Performance Characterization of the DSS-28 GAVRT-II Antenna Drive System

Farrokh Baher,* Barzia Tehrani,* and Wodek Gawronski†

ABSTRACT. — The existing Deep Space Network (DSN) 34-m antenna was retrofitted with a new PC-based industrial controller, upgraded interface hardware, high-frequency feed and receiver, and a tertiary assembly placed at the vertex of the main reflector. The upgraded wideband radio telescope was designed and built for use in the Goldstone Apple Valley Radio Telescope (GAVRT) outreach program. The servo performance due to the wind disturbance and mechanical components desired for the educational outreach program would be poor if a well-balanced rate loop and new linear-quadratic-Gaussian (LQG) controller were not performed and implemented. This article investigates and addresses antenna servo rate-loop anomalies and the effect of the LQG controller to meet the pointing requirement.

The anomalies under investigation are:

- Low-level azimuth oscillations (~1 mdeg rms)
- Elevation oscillations at a rate of 0.6 deg/s (1.4 mdeg rms error)
- Poor coherence in elevation compared to DSS-27 (similar antenna)

Prior to the servo rate-loop measurement, the servo rate-loop alignment (amplifier parameter configuration and percent torque bias) was performed for both azimuth (AZ) and elevation (EL). Due to the lack of servo rate-loop requirements, the results of the DSS-28 servo rate-loop measurements are compared with the measured values from DSS-27 using a step-function waveform to evaluate percent overshoot, settling time, and rise time, and to address AZ and EL oscillations. The results of both measurements are summarized in Table 4 and Table 5. Figures 9 through 13 illustrate different step amplitudes (0.06 deg/s, 0.6 deg/s, and 1 deg/s), which correspond to different rate commands to show these parameters.

I. Introduction

The Goldstone Apple Valley Radio Telescope (GAVRT) outreach program is a partnership involving the Lewis Center for Educational Research (LCER), the Apple Valley Unified High

* Communications Ground Systems Section.
† Communications Ground Systems Section, retired.

Note — This article originally appeared in *The Interplanetary Network Progress Report*, vol. 42-193, May 15, 2013, issue, but its publication had to be delayed until the November 15, 2013, issue.

The research described in this publication was carried out by the Jet Propulsion Laboratory, California Institute of Technology, under a contract with the National Aeronautics and Space Administration. © 2013 California Institute of Technology. U.S. Government sponsorship acknowledged.

School District (AVUHSD), NASA, and JPL, in which teachers and students nationwide access the 34-m radio telescope antenna via the Internet to carry out classroom radio astronomy observations. The LCER and AVUHSD are located east of Los Angeles, California, near the NASA Goldstone Deep Space Communications Complex (GDSCC). The DSS-28 antenna was designed for the Deep Space Network (DSN) to support radar and radio astronomy observations in the exploration of the solar system and the universe. Recently, the antenna was given to LCER and was retrofitted to perform as a telescope (downlink only) in support of the educational outreach program in Apple Valley.

This article describes the servo rate-loop issues and linear-quadratic-Gaussian (LQG) controller design to significantly improve telescope performance and satisfy the servo requirement of 1 mdeg rms error, less than 20 percent overshoot, and reduction of settling time below 6 s. The article provides information on the servo rate-loop tuning, rate-loop results when step and triangle signal are applied to the controller, and system identification performance, magnitude, phase, and the coherence function to describe the linearity of the system between the input and the output.

II. Executive Summary

The DSS-28 antenna drive system and position-loop controller design and tuning were conducted in early calendar year 2012 and final parameters were installed on March 1, 2012. The performance of the servo system is quantified using various methods, including visual inspection of the tachometer coupling, analog measurement of the rate-loop motor controller, and digital analysis of the position-loop responses. Furthermore, a comparison baseline data set with specific focus on rate-loop behavior and position-loop stability margin was collected from DSS-27, which has similar structural features as DSS-28. This large volume of measurement data is used to assess the performance characteristics of the DSS-28 servo system against the following derived criteria:

A. Obliging Structural Safety

The DSS-28 servo is safe to operate with no additional limitations imposed by the servo system over the existing safety procedures and guidelines. Even though some small level of sustained oscillation is visible in the azimuth axis, the magnitude of oscillation is very low, and the frequency of oscillation is far from the structural resonance frequency; consequently, such oscillation does not add any risk to the safety of the structure nor does it increase wear and tear on the antenna.

B. GAVRT Tracking Requirements

The DSS-28 servo performance meets GAVRT tracking requirements under all conditions except when the tracking elevation rate is at 0.6 deg/s. Since sustained tracking at 0.6 deg/s is seldom used, the impacts of the anomaly on tracking observations are considered very low.

C. Comparison with the DSS-27 Baseline

The DSS-28 open-loop servo system performance shows substandard performance when compared with the DSS-27 baseline. The exact root cause for the inferior performance is not known. This article shows a detailed comparison analysis and provides the baseline and model for further analysis. Likewise, this article recommends a set of additional analyses in the area of both structural verification and servo drive testing to identify the root cause.

III. Measurement Methods and Summary of Results

A. Closed-Loop Control Characteristics (Operational Mode)

The closed-loop characteristics define the overall antenna servo control system performance in an integrated environment that includes a position-loop controller, rate-loop controller, drive system components, and the antenna structure. To measure the overall servo performance, the antenna controller software is used to generate commanded steps and fixed-rate signals and inject them to the point of position input while simultaneously logging command and encoder values. The closed-loop measurement methods are further classified into the following distinct test sets:

- Linear position step response measurement
- Nonlinear position step response measurement
- Position-loop fixed-rate tracking response

1. Linear Position Step Response Measurement

The position-loop response is linear on small steps when the total integral error is less than the maximum integral saturation point. In order to restrain measurement to the linear region, a step input of less than 0.05 deg magnitude is injected into the position loop. In addition, given the dependency of azimuth structural response with elevation angle, azimuth step response is measured in three elevation positions of high, minimum, and low angles. The overshoot and settling time are measured. The combination of overshoot and settling time indirectly represents the wind disturbance characteristics of the servo system. Table 1 shows the summary of measurement and analysis results.

Table 1. DSS-28 position-loop linear step response performance characteristics.

Test Case	Settling Time	Overshoot Small Step
AZ Step at EL=45 deg	4.3 s	5%
AZ Step at EL=10 deg	4.8 s	5%
AZ Step at EL=80 deg	4.4 s	6%
EL Step	8.8 s	11%

Settling Time. Settling time is defined as the time at which the antenna encoder output remains within a 3 percent threshold of the nominal value of the step command and indicates how fast the antenna reacts to the command. The settling time of a step response is illustrated in Figure 1 with settling time of 8.8 s for 0.04-deg step size.

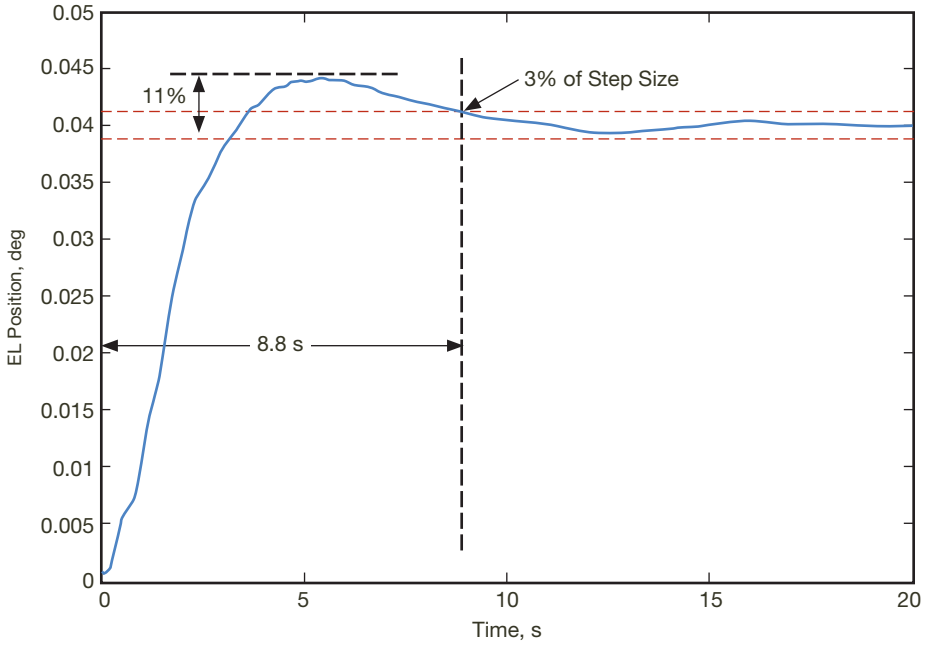

Figure 1. Elevation step response with 0.04-deg step size. Settling time is 8.8 s and overshoot is 11 percent of the step size.

The typical settling time achieved by DSN beam-waveguide (BWG) antennas is approximately 6 s on average, and varies between 4 to 9 s depending on the servo characteristics and loop compensation parameters.

Percent Overshoot. Percent overshoot is the relative difference between the maximal encoder output and the commanded step with respect to the value of the commanded step. Percent overshoot of a small step response is illustrated in Figure 1 with an overshoot of 11 percent for 0.04-deg step size. The typical linear step response overshoot of DSN BWG antennas is less than 20 percent of the step size.

The azimuth performance is remarkably good, with a settling time less than the average DSN BWG antennas, and a low overshoot at all elevation angles. The small overshoot is the result of a small integral gain of the LQG controller. The low overshoot also indicates that better overall performance may be achievable with additional tuning, but conditioned to the stability margin and LQG damping capability near resonance frequency. To achieve the potential better performance, high-coherence frequency response data are needed. See Section III.B for open-loop frequency response measurement results.

In contrast to azimuth step response, the elevation axis shows much slower response to commands, and a longer settling time. The long settling time is the result of low proportional gain of the controller, which is specifically designed low to manage the instability in

the elevation rate loop. Figure 1 shows the elevation step response for a 0.04-deg step. As shown in the figure, the response to the command follows with very slow rise time and low starting acceleration. Further stability tests have shown that increases in the proportional gain and therefore rise-time results is oscillation at settling.

2. Nonlinear Position Step Response Measurement

The position-loop response is nonlinear on large steps when the total integral error exceeds the maximum integral saturation point. While the performance of nonlinear control regions has no impact on tracking, it implicates the slew behaviors for source-to-source transitions and may complicate going to stow operation. In order to measure the controller performance in nonlinear regions, a step input of 10-deg magnitude is injected into the position loop. The following quality characteristics are measured:

Total Overshoot. Total overshoot of a large step response is illustrated in Figure 2 with overshoot of 0.007-deg magnitude for a 10-deg step size. Total overshoot is the difference between the maximal encoder output and the commanded step with respect to the value of the commanded step. The typical nonlinear step response overshoot of DSN BWG antennas is less than 0.1-deg magnitude.

As shown in the summary of nonlinear measurement results (Table 2), the total overshoot on both azimuth and elevation axes and all conditions is extremely low. This low total overshoot is best suited for observational modes that require numerous slewing from source to source.

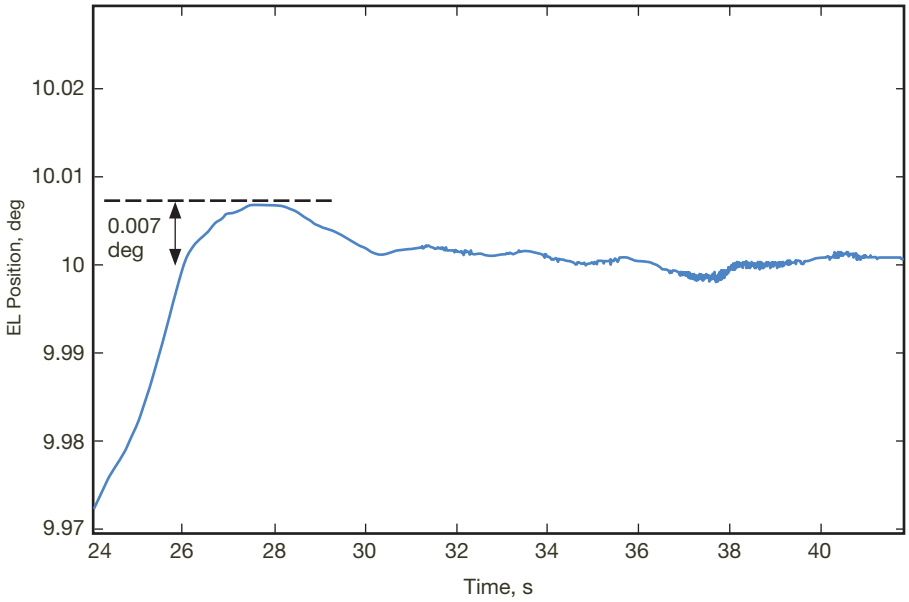

Figure 2. Elevation step response with 10-deg step size. Total overshoot is 0.007 deg.

Table 2. DSS-28 position-loop nonlinear step response performance characteristics.

Test Case	Overshoot Large Step
AZ Large Step at EL=45 deg	0.004 deg
AZ Large Step at EL=10 deg	0.004 deg
AZ Large Step at EL=80 deg	0.004 deg
EL Large Step	0.007 deg

3. Position-Loop Fixed-Rate Tracking Response

The response of the antenna axes to tracking commands is measured in fixed rate controlled by updating position input in regular intervals equal to the controller position-loop closure frequency. The fixed-rate tracking response is measured for rates from 0.0001 to 0.9 deg at each direction. In addition, given the dependency of azimuth structural response with elevation angle, azimuth fixed-rate tracking response is measured in three elevation positions of high, minimum, and low angles. The following quality characteristics are measured:

Steady-State Mean Error. Steady-state mean error in rate offsets is illustrated in Figure 3. This represents a lagging of the antenna when commanded at a constant rate. The steady-state mean error is expected to approach zero overtime and not exceed 0.0001 deg in a 30-s integration period.

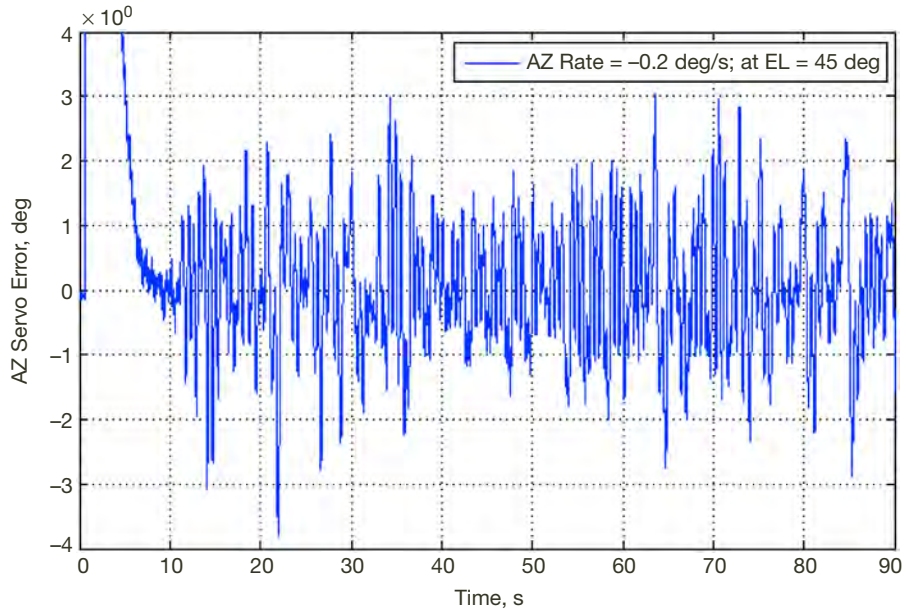

Figure 3. Azimuth response to 0.2 deg/s fixed rate at mid-elevation. Total steady state is reached after 11 s; mean error is 0.0000 and tracking rms is 0.00096 deg.

Steady-State rms Servo Error. Steady-state rms servo error in rate offsets, illustrated in Figure 3, represents the magnitude of tracking noise that is not corrected by the servo system. The typical tracking rms achieved by DSN BWG antennas is less than 0.001 deg in a 30-s integration after steady state is reached. Tracking rms of 0.001 deg meets the GAVRT observation requirements.

Since performance measurement at all possible rates is extensive and almost impossible, the fixed-rate tracking tests were reduced to a limited number of rates distributed to cover the full range with concentration on low rates in [–0.9, –0.7, –0.5, –0.3, –0.2, –0.1, –0.01, –0.001, –0.0001, 0.0001, 0.001, 0.01, 0.1, 0.2, 0.3, 0.5, 0.7, 0.9]. Each of these rates is used four times — one for elevation and three for azimuth — on low, medium, and high elevation angles. The results of all test cases show mean error is 0.0000. The summary of measured rms tracking-error values is shown in Table 3.

Table 3. DSS-28 position-loop linear fixed-rate tracking response performance characteristics.

Rate, deg/s	AZ rms Error, mdeg, at EL=45 deg	AZ rms Error, mdeg, at EL=10 deg	AZ rms Error, mdeg, at EL=80 deg	EL rms Error, mdeg,
+0.0001	0.1	0.1	0.1	n/a
–0.0001	0.1	n/a	0.1	n/a
+0.001	0.2	0.3	0.1	1.5**
–0.001	0.3	0.2	0.1	1.1**
+0.01	0.5	0.5	0.4	0.9
–0.01	0.5	0.7	0.4	0.8
+0.1	1.0	0.6	0.8	1.0
–0.1	1.1	0.5	0.8	0.8
+0.2	0.9	0.9	0.9	1.1**
–0.2	1.0	1.1	0.7	2.6**
+0.3	0.8	0.7	0.5	0.8
–0.3	0.9	0.8	0.8	0.7
+0.5	0.6	1.5*	0.5	0.6
–0.5	1.0	0.6	0.9	0.8
+0.6	n/a	n/a	n/a	1.8*
+0.7	0.6	0.9	0.4	0.9
–0.7	0.8	0.6	0.9	0.8
+0.9	0.6	0.6	0.6	0.7
–0.9	0.8	0.8	0.96	0.6

* Does not meet <0.001-deg rms requirement. ** High wind during measurement.

As shown in Table 3, several test cases failed to meet the <0.001-deg rms requirement, with highest value reaching above 2.5 mdeg at –0.2 deg/s tracking. However, in several cases (marked with **), the measured wind speed at the time of data collection exceeded the level at which the 1-mdeg rms requirement is applicable. Studying the data also shows that the large rms errors in those cases are not the result of structural or control system injected oscillations.

Azimuth at +0.5 deg/s on low-elevation, rms = 1.5 mdeg

As shown in Figure 4, during this test case the azimuth tracked at a rate of 0.5 deg/s for at least 40 s in steady state with tracking rms of less than 1 mdeg, with a sudden jump to rms of approximately 2 mdeg for the rest of the test duration. Given that servo response is independent of the absolute azimuth position, such change after reaching the steady state can only be caused by external factors such as azimuth track unevenness or wind disturbance. However, since two other similar test cases covering the same azimuth angles (only differ on elevation angle) do not show such behavior, it is safe to conclude that azimuth track unevenness is not contributing to the large error rms. Wind gust could be another possibility, which can be substantiated by variable frequency in the response. Nevertheless, given no detailed weather data at the time of this measurement, the conclusion cannot be made with certainty.

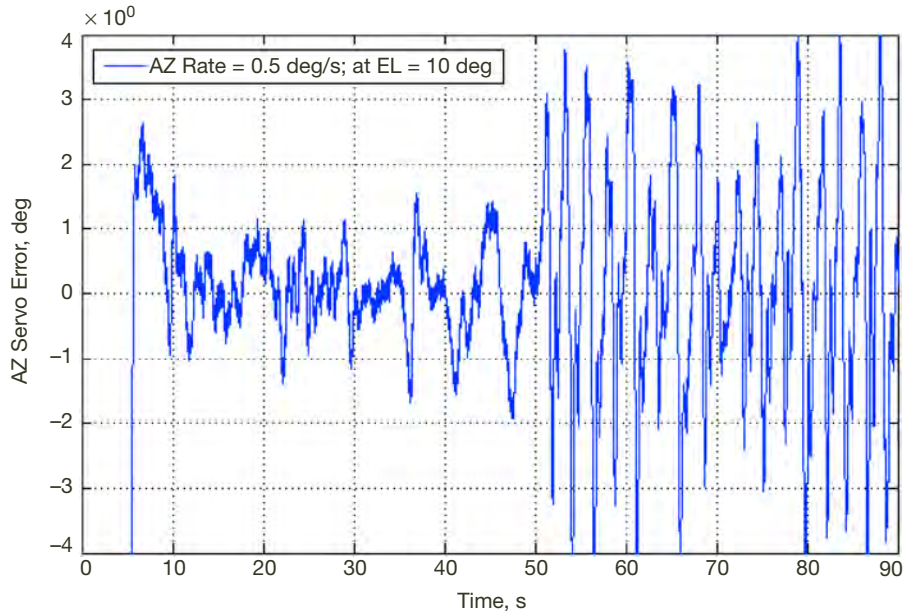

Figure 4. Azimuth response to 0.5 deg/s fixed rate at low elevation. Total steady state is reached after 11 s; mean error is 0.0000 and tracking rms is 0.0015 deg.

Elevation at 0.6 deg/s, rms = 1.8 deg

As shown in Figure 5, a high-elevation tracking rms at 0.6 deg/s rate is caused by unremitting high-frequency oscillation in steady state. The oscillation frequency matches structural resonance, which indicates that control functions are not fully stable. However, detailed study and comparison of rate-loop response does not show any specific behavior or unexpected changes at exactly 0.6 deg/s. Further analysis and testing is required to identify the root cause and the trigger. However, multiple tests have shown that such resonance only exists at a sustained rate of 0.6 deg/s. Since such sustained fixed tracking is not a norm in operational observations, the impact of this anomaly is considered very low.

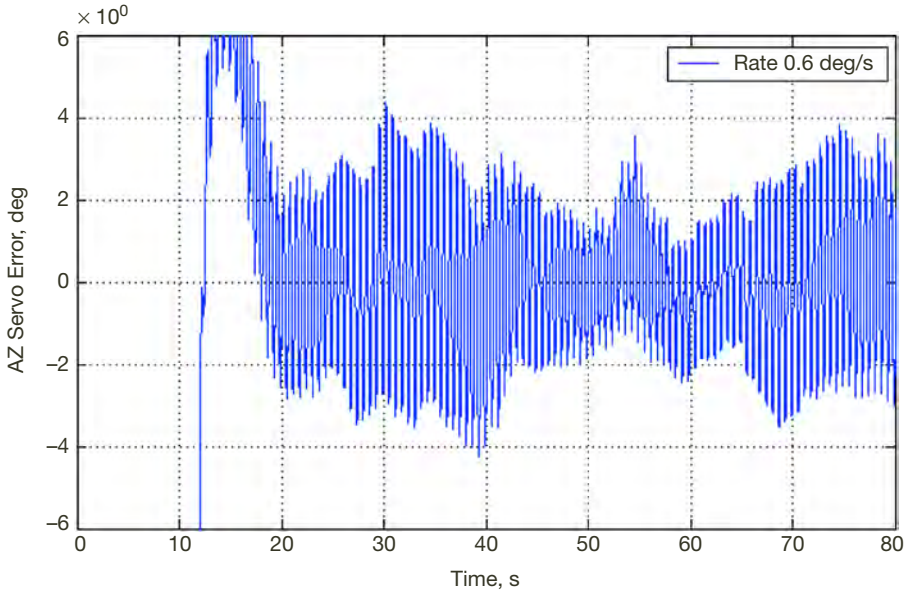

Figure 5. Elevation response to 0.6 deg/s fixed rate. Total steady state is reached after 18 s; mean error is 0.0000 and tracking rms is 0.0018 deg.

B. Open-loop Control Characteristics

The open-loop characteristics define the antenna drive's performance in an integrated environment that includes rate-loop controller, drive components, and antenna structure. The rate-loop characterization is performed in two distinct test environments:

1. White Noise Injection

White noise injection is performed by injecting the uniform white noise into the rate output of the position-loop controller in open-loop mode. The controller logs both the injected signal and encoder reading in 10-ms cycles.

2. Drive Cabinet Signal Injection

Drive cabinet signal injection is performed using an external signal generator and signal recorder (Nicolet) connected to the antenna drive cabinet (ADC) test ports. The signal generator is then configured to generate test signal waveforms for each specific test case. Figure 6 shows the test environment and ADC signal injection and monitor points.

The closed-loop measurement methods are further classified into the following distinct test sets:

- Open-loop frequency response
- Square-function waveform tachometer and current response
- Triangle (ramp) waveform tachometer and current response

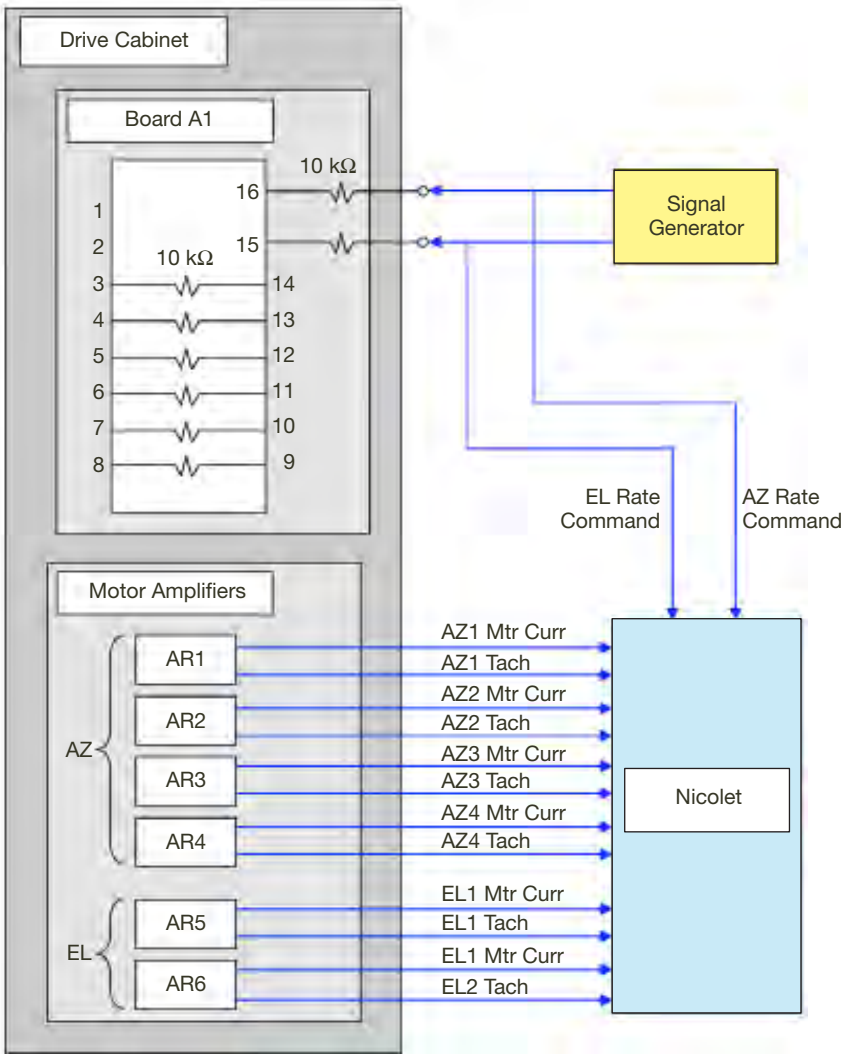

Figure 6. Test-bed configuration: ADC signal injection.

3. Open-Loop Frequency Response

The open-loop response of the antenna drive system to rate commands is represented in frequency response. The frequency response plot is the closest approximate representation of the plant transfer function from rate input to the antenna servo interface (ASI) to position output from encoder to the position controller. The frequency response is also used in system identification to generate best estimation for the open-loop linear state space model used as the estimator by the LQG controller. In addition to system identification, the frequency response can be used to derive the following performance parameters:

Gain Margin. Gain margin is illustrated in Figure 7 (AZ) and Figure 8 (EL). Gain margin is defined as the difference between the two values of open-loop gain at phase crossover and gain crossover. It represents the factor by which the open-loop magnitude must be multiplied to destabilize the closed-loop system.

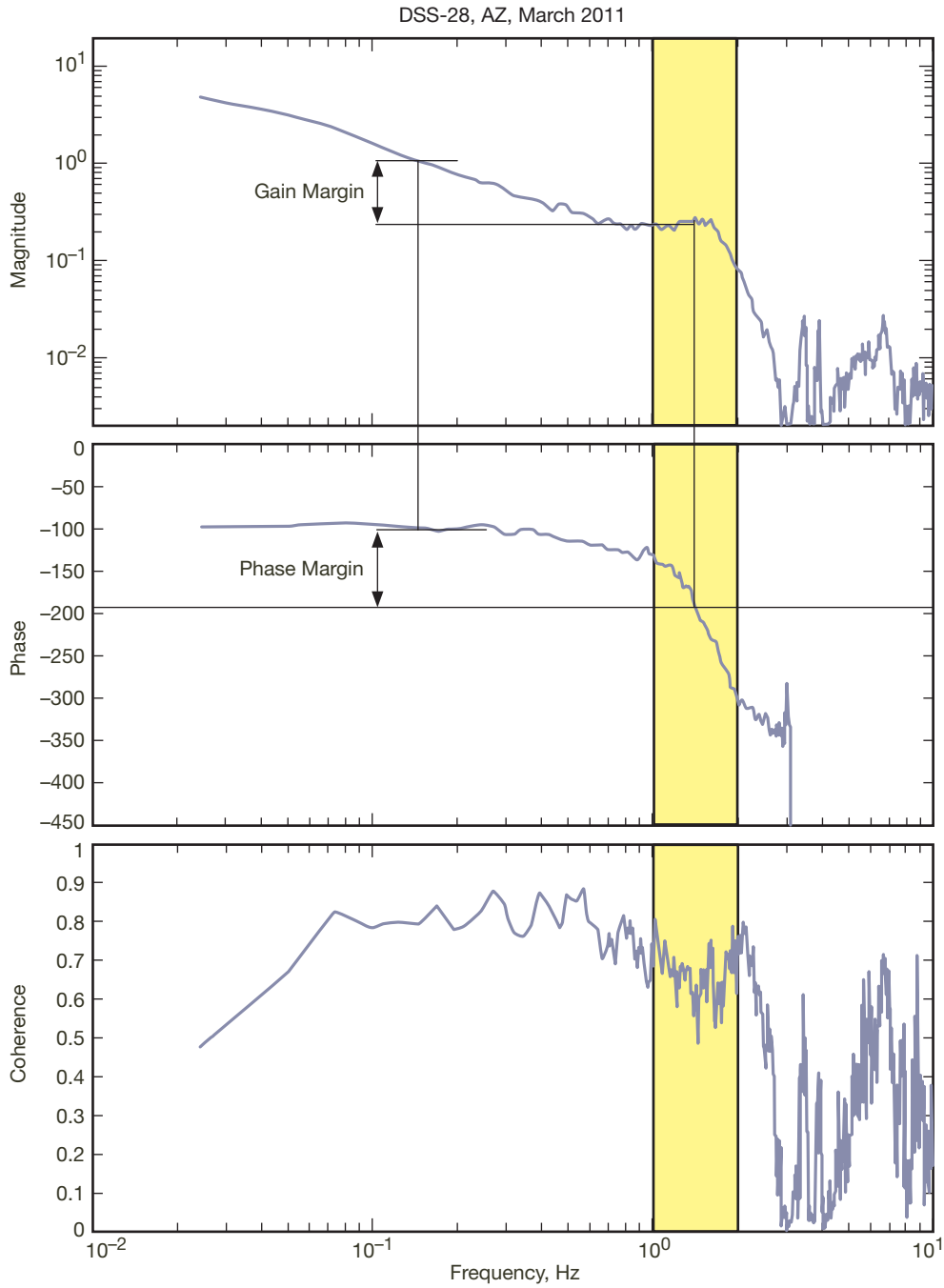

Figure 7. Magnitude, phase, and coherence responses of azimuth. From the graph, the gain and phase margin are found to be approximately 1.6 dB and 75 deg, respectively. The coherence plot shows that it is good for frequencies below 0.6 Hz and is a problematic issue about frequency range of 1–2 Hz (yellow area). At the resonance, it should be high. However, it drops and is an indication of some hardware problem.

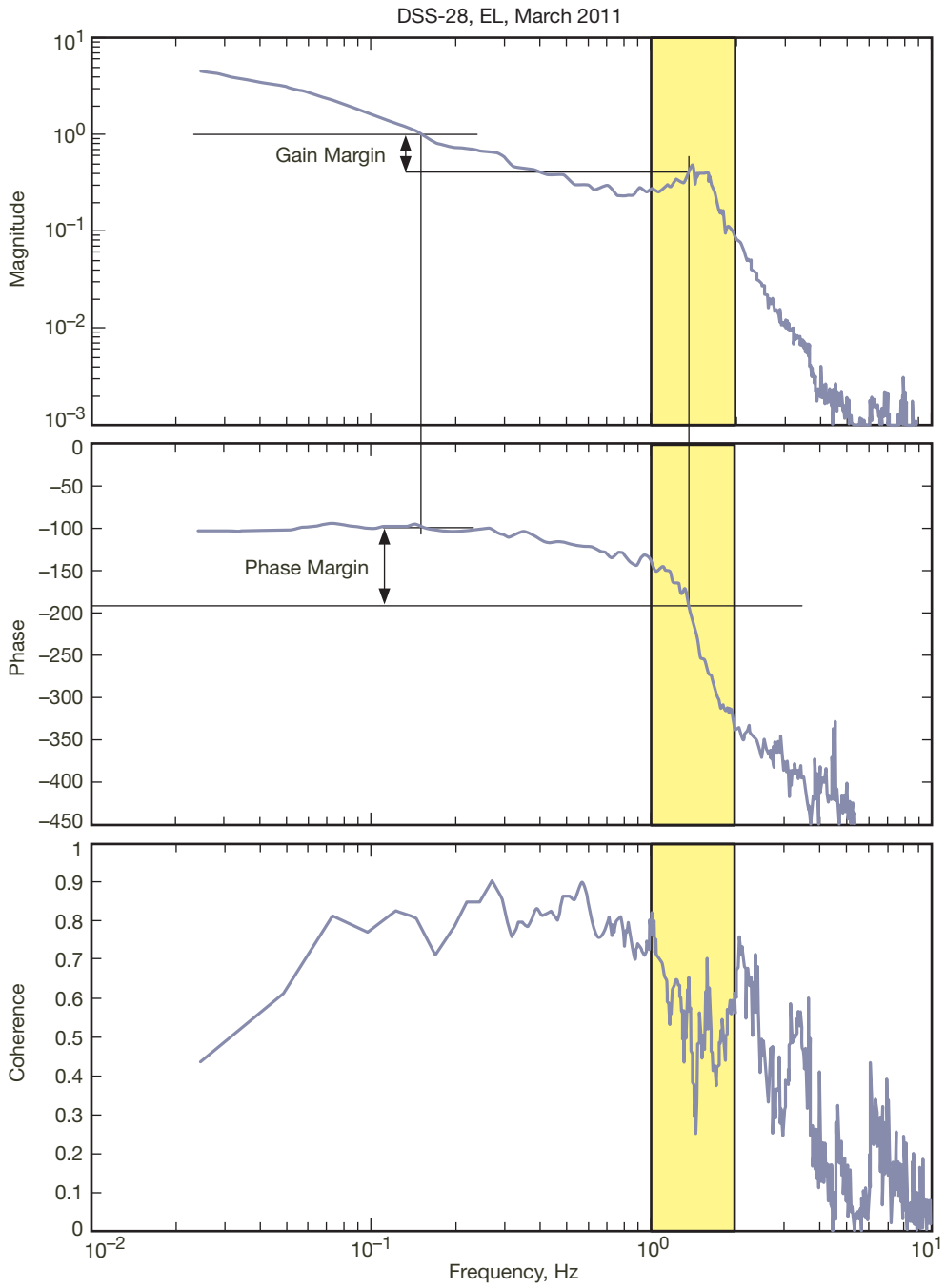

Figure 8. Magnitude, phase, and coherence responses of elevation. From the graph, the gain and phase margin are found to be approximately 3 dB and 75 deg, respectively. The coherence plot shows that it is good for frequencies below 0.6 Hz and is a problematic issue about frequency range of 1–2 Hz (yellow area). At the resonance, it should be high. However, it drops and is an indication of some hardware problem.

Phase Margin. Phase margin is illustrated in Figure 7 (AZ) and Figure 8 (EL). Phase margin is defined as the difference between the two values of open-loop phase at phase crossover and gain crossover. It represents the number of degrees of phase shift to destabilize the closed-loop system.

Coherence Function. Coherence function is an indicator for approximation error. It is defined as the ratio of the square of cross power spectral density between input and output over the products of independent auto-spectral density of input and output. It represents the amount of uncertainty in the measurement. Low coherence can be caused by noise during measurement (i.e., wind) or may be caused by anomalies and unpredictable structural response (i.e., loose coupling, slips, etc.).

4. Square-Function Waveform Tachometer Response

The square-waveform tests are performed to measure the step response characteristics of the rate loop for each drive (4 on azimuth, 2 on elevation). The following characteristics are measured:

Percent Overshoot. Percent overshoot in the square-waveform test is illustrated in Figure 9 with overshoot of 35 percent for 0.04-deg step size. Percent overshoot is the relative difference between the maximal tachometer output and the step size defined by the difference between the minimal and maximal steady state values.

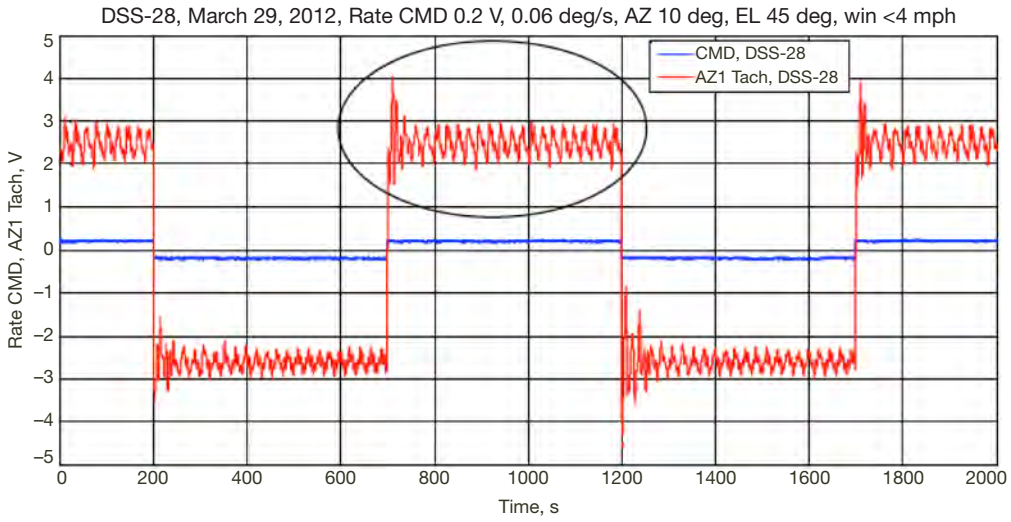

Figure 9. Azimuth drive-1 tachometer voltage during waveform test of 0.2 V magnitude.

Rise Time. Rise time is the time required for the response to go from 10 percent to 90 percent of the steady-state value. It represents the gain of response to rate command. The rise time typically correlates closely with the average gain of the frequency response within the frequency bandwidth of the open-loop system.

Symmetry. Symmetry around the zero rate measures the amount of rate bios in analog measurements and rate-loop control functions. Large asymmetric response is an indication of an unexpected problem in the drive system (i.e., A2D bios, tachometer problem, etc.).

Oscillation. Oscillation during the square-waveform test is illustrated in Figure 10 with oscillation frequency of 0.12 Hz and magnitude of 0.3 V peak to peak.

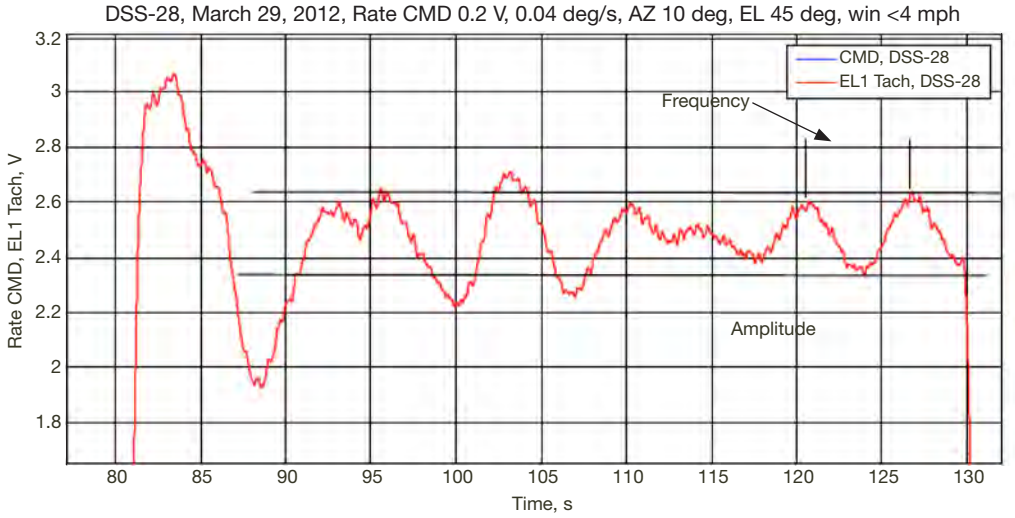

Figure 10. Azimuth drive-1 oscillation during waveform test of 0.2 V magnitude.

Table 4 and Table 5 show the summary of the square-waveform test results and azimuth and elevation, respectively. Given the large variability between BWG antennas, the DSS-27 baseline is used to compare and validate each performance parameters. As shown in the results, azimuth response is very similar to DSS-27 for overshoot and rise time but shows higher magnitude and lower frequency of oscillations.

Table 4. DSS-28 azimuth rate-loop square-waveform performance summary and comparison with DSS-27 baseline.

	Percent Overshoot		Frequency of Oscillation, Hz		Amplitude of Oscillation, V p–p		Rise Time, s	
Rate	DSS-27	DSS-28	DSS-27	DSS-28	DSS-27	DSS-28	DSS-27	DSS-28
0.2 V (0.06 deg/s)	14–19	17–25	0.5	0.045	0.45	1	<1	<1
2 V (0.6 deg /s)	5–7	3–4	0.6	0.045	0.6	0.66	<1	<1
3.3 V (1 deg /s)	1.5–4	2–3	0.8	0.048	0.8–1.05	1.36	<1	<1

Table 5. DSS-28 elevation rate-loop square-waveform performance summary and comparison with DSS-27 baseline.

	Percent Overshoot		Frequency of Oscillation, Hz		Amplitude of Oscillation, V p–p		Rise Time, s	
Rate	DSS-27	DSS-28	DSS-27	DSS-28	DSS-27	DSS-28	DSS-27	DSS-28
0.2 V (0.04 deg/s)	9–12	10	1.2	0.15	0.1	0.3	0.2	1
2 V (0.4 deg /s)	2	2.5	1.2	0.15	0.4	0.6	1	11
3.3 V (0.66 deg /s)	1.6	0.7	0.8	0.2	0.5	1	1.6	18.5

5. Triangle (Ramp) Waveform Tachometer Response

The triangle (ramp) waveform signal is injected to the amplifier input and the output response (tachometer) is recorded. The triangular waveform test is performed to measure the following characteristics:

Linearity. Linearity around zero crossing represents the behavior of the system as it slows down to zero (rest) and then switches to the opposite direction.

Command Following. Command following is the function representing the tachometer response to input command. The direction and scale factor of the response is expected to stay constant for the duration of the test.

The comparison between DSS-28 and DSS-27 shows very similar performance with the exception of zero crossing (dead-band) on elevation drive no. 2, shown in Figure 11. Even though the 1-s-wide dead-band is much larger than DSS-27, its magnitude is still very small and impact to the position loop is almost negligible.

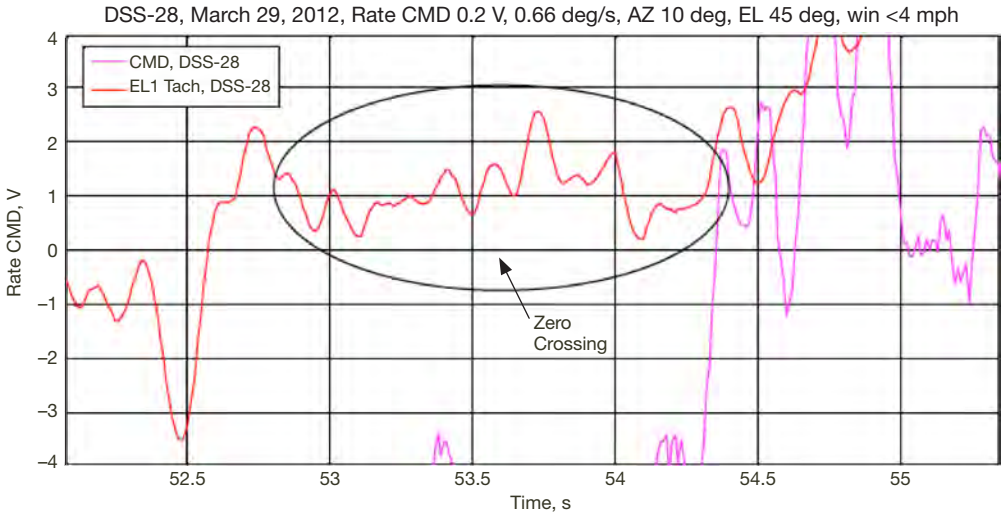

Figure 11. Elevation drive no. 2 zero crossing (dead-band) of approximately 1 s.

In addition, the triangle waveform test is used to further eliminate rate-loop response as the root cause of excess position-loop oscillation at 0.6 deg/s elevation fixed rate (shown in Figure 5). As shown in Figure 12 and Figure 13, the tachometer response at 35 VDC, which corresponds to the 0.6 deg/s rate command, does not show any discontinuity (flatness) as the command crosses ±3 VDC (±0.6 deg/s).

C. Other Tests and Measurements

1. Gain Stability Test

New controller coefficients were developed for both AZ and EL LQG controller (proportional and integral [PI] gain of AZ LQG Kp=2.078 and Ki=0.96; for EL, Kp=1.392 and Ki=0.488).

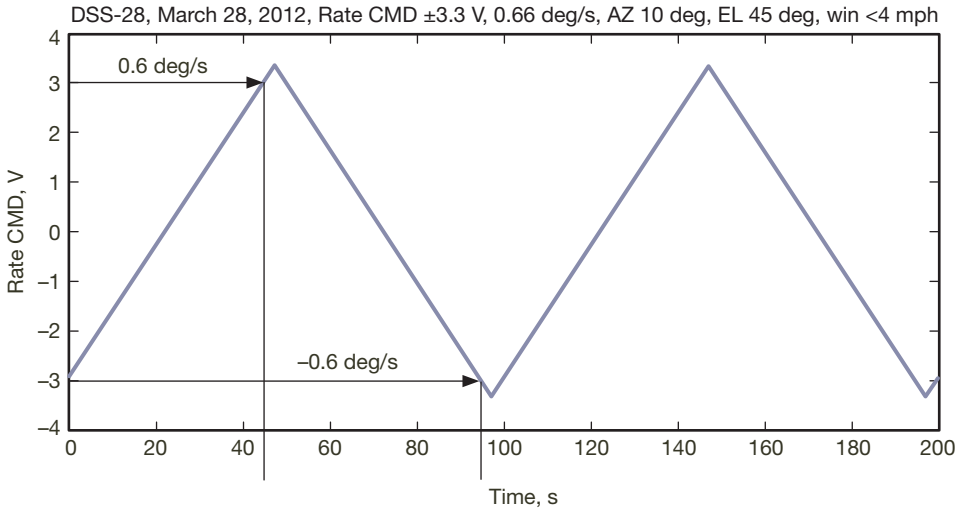

Figure 12. Elevation tach-1 response with ±3.3 V rate input showing no discontinuity at rate crossing 3 V.

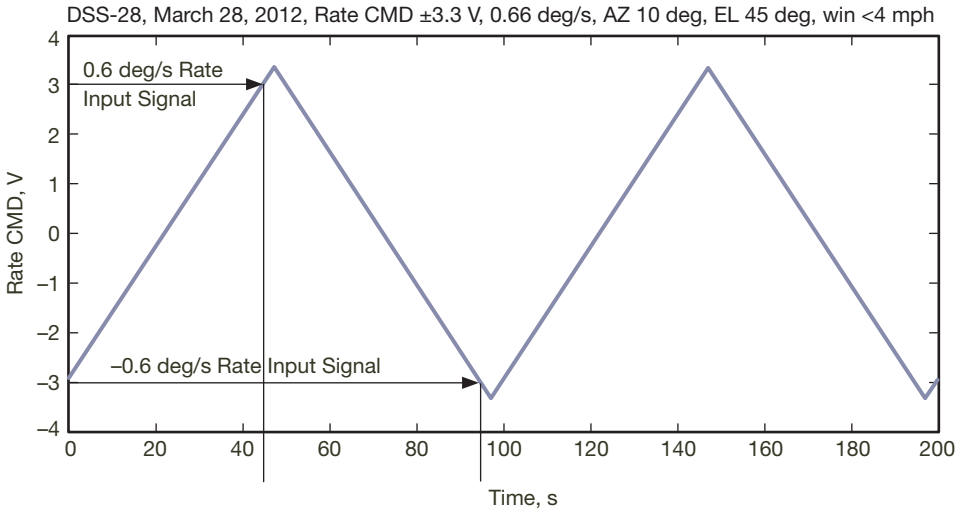

Figure 13. Elevation tach-2 response with ±3.3 V rate input showing no discontinuity at rate crossing 3 V.

Significant improvement was observed with respect to the PI controllers, and the performance is shown in Appendix A through Appendix D.

2. Encoder Coupling Visual Inspection

Visual inspection of the coupling located between the motor shaft and tachometer with the cover removed was performed using a video camera. The antenna was commanded to move both directions at very low speed to observe any stiction at zero crossing. There was no nonlinearity at zero crossing. However, a very short pause (stutter) in rotation at different rotation positions of the shaft was observed on both antennas. Further gearbox or coupling investigation is required to find the root cause of this behavior.

IV. Unresolved Issues

Since the initial effort to improve the DSS-28 servo performance to the level suitable for observation and research campaigns, a large number of issues have been resolved. The servo is ready for operational use and meets the tracking requirements. Nevertheless, a few performance-related issues are still outstanding, which require additional work and attention to optimize the performance. The following list is documented here in the order of recommended priority based on their impact to the overall system performance.

(1) *Sluggish Elevation Rate-Loop Response* is quantified by extremely slow rise time to rate steps. The slow rise time and consequently under-gained response to rate commands adversely impacts the elevation positioning and tracking by reducing the effective control bandwidth of the position loop and undesirably diminishes the wind disturbance rejected capability of the system. In addition, the sluggish response at low frequency rate commands will reduce the ability of the LQG designer to damp the structural oscillation by forcing minimal gain-margin.

(2) *Azimuth Oscillation at 0.6 deg/s* with structural resonance signature is shown in position-loop measurements. Such oscillation that is restricted to the position loop is unpredictable by modeling and indicates an existence of an anomalous condition that is not correctable by control system design or tuning. The source of this behavior is currently unknown.

(3) *Low Coherence of Frequency Response* represents an excess error in the frequency-response measurement and causes inaccuracy in the system identification and LQG estimator error. Even though the low coherence may simply be the result of measurement noise, it may be an indication of some form of mechanical instability that results in randomness in response.

(4) *Small Azimuth Rate-Loop Oscillation* measured by square-waveform signal injection indicates a potential problem in the drive system that may include mechanical. Even though this low level of oscillation is completely compensated in the position loop and has no impact on the system performance, it may be an early indication of a problem in the system that could escalate over time.

V. Recommendations

To determine the root cause of the DSS-28 azimuth and elevation axes' oscillations and the slow elevation transient state (rise time), and in order for the DSS-28 antenna to operate properly, the following recommendations are made:

1. Mechanical

- Investigate AZ and EL drive rotation stutter by decoupling the motor from the gearbox and applying a very low rate command. Observe and record the shaft rotation. This will determine if the stutter is caused by the gearbox.
- Check and verify that the motor bearings do not bind at slow speed rotation.

2. Servo Rate-Loop

- Ensure that both antennas' analog boards in the antenna drive cabinets were built to the same drawing.
- Review circuits of the analog boards to verify that the EL rate-loop circuitry integration time is the same as AZ to investigate the rise time.
- Retest DSS-28 elevation axes for slow rise time.
- Perform motor armature current to analyze imbalance, friction, and countertorque of the AZ and EL drives.
- Perform individual drive response test.

3. Servo Position-Loop

- Measure closed-loop frequency response of the controller and compare the results with the open-loop response. Verify position-loop does not inject additional unexpected phase shift in the control system.

4. Perform Annual Servo Performance Measurement per 869-000129.[1]

Acknowledgment

The authors gratefully acknowledge the support of the Lewis Center for Educational Research (LCER) personnel; John Leflang and Ryan Dorcey for their work on data collection and remote computer control support; the LCER and the Apple Valley Unified School District, located near NASA's Goldstone Deep Space Communications Complex, with a partnership involving NASA, JPL, and the Goldstone Apple Valley Telescope (GAVRT) support outreach project. Special thanks to program manager Dr. Lawrence Teitelbaum for his funding support. Also, thanks to Fred Soria and Tyler Lentz from ITT Exelis at the Goldstone complex in support of servo rate loop data gathering and Karen Ross Wilson for documentation assistance. Thanks to Marilyn Morgan for work on editing and production of this article for *The Interplanetary Network Progress Report*.

[1] *DSN Antenna Servo Performance Verification Procedure*, DSN document 869-000129, Rev. F (internal document), Jet Propulsion Laboratory, Pasadena, California, June 2, 2010.

Appendix A

Azimuth LQG Closed-Loop Performance at Elevation of 45 Degrees

The measurements in Appendix A were all taken at DSS-28 on March 2, 2012.

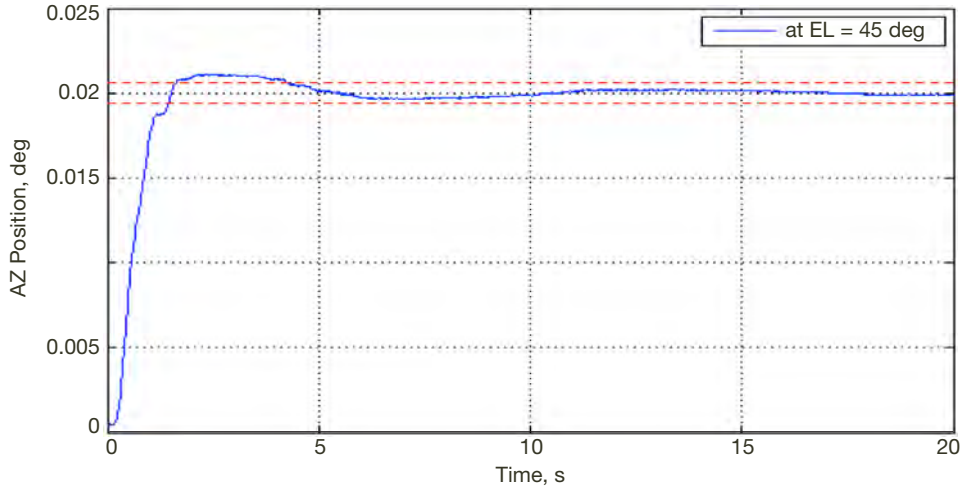

Figure A-1. Overshoot of 5 percent and settling time of 4.3 s, which satisfies the requirements when a positive small position offset of 0.02 deg is applied to the azimuth drives.

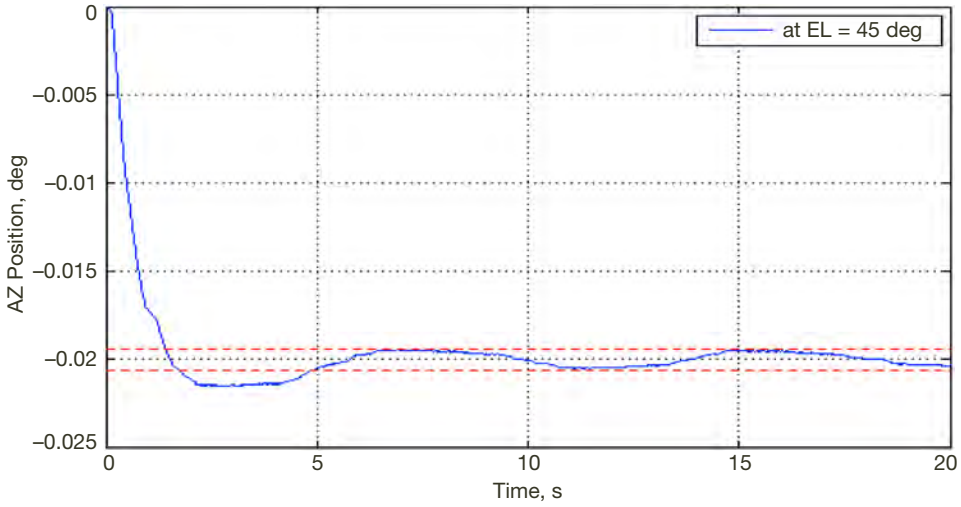

Figure A-2. Overshoot of 7 percent and settling time of 4.9 s when a negative small position offset of 0.02 deg is applied to the azimuth drives. Both parameters satisfy the requirements.

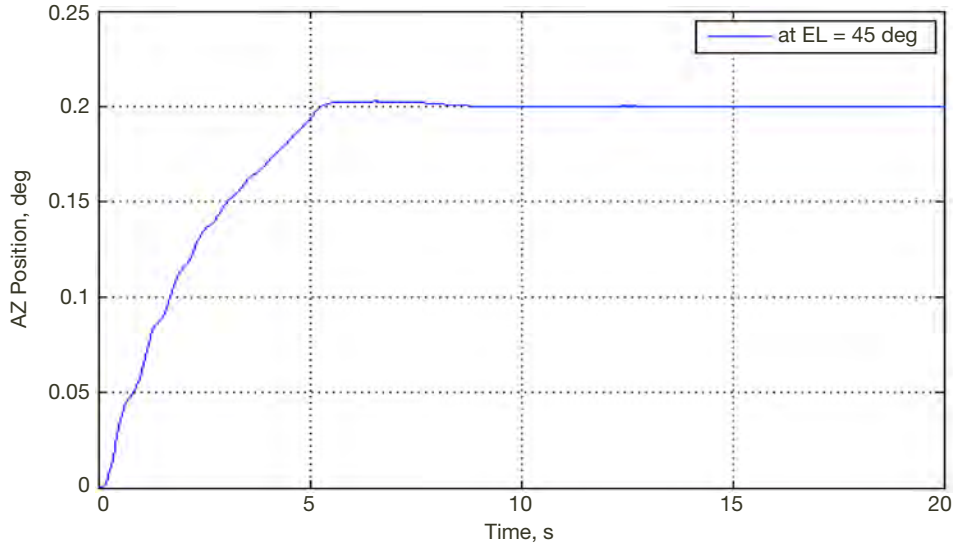

Figure A-3. Overshoot of 0.003 deg when a positive position offset of 0.2 deg is applied to the azimuth drives, which satisfies the requirement of less than 0.1 deg.

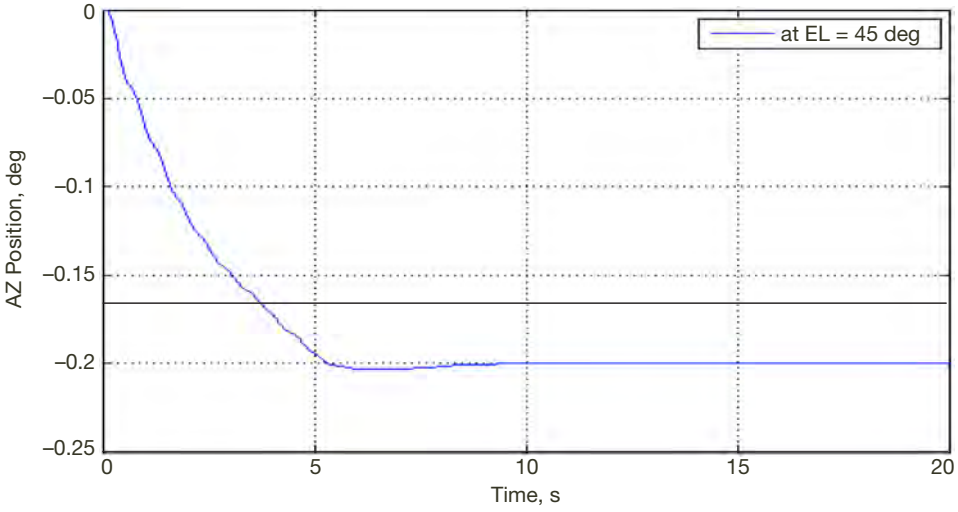

Figure A-4. Overshoot of 0.003 deg when a negative position offset of 0.2 deg is applied to the azimuth drives, which satisfies the requirement of less than 0.1 deg.

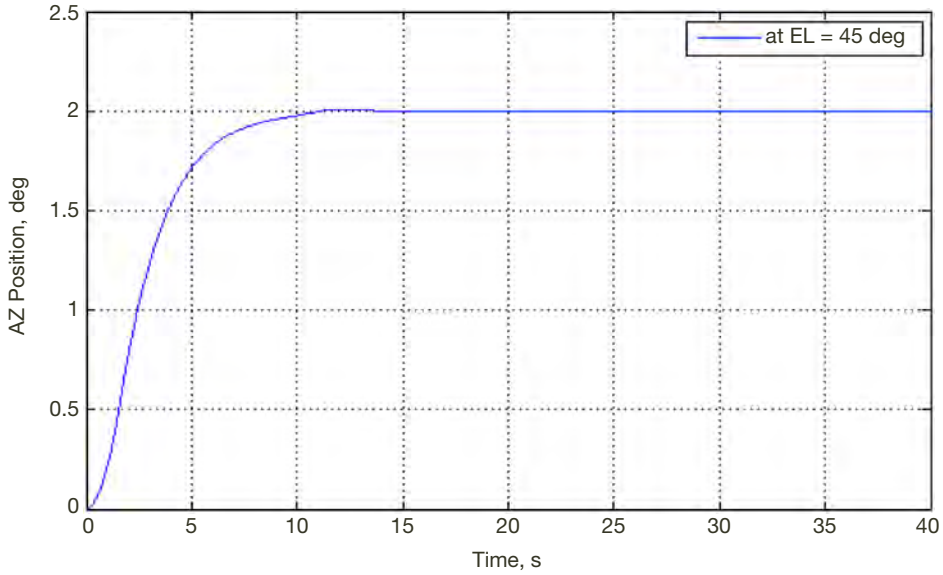

Figure A-5. Overshoot of 0.004 deg when a positive position offset of 2 deg is applied to the azimuth drives, which satisfies the requirement of less than 0.1 deg.

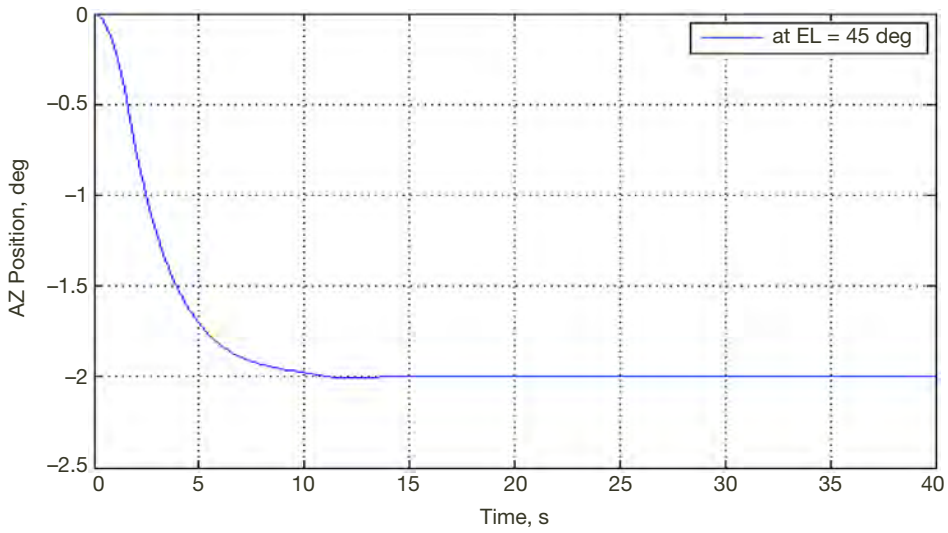

Figure A-6. Overshoot of 0.003 deg when a negative position offset of 2 deg is applied to the azimuth drives, which satisfies the requirement of less than 0.1 deg.

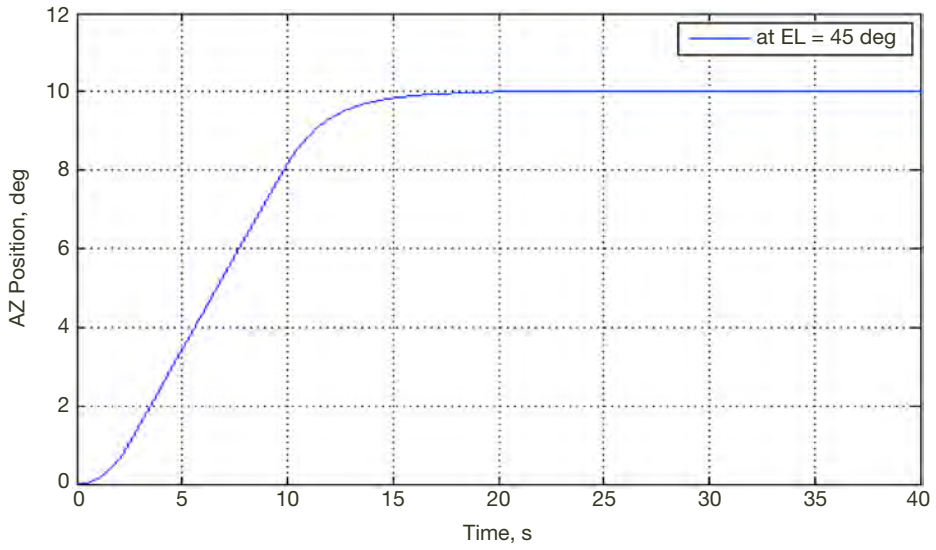

Figure A-7. Overshoot of 0.004 deg when a positive large position offset of 10 deg is applied to the azimuth drives, which satisfies the requirement of less than 0.1 deg.

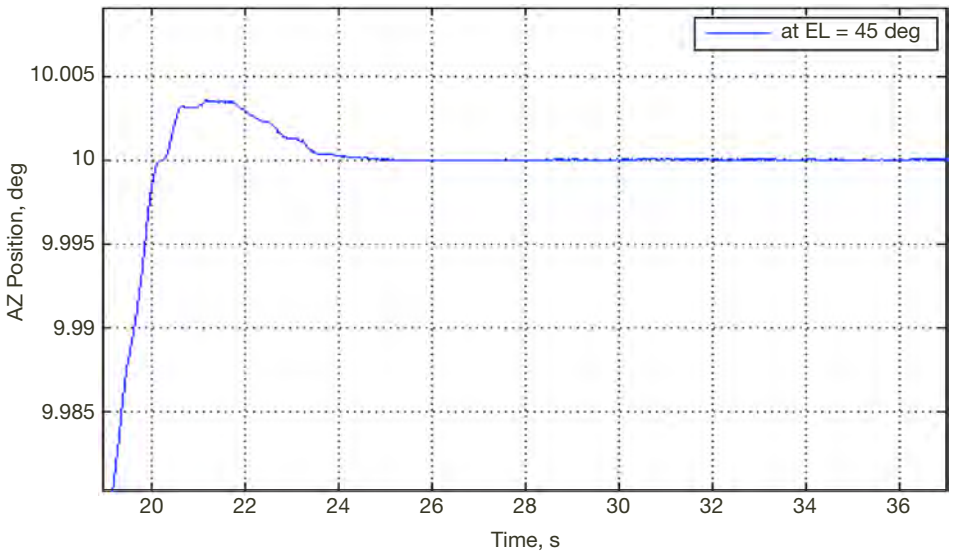

Figure A-8. Zoom of Figure A-7 to show overshoot of 0.004 deg.

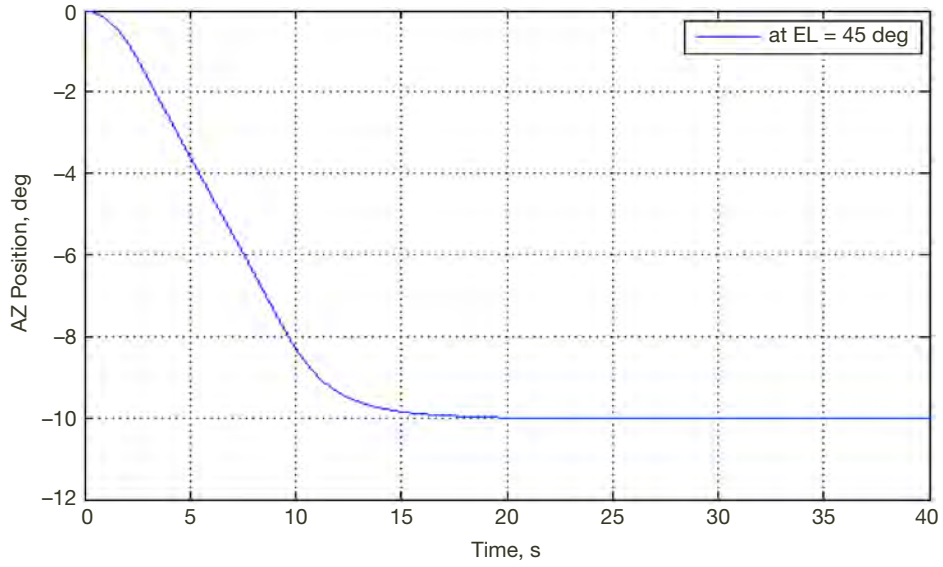

Figure A-9. Overshoot of 0.004 deg when a negative large position offset of 10 deg is applied to the azimuth drives, which satisfies the requirement of less than 0.1 deg.

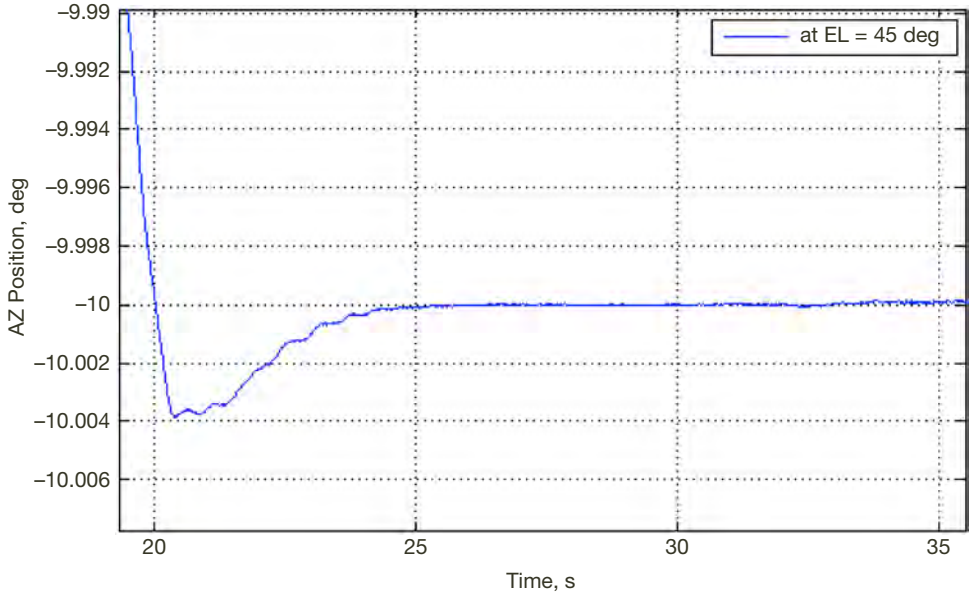

Figure A-10. Zoom of Figure A-9 to show overshoot of 0.004 deg and the response attained at maximum speed.

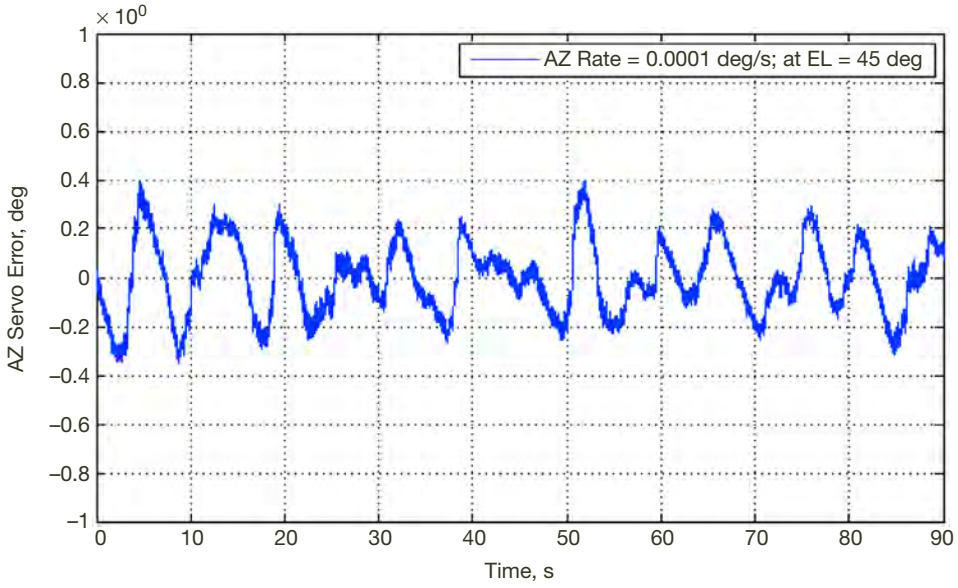

Figure A-11. Azimuth rms mean servo error of 0.1 mdeg when a small positive rate offset of 0.0001 deg/s is applied to the azimuth drives. The mean servo error does meet the requirement of less than 0.001 deg rms.

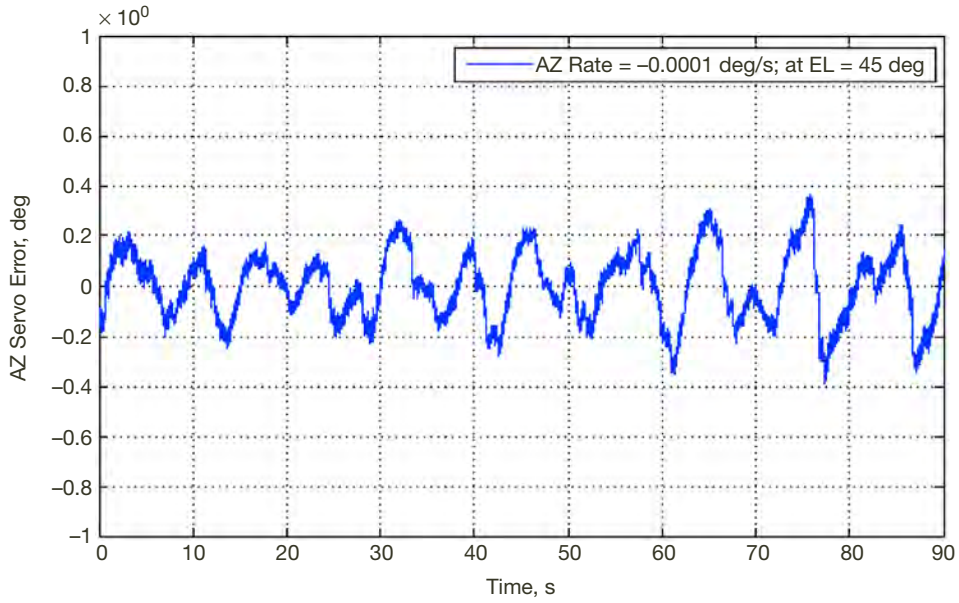

Figure A-12. Azimuth rms mean servo error of 0.1 mdeg when a small negative rate offset of 0.0001 deg/s is applied to the azimuth drives. The mean servo error does meet the requirement of less than 0.001 deg rms.

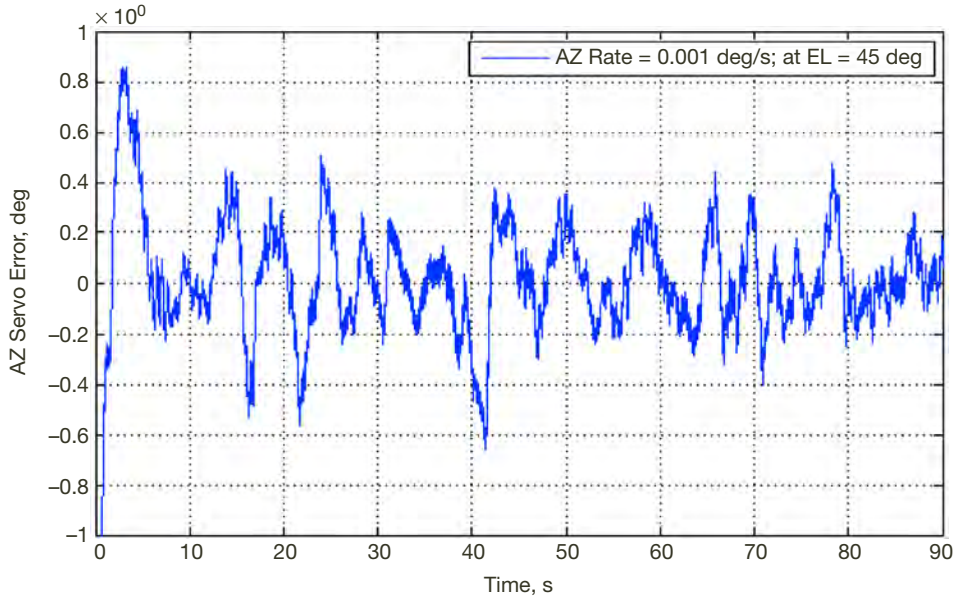

Figure A-13. Azimuth rms mean servo error of 0.2 mdeg when a small positive rate offset of 0.001 deg/s is applied to the azimuth drives. The mean servo error does meet the requirement of less than 0.001 deg rms.

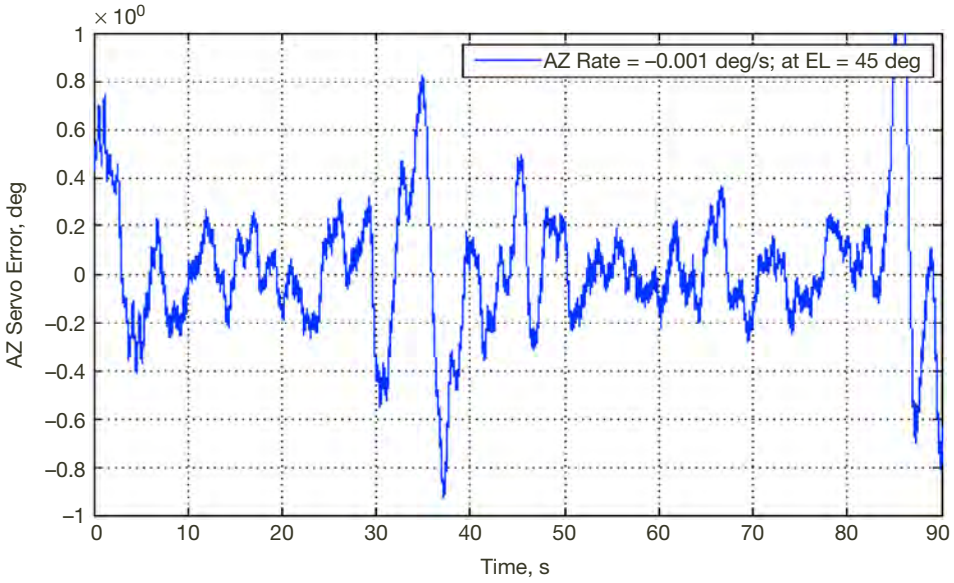

Figure A-14. Azimuth rms mean servo error of 0.3 mdeg when a small negative rate offset of 0.001 deg/s is applied to the azimuth drives. The mean servo error does meet the requirement of less than 0.001 deg rms.

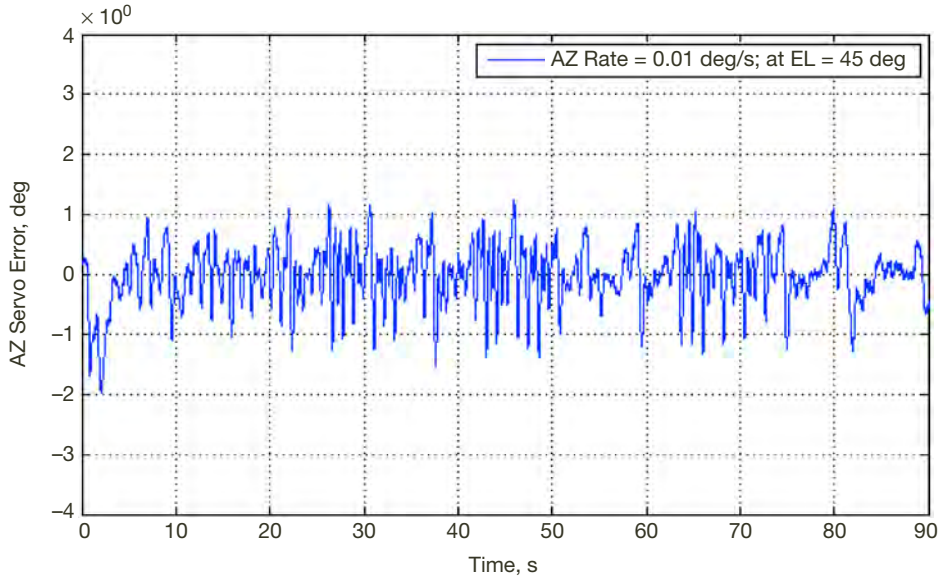

Figure A-15. Azimuth rms mean servo error of 0.5 mdeg when a positive rate offset of 0.01 deg/s is applied to the azimuth drives. The mean servo error does meet the requirement of less than 0.001 deg rms.

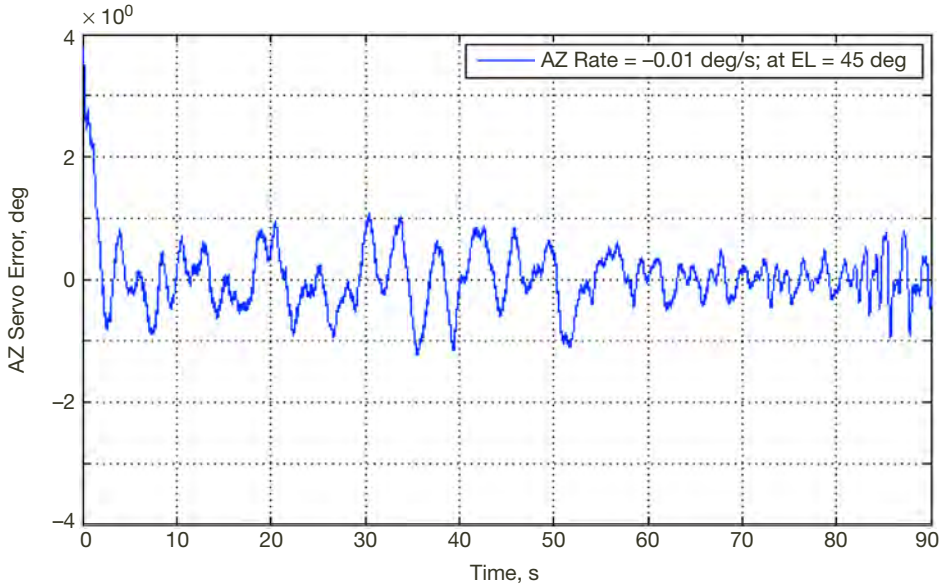

Figure A-16. Azimuth rms mean servo error of 0.5 mdeg when a negative rate offset of 0.01 deg/s is applied to the azimuth drives. The mean servo error does meet the requirement of less than 0.001 deg rms.

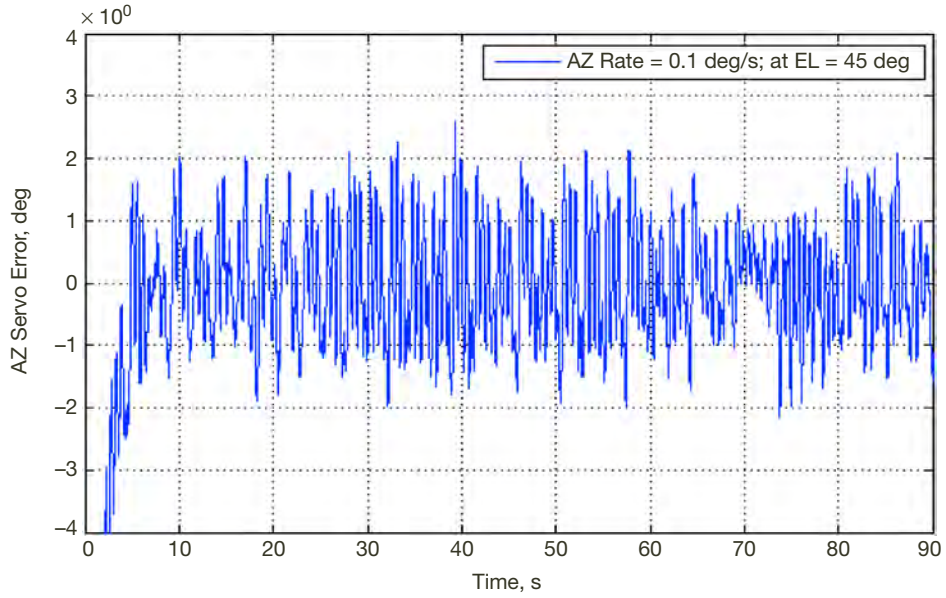

Figure A-17. Azimuth rms mean servo error of 0.96 mdeg when a positive rate offset of 0.1 deg/s is applied to the azimuth drives. The mean servo error does meet the requirement of less than 0.001 deg rms.

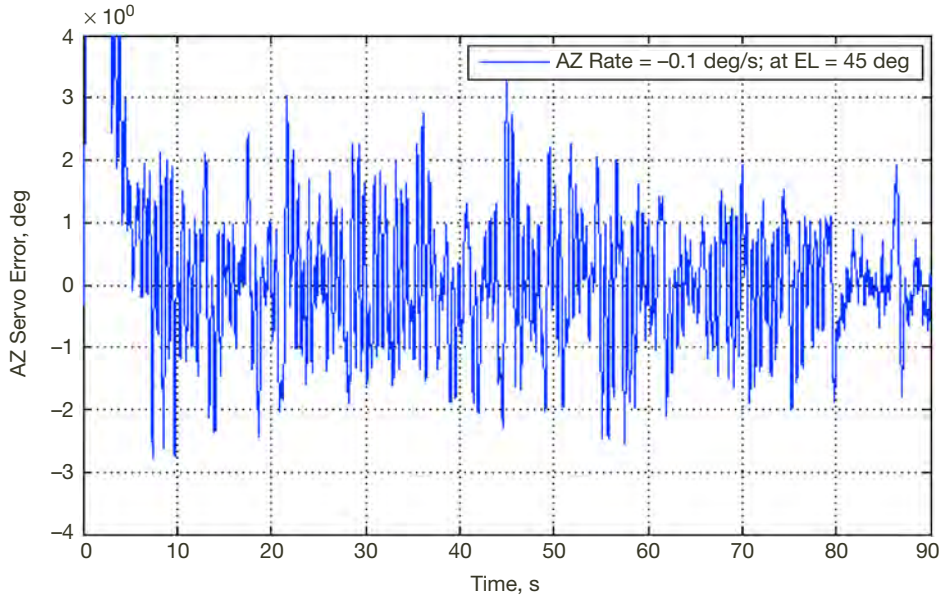

Figure A-18. Azimuth rms mean servo error of 0.96 mdeg when a negative rate offset of 0.1 deg/s is applied to the azimuth drives. The mean servo error does meet the requirement of less than 0.001 deg rms.

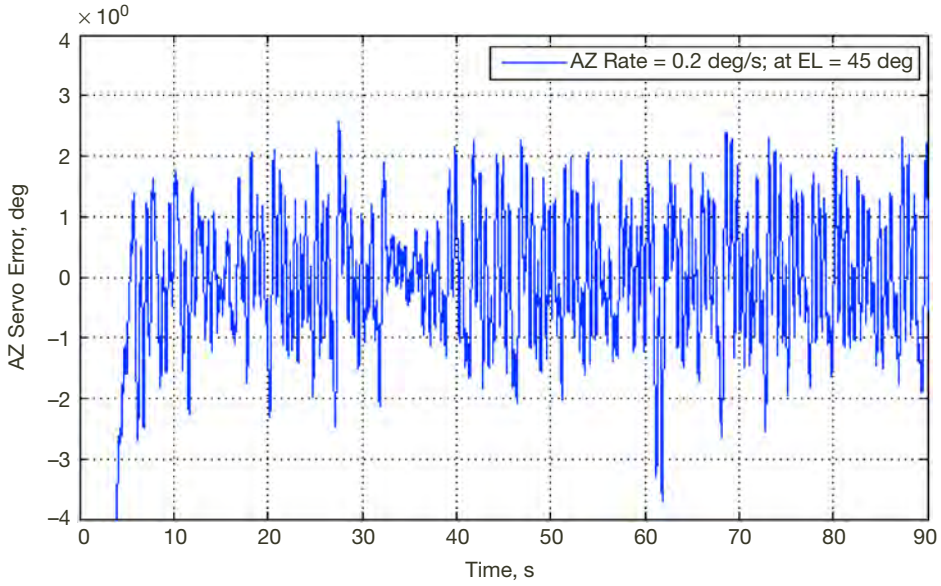

Figure A-19. Azimuth rms mean servo error of 0.9 mdeg when a positive rate offset of 0.2 deg/s is applied to the azimuth drives. The mean servo error does meet the requirement of less than 0.001 deg rms.

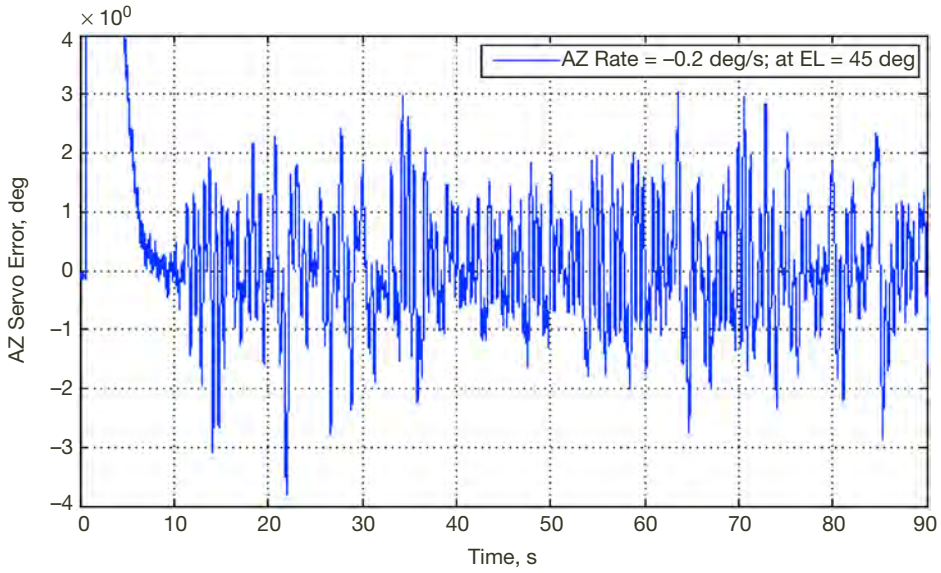

Figure A-20. Azimuth rms mean servo error of 0.9 mdeg when a negative rate offset of 0.2 deg/s is applied to the azimuth drives. The mean servo error does meet the requirement of less than 0.001 deg rms.

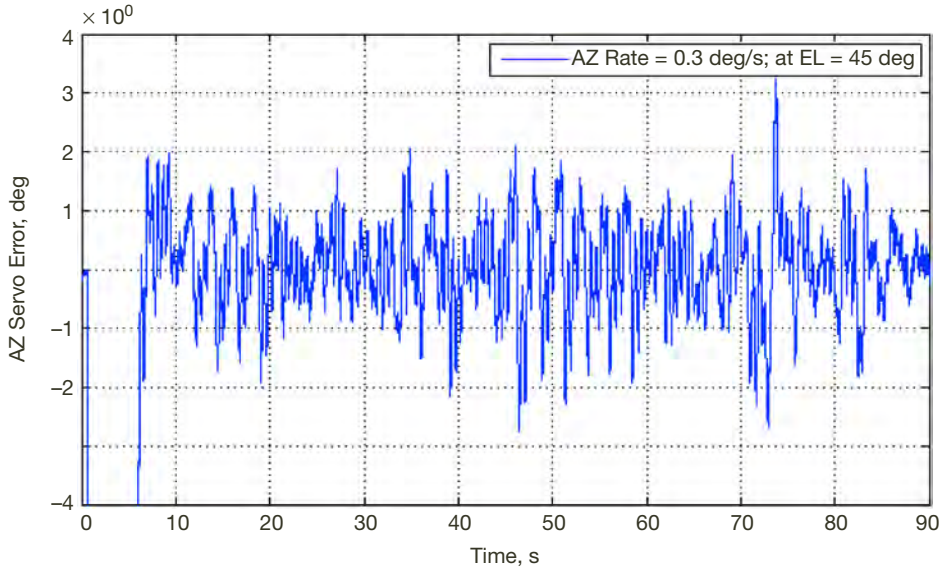

Figure A-21. Azimuth rms mean servo error of 0.8 mdeg when a positive rate offset of 0.3 deg/s is applied to the azimuth drives. The mean servo error does meet the requirement of less than 0.001 deg rms.

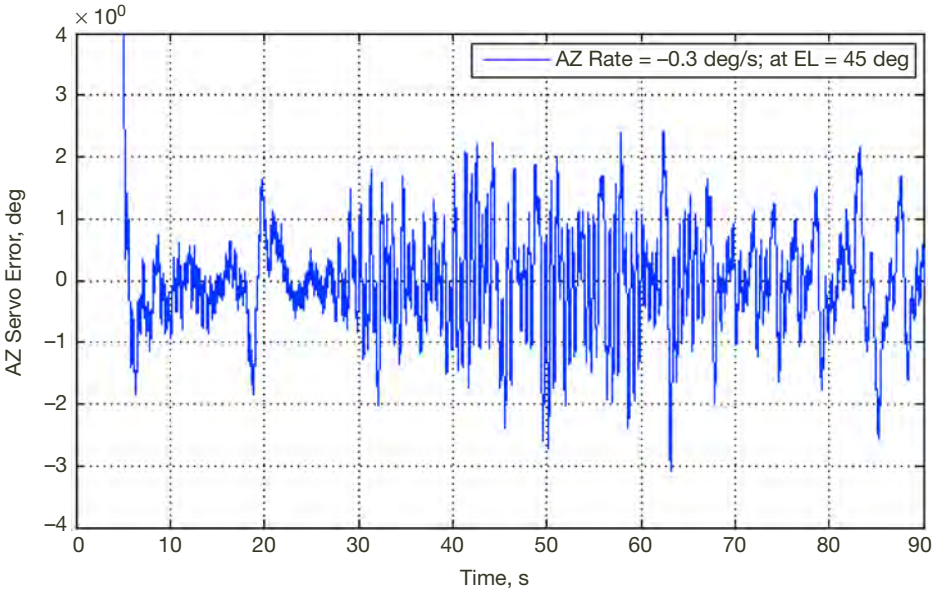

Figure A-22. Azimuth rms mean servo error of 0.9 mdeg when a negative rate offset of 0.3 deg/s is applied to the azimuth drives. The mean servo error does meet the requirement of less than 0.001 deg rms.

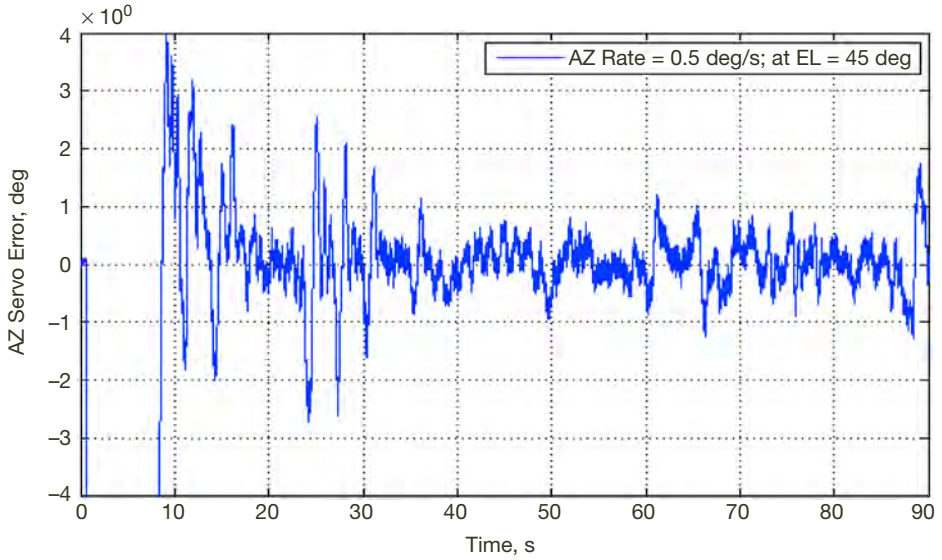

Figure A-23. Azimuth rms mean servo error of 1 mdeg when a positive large rate offset of 0.5 deg/s is applied to the azimuth drives. The mean servo error does meet rthe equirement of less than 0.001 deg rms.

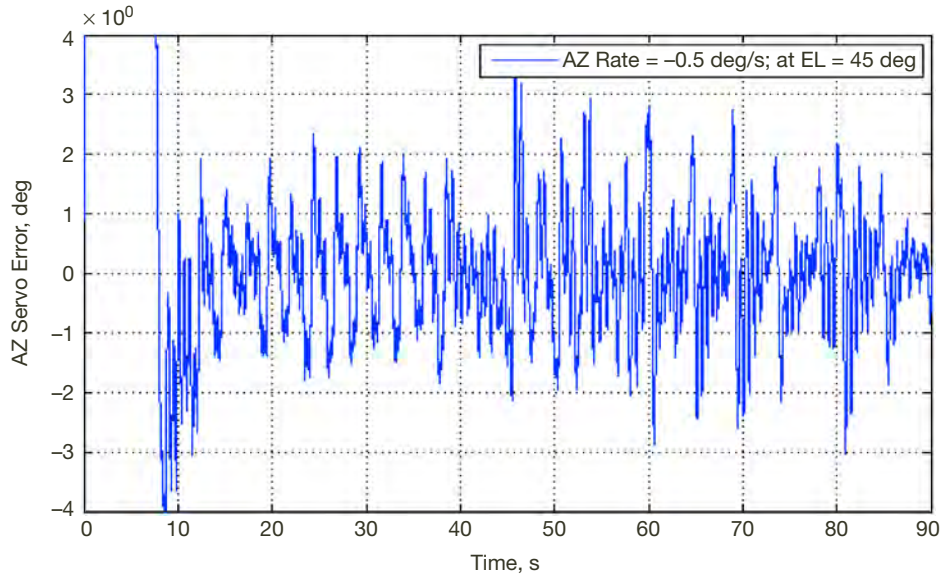

Figure A-24. Azimuth rms mean servo error of 1 mdeg when a negative large rate offset of 0.5 deg/s is applied to the azimuth drives. The mean servo error does meet the requirement of less than 0.001 deg rms.

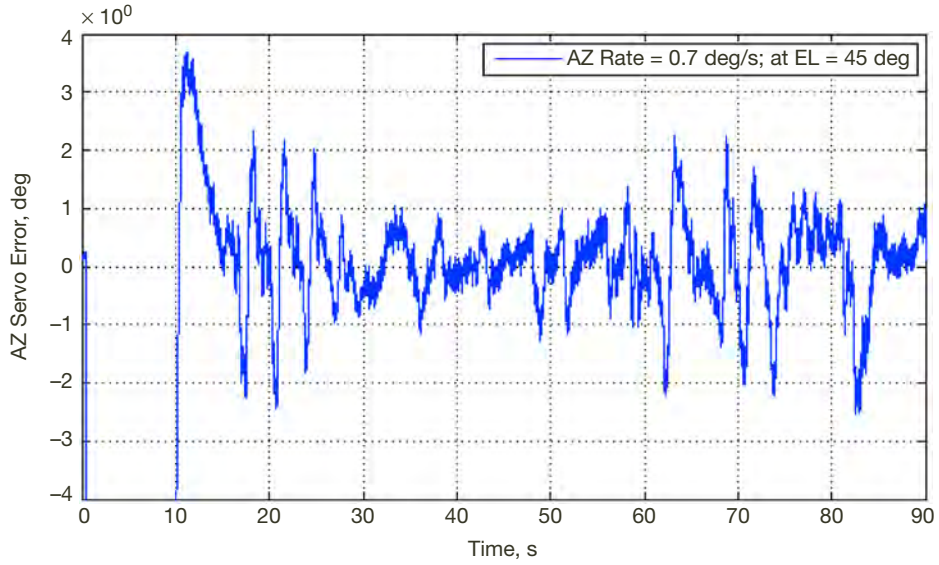

Figure A-25. Azimuth rms mean servo error of 0.6 mdeg when a positive large rate offset of 0.7 deg/s is applied to the azimuth drives. The mean servo error does meet the requirement of less than 0.001 deg rms.

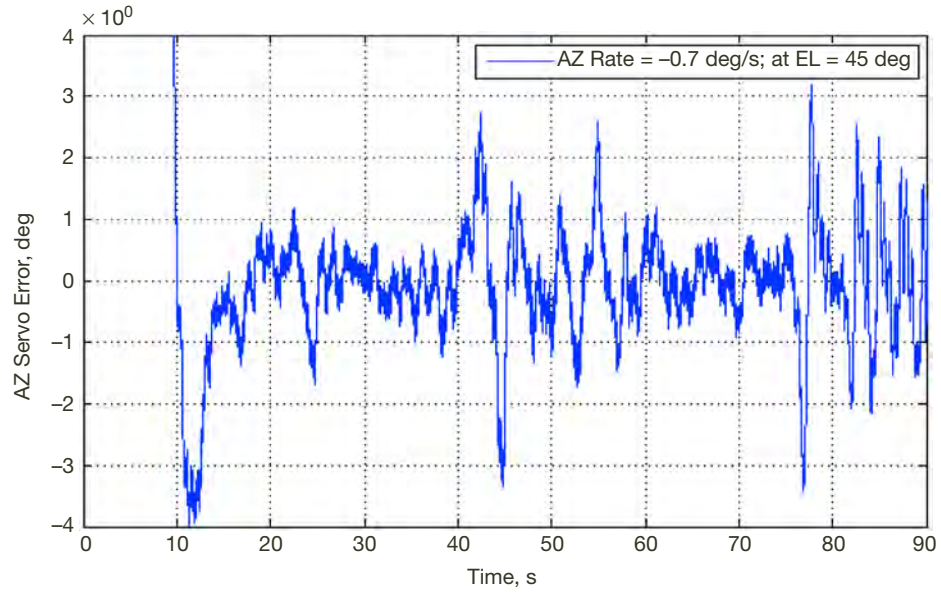

Figure A-26. Azimuth rms mean servo error of 0.96 mdeg when a negative large rate offset of 0.7 deg/s is applied to the azimuth drives. The mean servo error does meet the requirement of less than 0.001 deg rms.

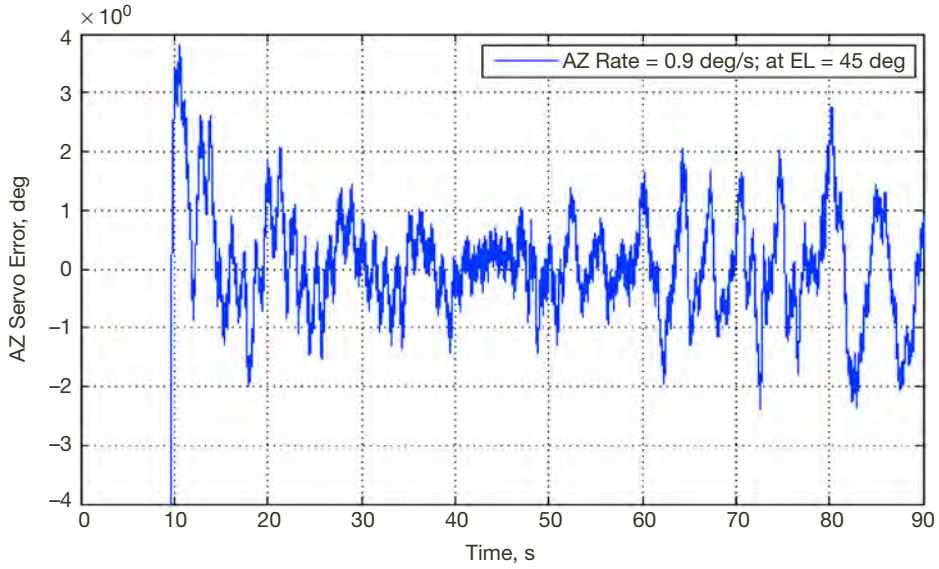

Figure A-27. Azimuth rms mean servo error of 0.6 mdeg when a positive large rate offset of 0.9 deg/s is applied to the azimuth drives. The mean servo error does meet the requirement of less than 0.001 deg rms.

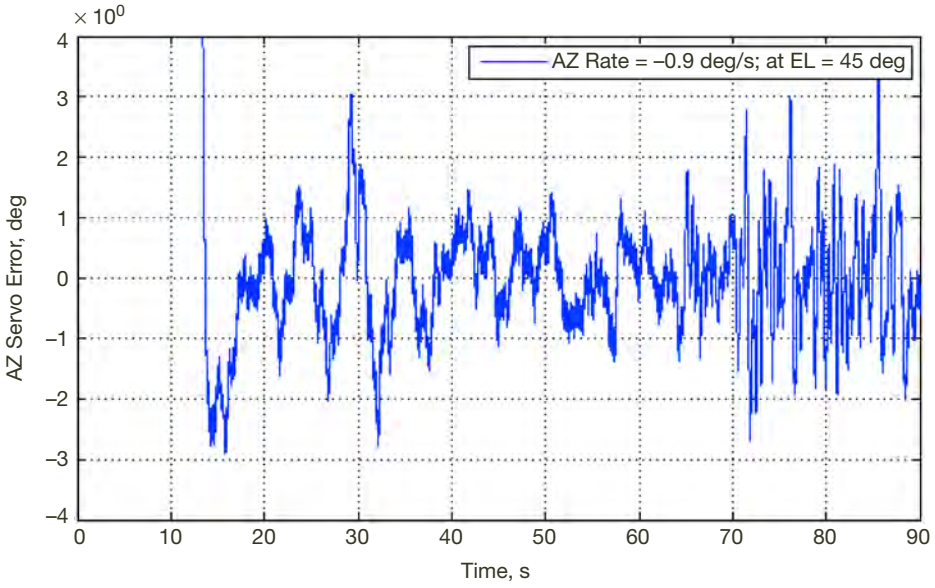

Figure A-28. Azimuth rms mean servo error of 0.96 mdeg when a negative large rate offset of 0.9 deg/s is applied to the azimuth drives. The mean servo error does meet the requirement of less than 0.001 deg rms.

Appendix B

Azimuth LQG Closed-Loop Performance at 10 Degrees Elevation

The measurements in Appendix B were all taken at DSS-28 on March 2, 2012.

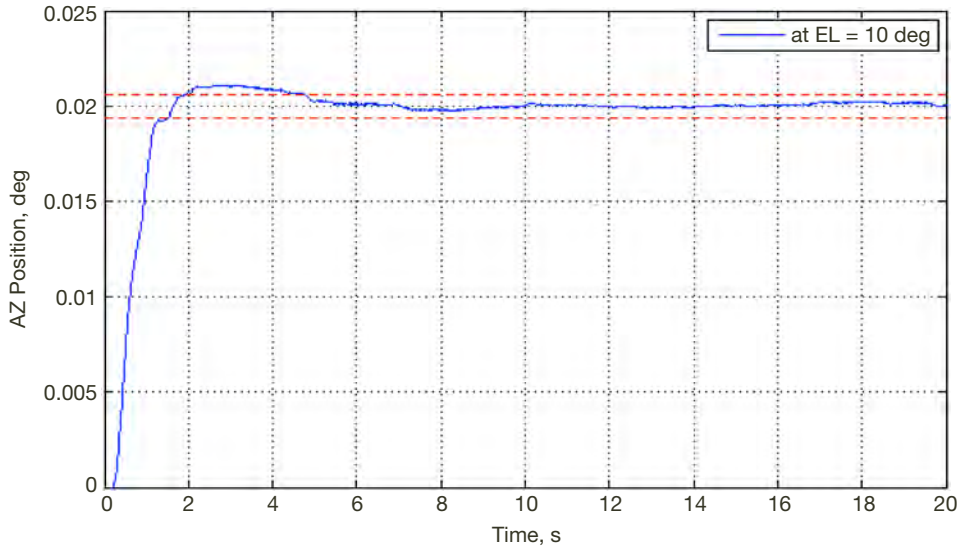

Figure B-1. Overshoot of 5 percent and settling time of 4.8 s, which satisfies the requirements when a positive small position offset of 0.02 deg is applied to the azimuth drives.

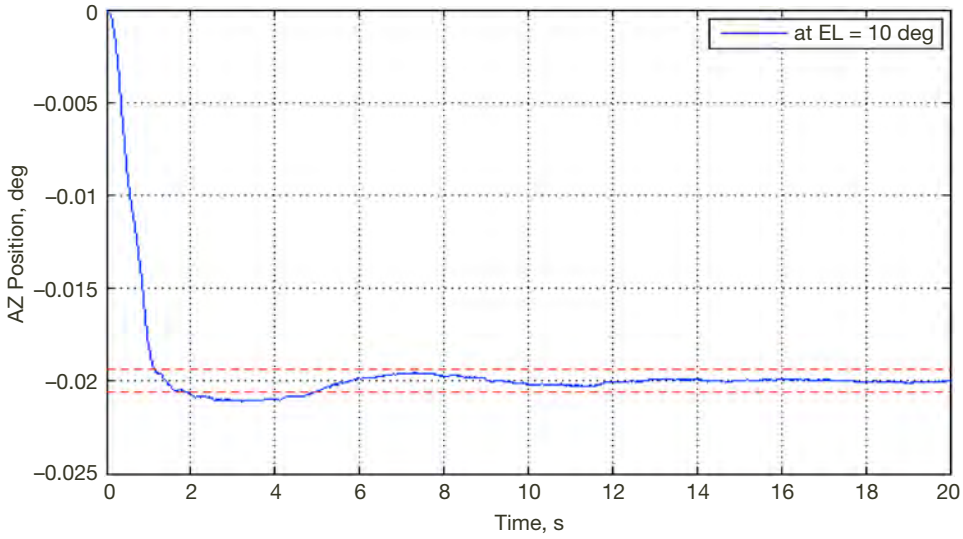

Figure B-2. Overshoot of 5 percent and settling time of 4.9 s, which satisfies the requirements when a negative small position offset of 0.02 deg is applied to the azimuth drives.

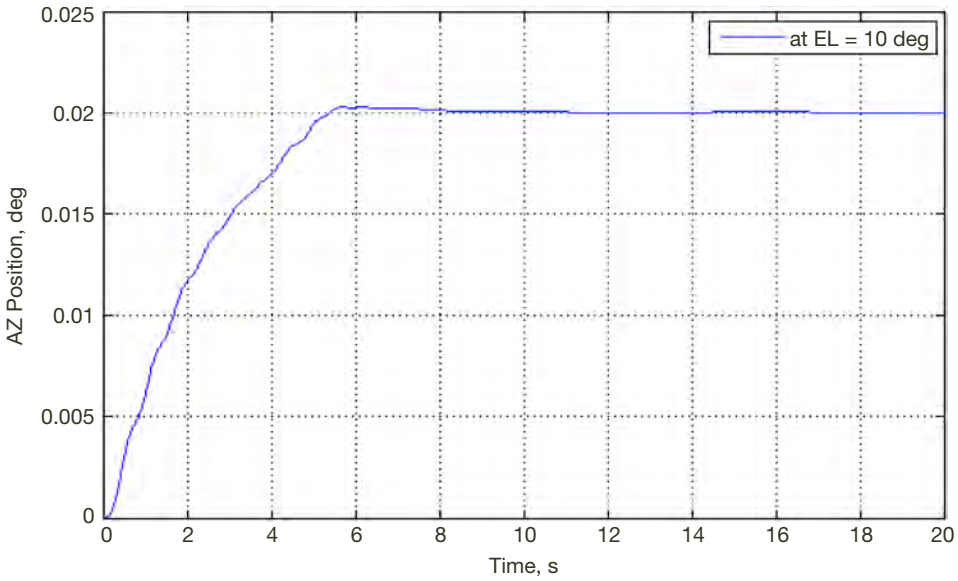

Figure B-3. Overshoot of 2 mdeg, which satisfies the requirements when a positive large position offset of 0.2 deg is applied to the azimuth drives.

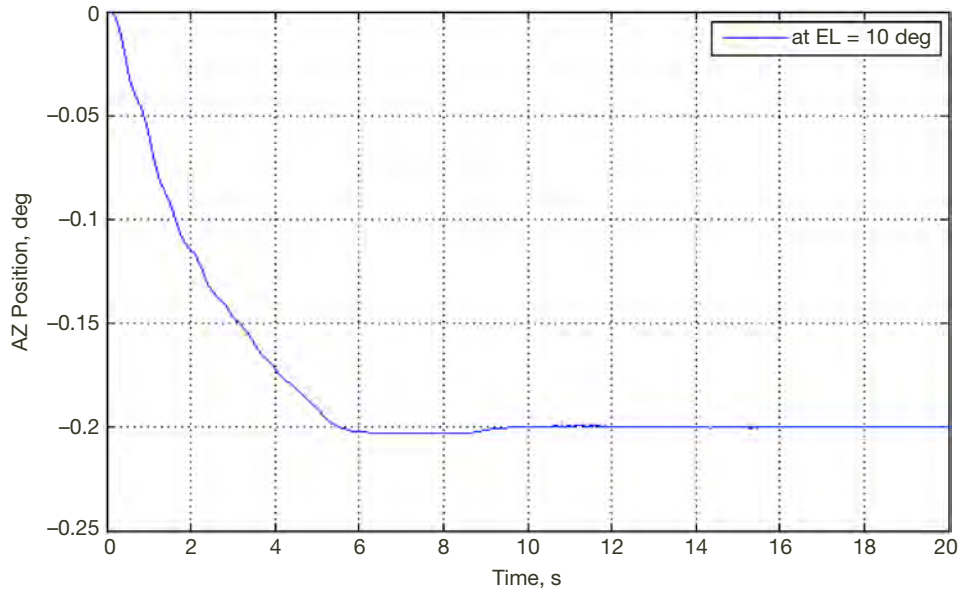

Figure B-4. Overshoot of 3 mdeg, which satisfies the requirements when a negative large position offset of 0.2 deg is applied to the azimuth drives.

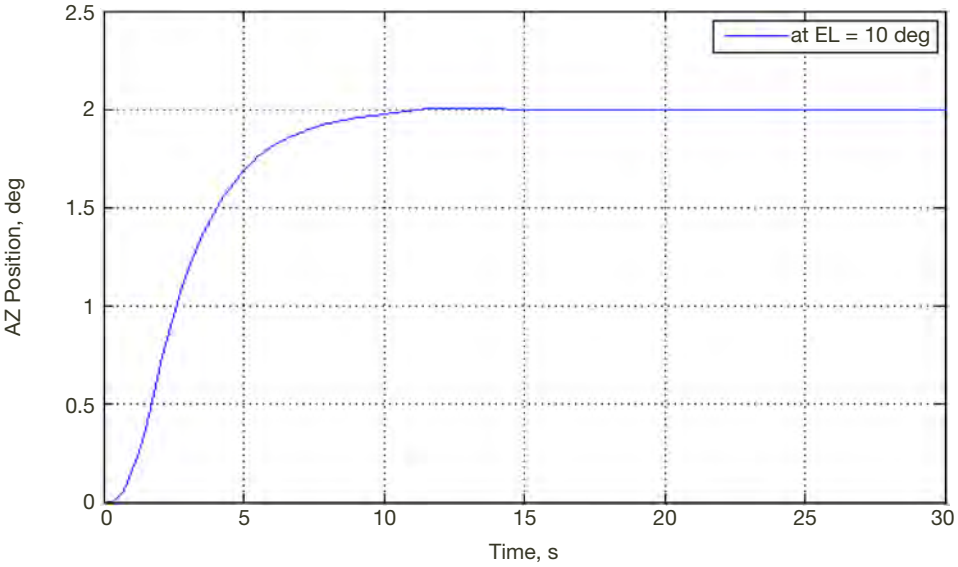

Figure B-5. Overshoot of 4 mdeg, which satisfies the requirements when a positive large position offset of 2 deg is applied to the azimuth drives.

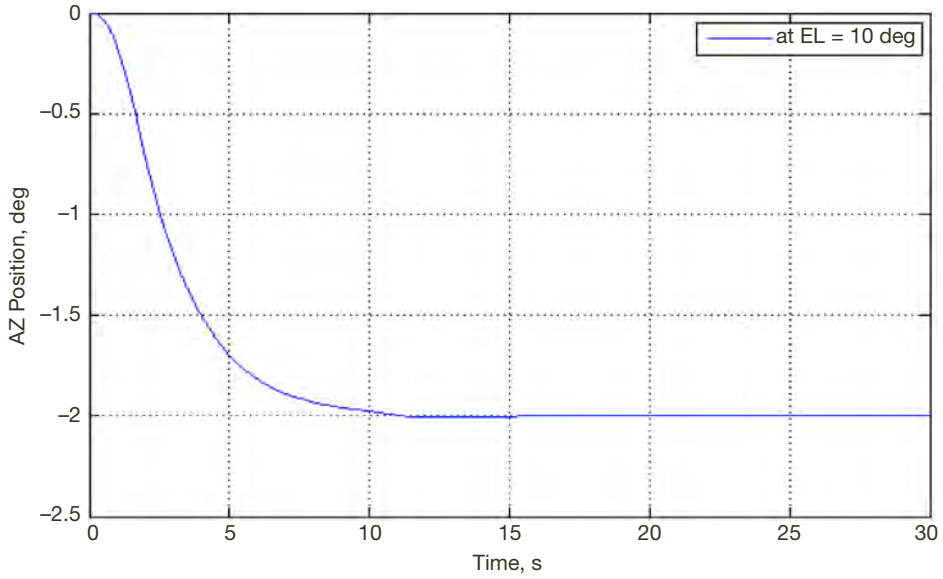

Figure B-6. Overshoot of 4 mdeg, which satisfies the requirements when a negative large position offset of 2 deg is applied to the azimuth drives.

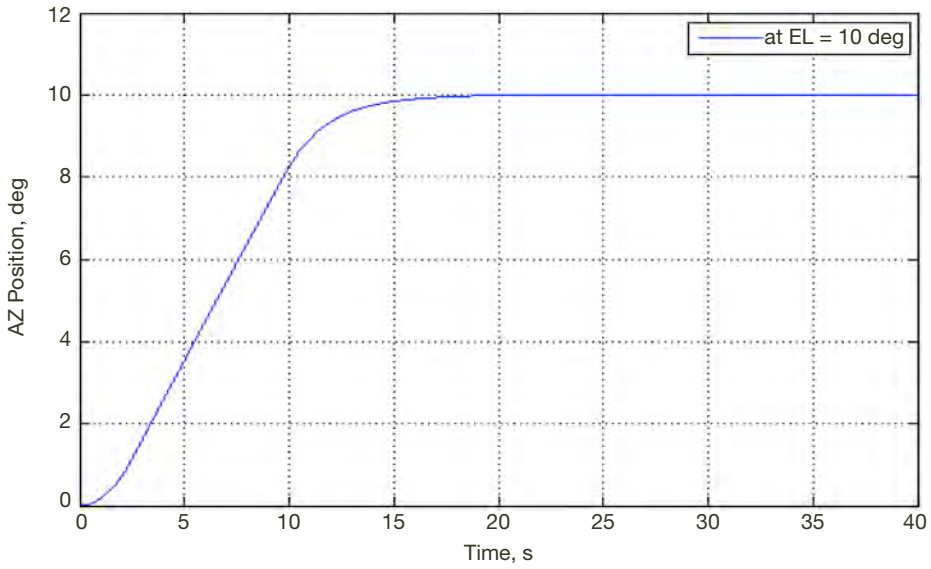

Figure B-7. Overshoot of 4 mdeg, which satisfies the requirements when a positive large position offset of 10 deg is applied to the azimuth drives.

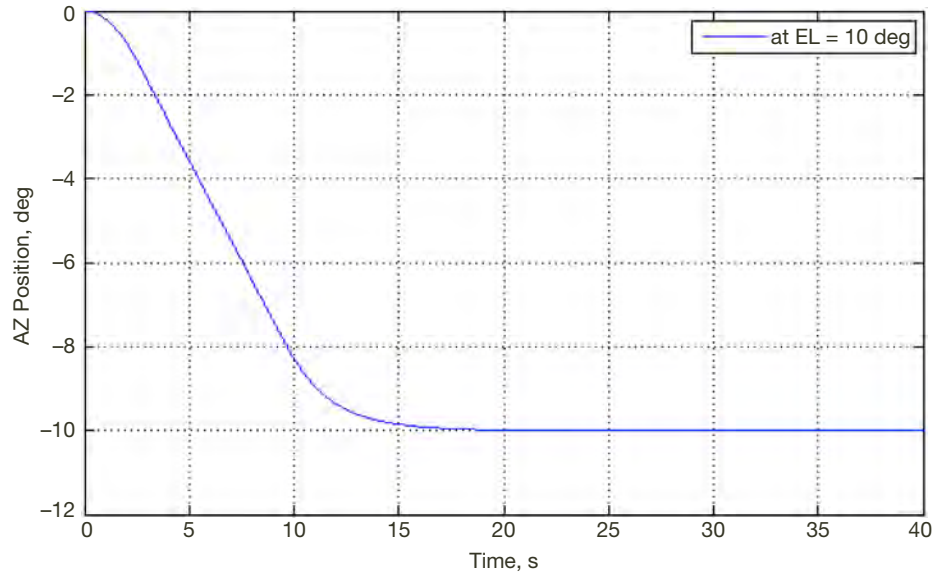

Figure B-8. Overshoot of 3 mdeg, which satisfies the requirements when a negative large position offset of 10 deg is applied to the azimuth drives.

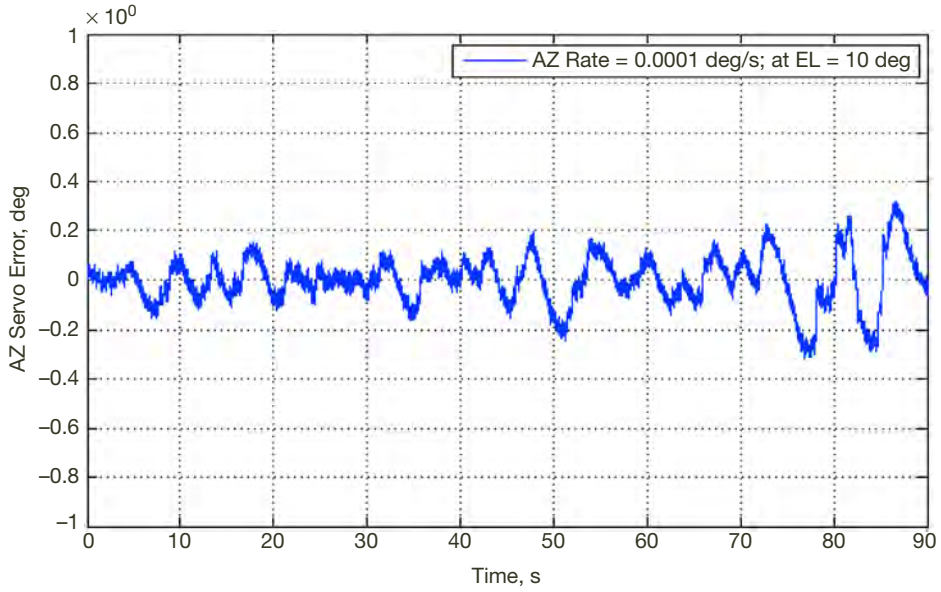

Figure B-9. Azimuth rms mean servo error of 0.1 mdeg when a small positive rate offset of 0.0001 deg/s is applied to the azimuth drives. The mean servo error does meet the requirement of less than 0.001 deg rms.

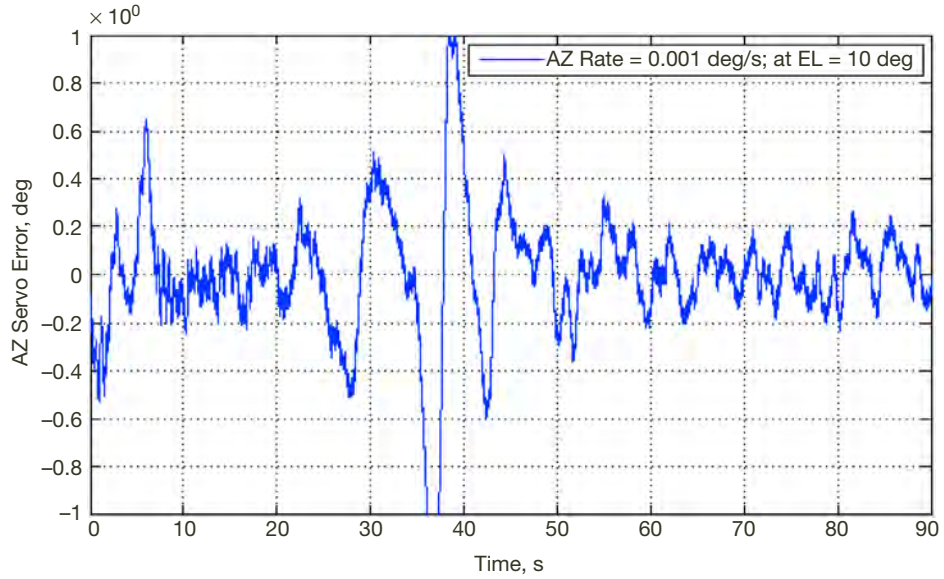

Figure B-10. Azimuth rms mean servo error of 0.3 mdeg when a small positive rate offset of 0.001 deg/s is applied to the azimuth drives. The mean servo error does meet the requirement of less than 0.001 deg rms.

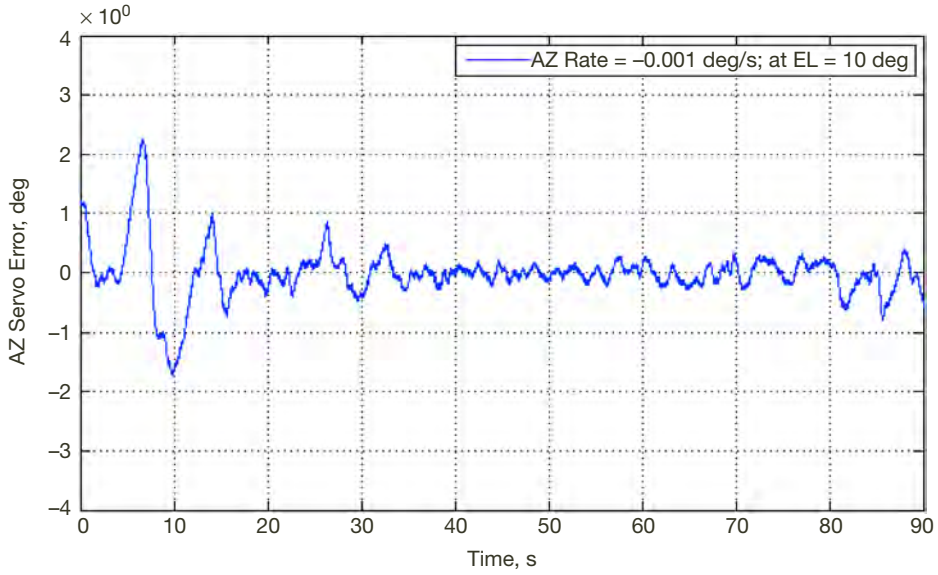

Figure B-11. Azimuth rms mean servo error of 0.2 mdeg when a small negative rate offset of 0.001 deg/s is applied to the azimuth drives. The mean servo error does meet the requirement of less than 0.001 deg rms.

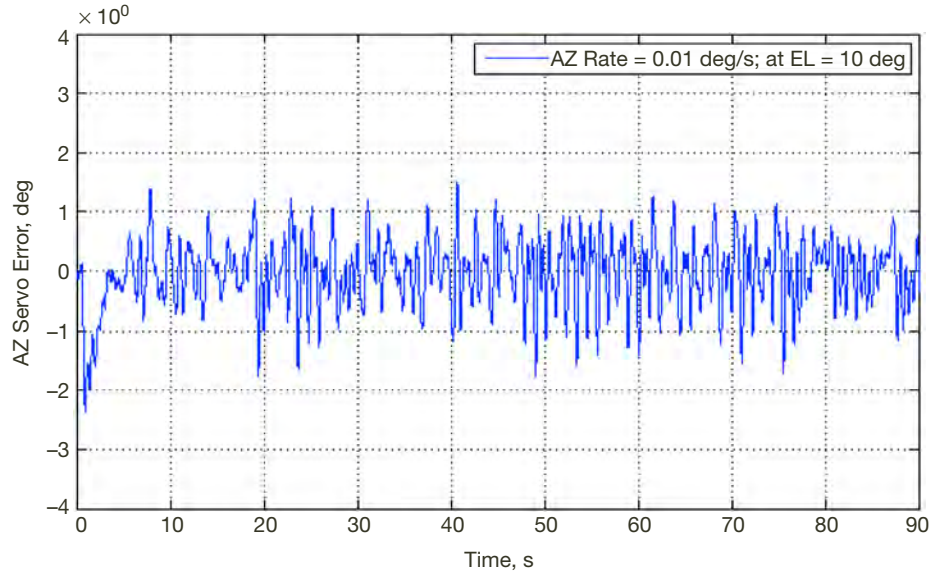

Figure B-12. Azimuth rms mean servo error of 0.5 mdeg when a positive rate offset of 0.01 deg/s is applied to the azimuth drives. The mean servo error does meet the requirement of less than 0.001 deg rms.

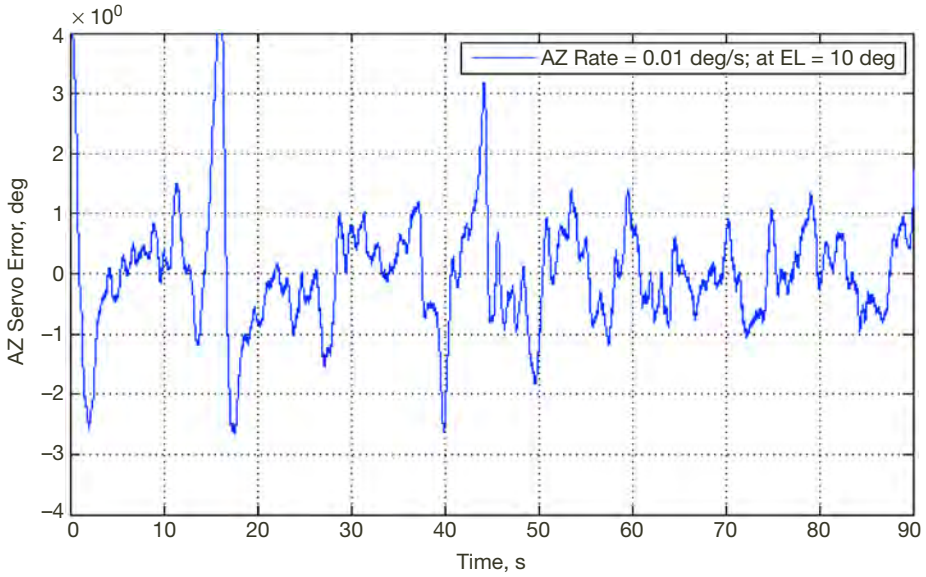

Figure B-13. Azimuth rms mean servo error of 0.7 mdeg when a negative rate offset of 0.01 deg/s is applied to the azimuth drives. The mean servo error does meet the requirement of less than 0.001 deg rms.

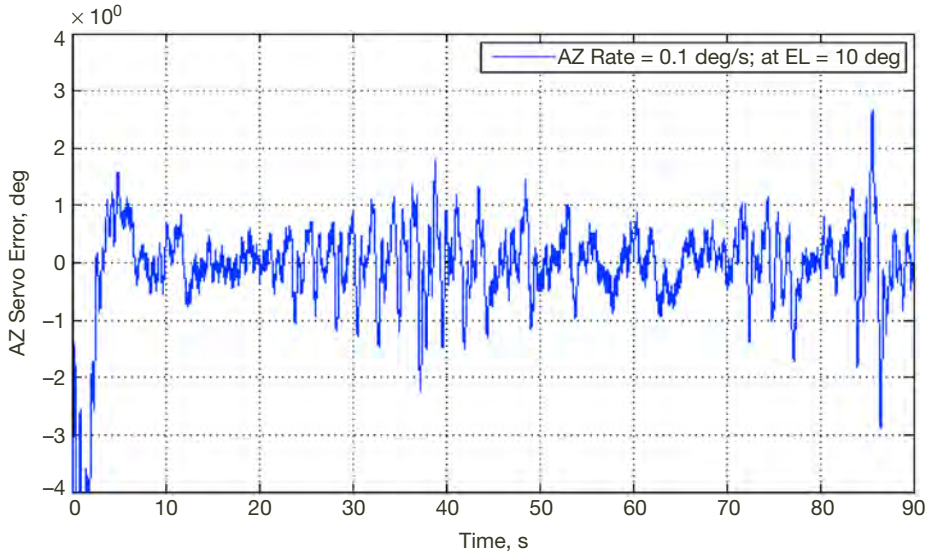

Figure B-14. Azimuth rms mean servo error of 0.6 mdeg when a positive rate offset of 0.1 deg/s is applied to the azimuth drives. The mean servo error does meet the requirement of less than 0.001 deg rms.

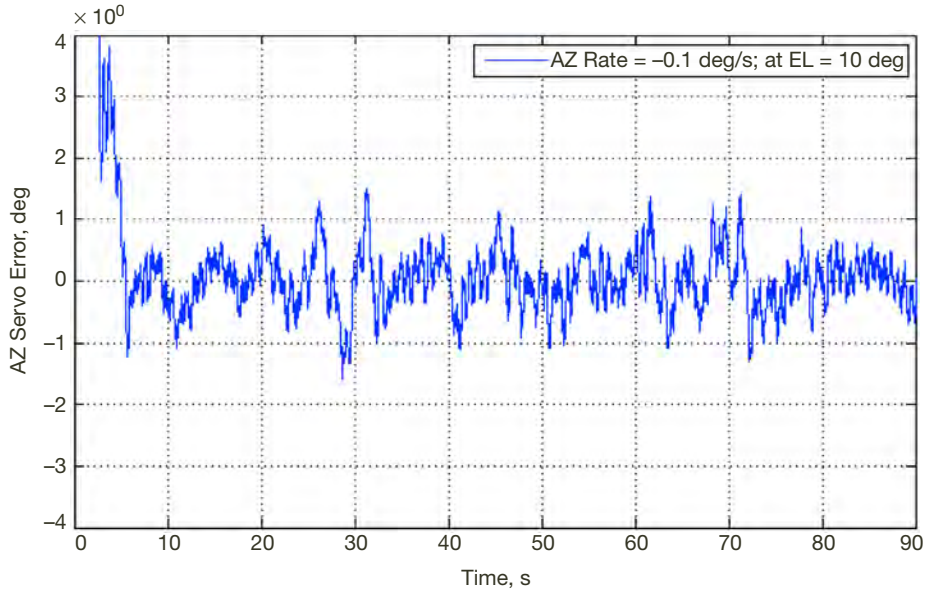

Figure B-15. Azimuth rms mean servo error of 0.5 mdeg when a negative rate offset of 0.1 deg/s is applied to the azimuth drives. The mean servo error does meet the requirement of less than 0.001 deg rms.

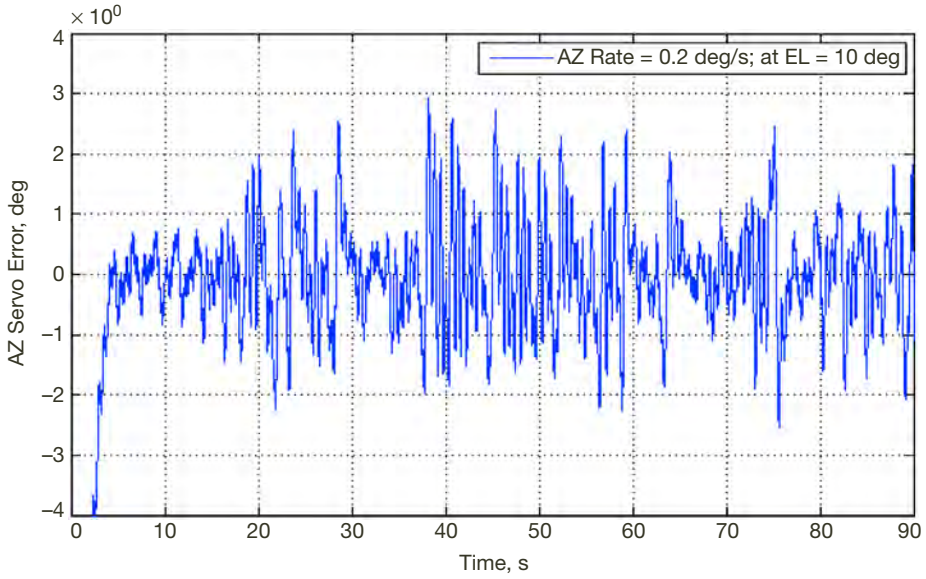

Figure B-16. Azimuth rms mean servo error of 0.9 mdeg when a large positive rate offset of 0.2 deg/s is applied to the azimuth drives. The mean servo error does meet the requirement of less than 0.001 deg rms.

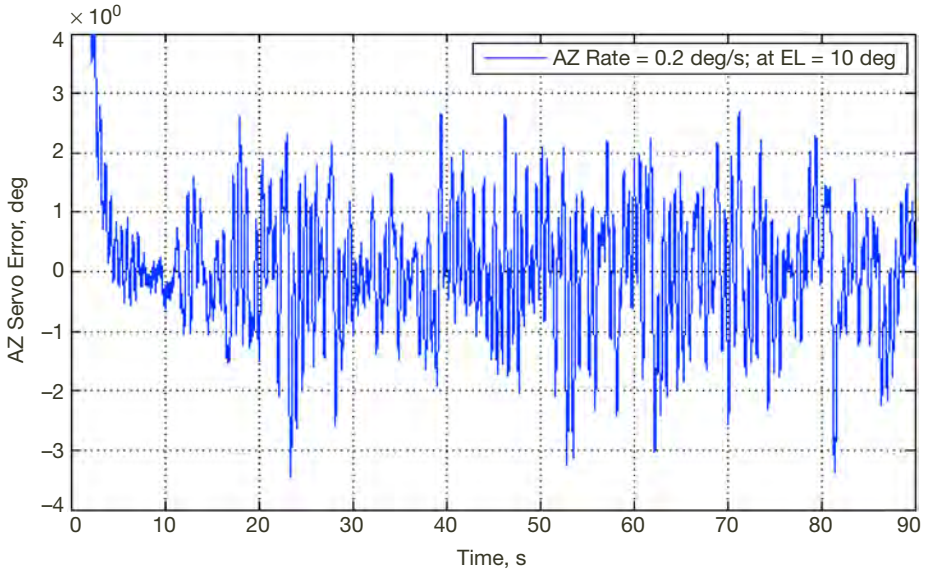

Figure B-17. Azimuth rms mean servo error of 1.1 mdeg when a positive rate offset of 0.2 deg/s is applied to the azimuth drives. The mean servo error does not meet the requirement of less than 0.001 deg rms.

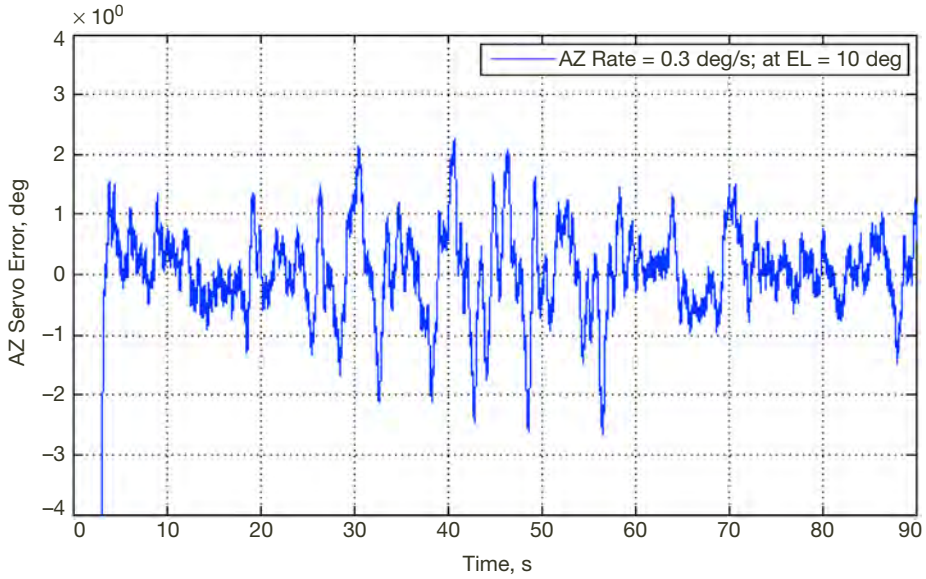

Figure B-18. Azimuth rms mean servo error of 0.7 mdeg when a large positive rate offset of 0.3 deg/s is applied to the azimuth drives. The mean servo error does meet the requirement of less than 0.001 deg rms.

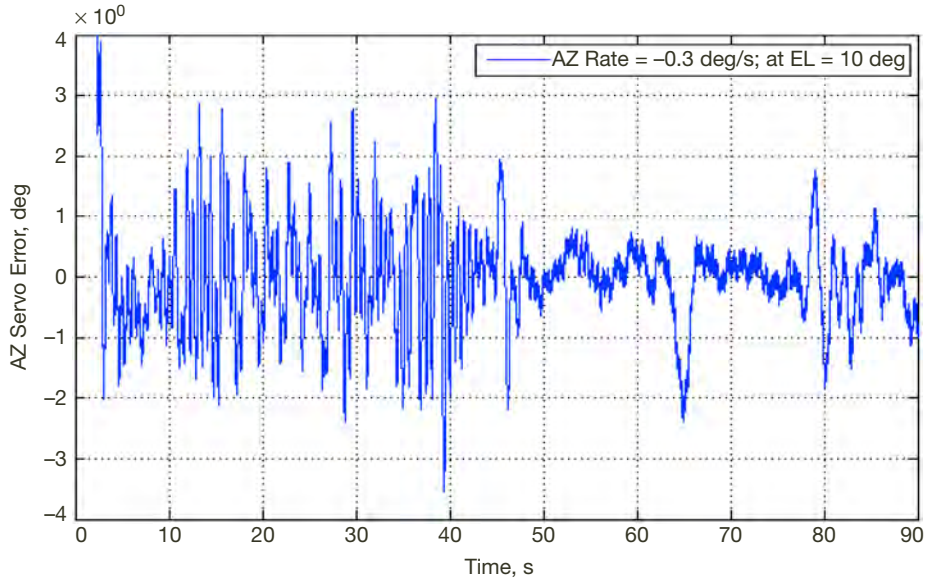

Figure B-19. Azimuth rms mean servo error of 0.8 mdeg when a negative large rate offset of 0.3 deg/s is applied to the azimuth drives. The mean servo error does meet the requirement of less than 0.001 deg rms.

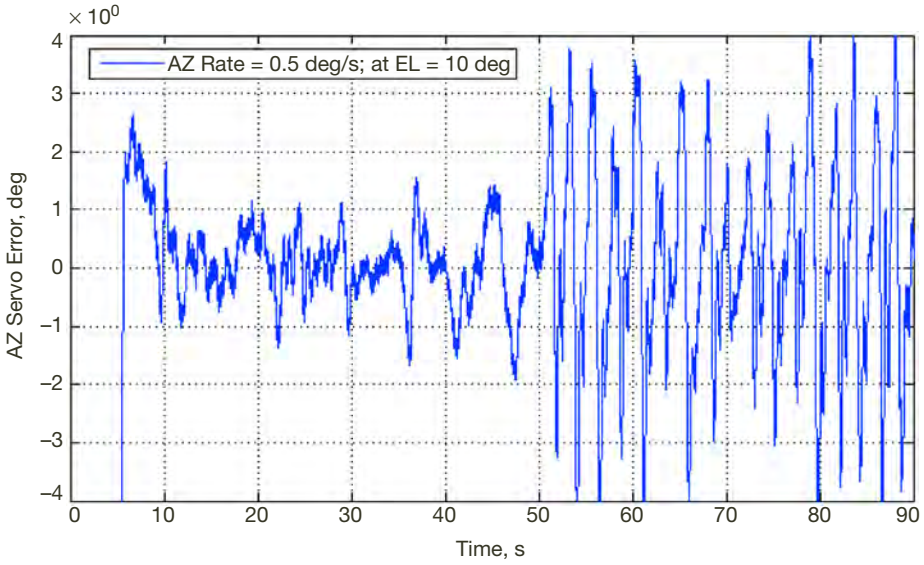

Figure B-20. Azimuth rms mean servo error of 1.5 mdeg when a large positive rate offset of 0.5 deg/s is applied to the azimuth drives. The mean servo error does not meet the requirement of less than 0.001 deg rms.

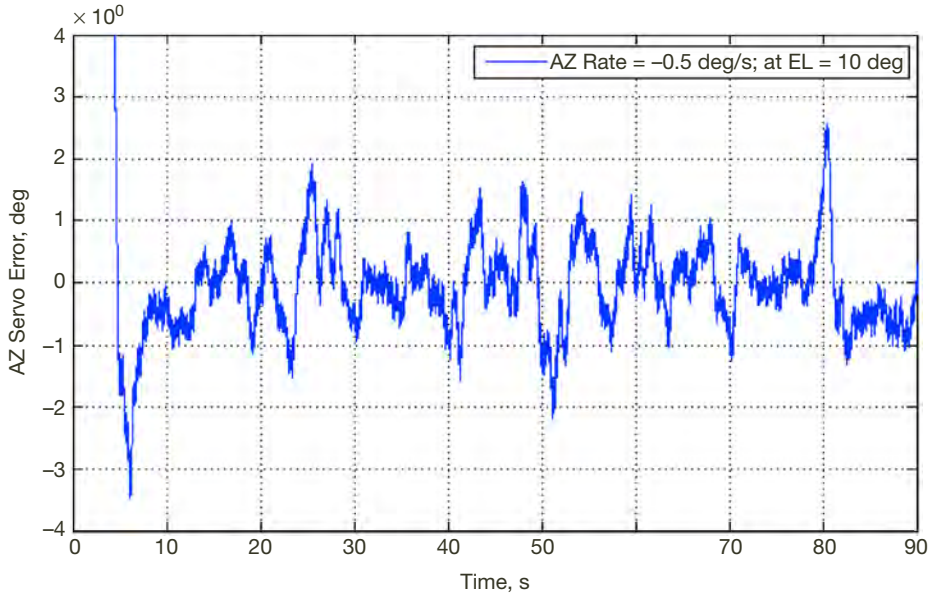

Figure B-21. Azimuth rms mean servo error of 0.6 mdeg when a negative large rate offset of 0.5 deg/s is applied to the azimuth drives. The mean servo error does meet the requirement of less than 0.001 deg rms.

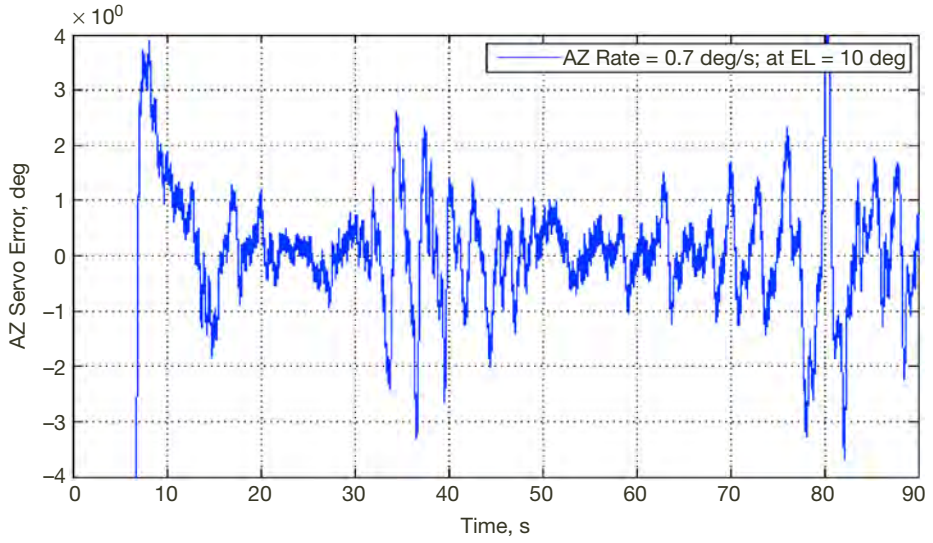

Figure B-22. Azimuth rms mean servo error of 0.9 mdeg when a large positive rate offset of 0.7 deg/s is applied to the azimuth drives. The mean servo error does meet the requirement of less than 0.001 deg rms.

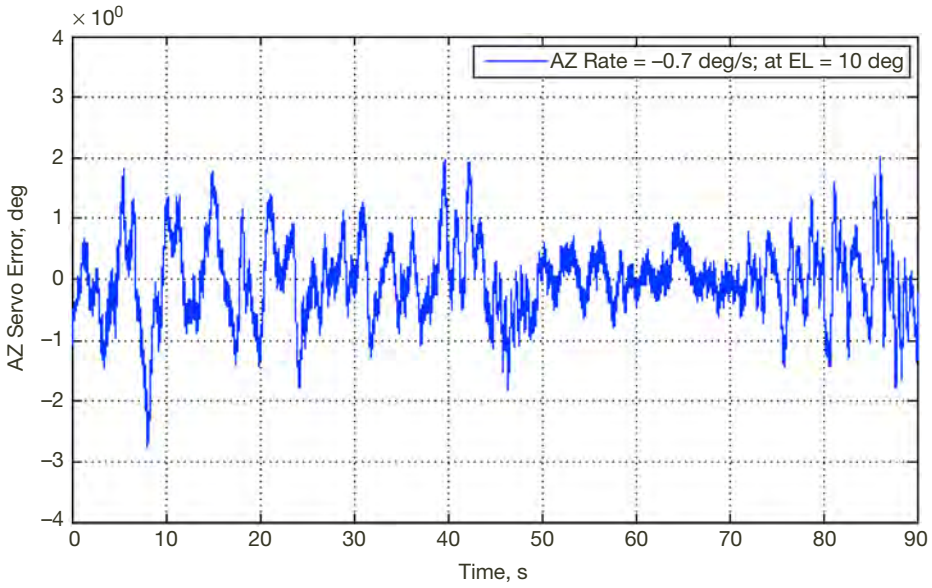

Figure B-23. Azimuth rms mean servo error of 0.6 mdeg when a positive large rate offset of 0.7 deg/s is applied to the azimuth drives. The mean servo error does meet the requirement of less than 0.001 deg rms.

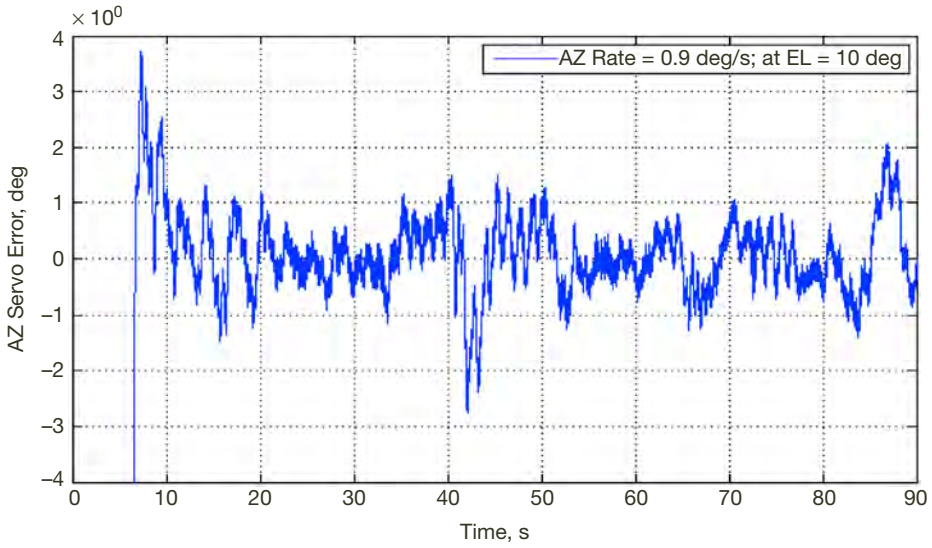

Figure B-24. Azimuth rms mean servo error of 0.6 mdeg when a negative large rate offset of 0.9 deg/s is applied to the azimuth drives. The mean servo error does meet the requirement of less than 0.001 deg rms.

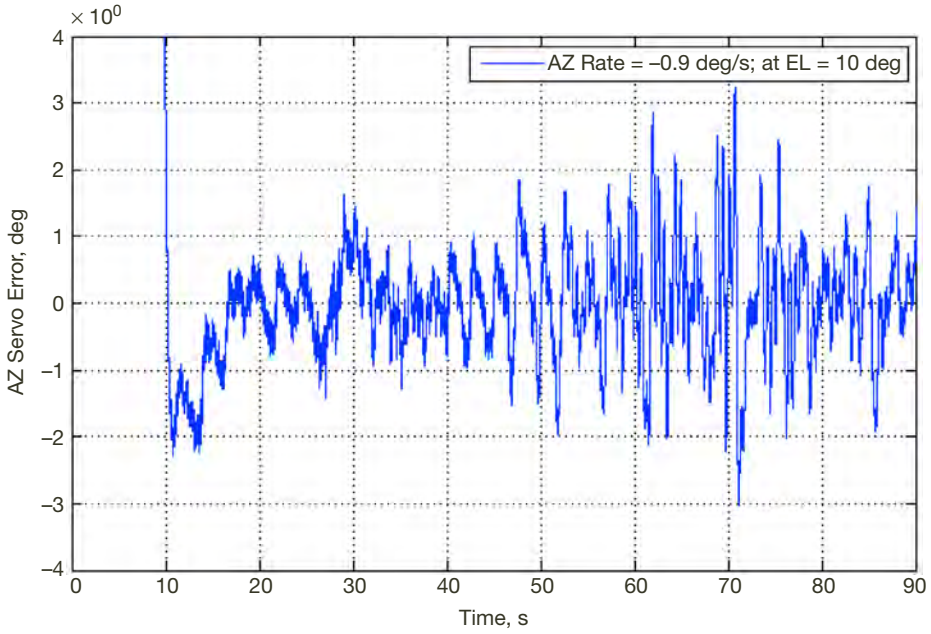

Figure B-25. Azimuth rms mean servo error of 0.8 mdeg when a negative large rate offset of 0.9 deg/s is applied to the azimuth drives. The mean servo error does meet the requirement of less than 0.001 deg rms.

Appendix C

Azimuth LQG Closed-Loop Performance at 80 Degrees Elevation

The measurements in Appendix C were all taken at DSS-28 on March 2, 2012.

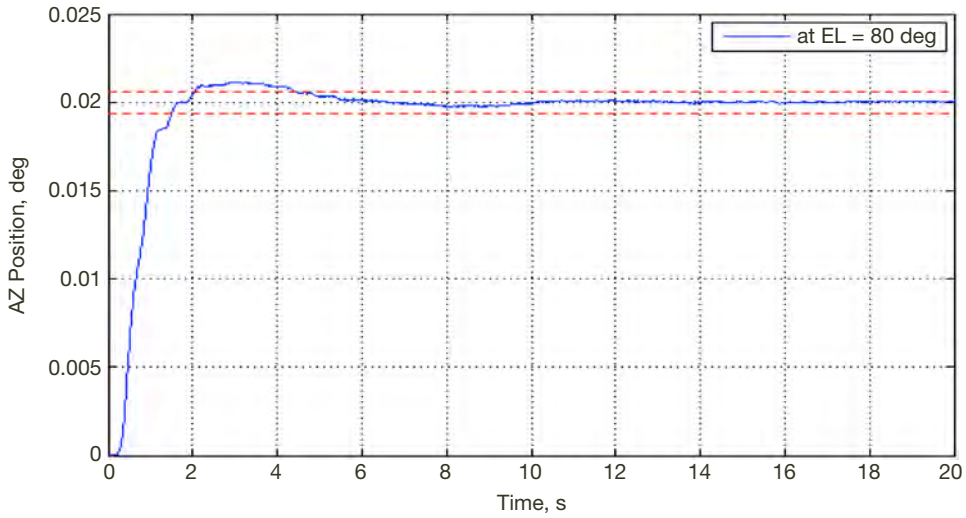

Figure C-1. Overshoot of 6 percent and settling time of 4.4 s, which satisfies the requirements when a positive small position offset of 0.02 deg is applied to the azimuth drives.

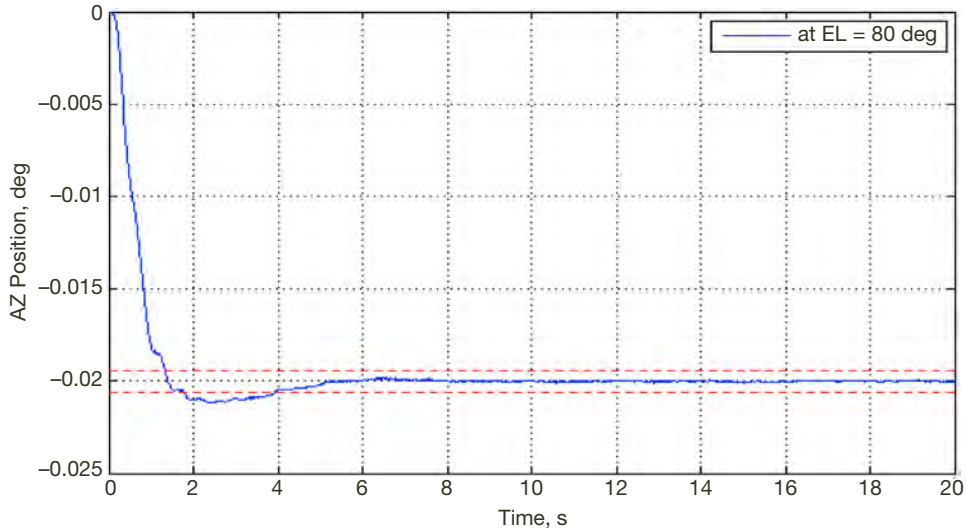

Figure C-2. Overshoot of 6 percent and settling time of 3.9 s, which satisfies the requirements when a negative small position offset of 0.02 deg is applied to the azimuth drives.

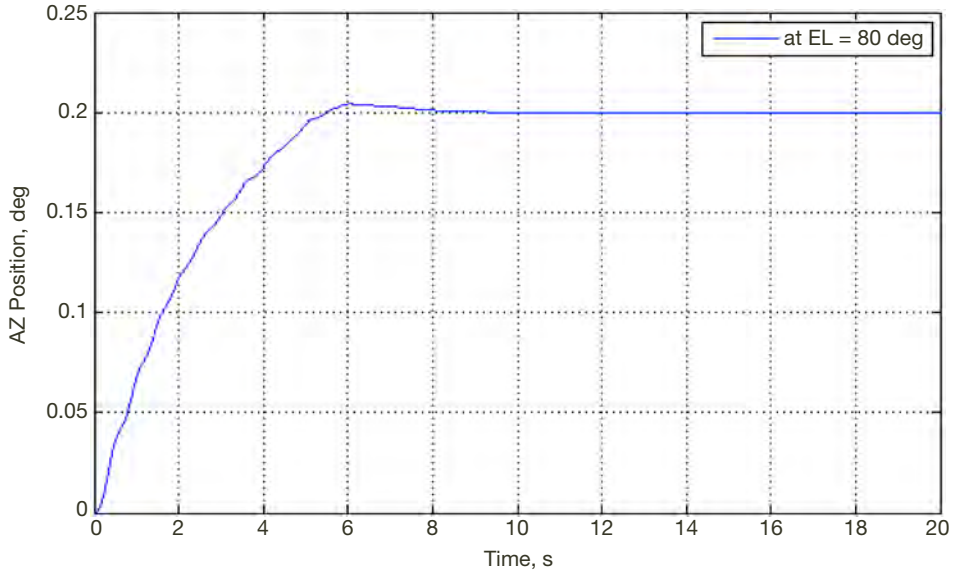

Figure C-3. Overshoot of 4 mdeg, which satisfies the requirements when a positive large position offset of 0.2 deg is applied to the azimuth drives.

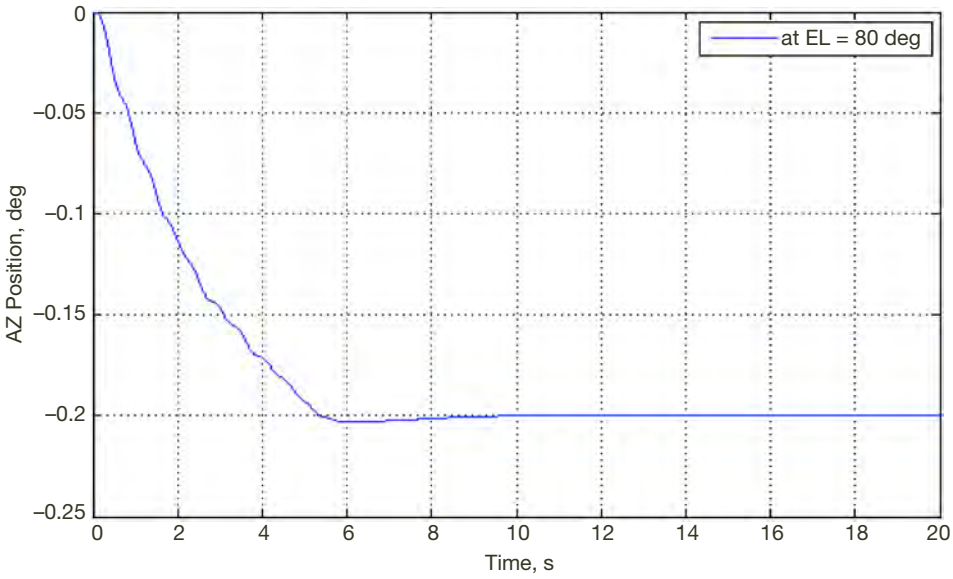

Figure C-4. Overshoot of 3 mdeg, which satisfies the requirements when a negative large position offset of 0.2 deg is applied to the azimuth drives.

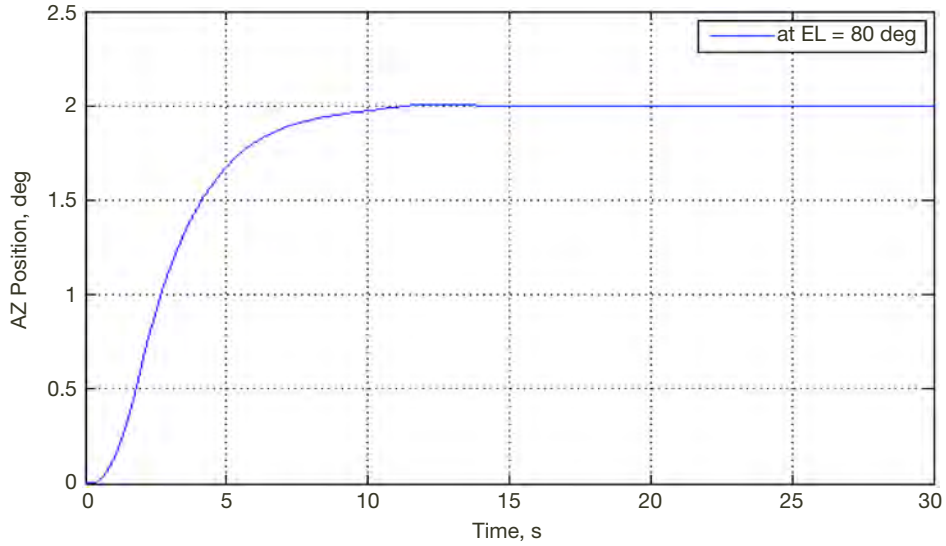

Figure C-5. Overshoot of 5 mdeg, which satisfies the requirements when a positive large position offset of 2 deg is applied to the azimuth drives.

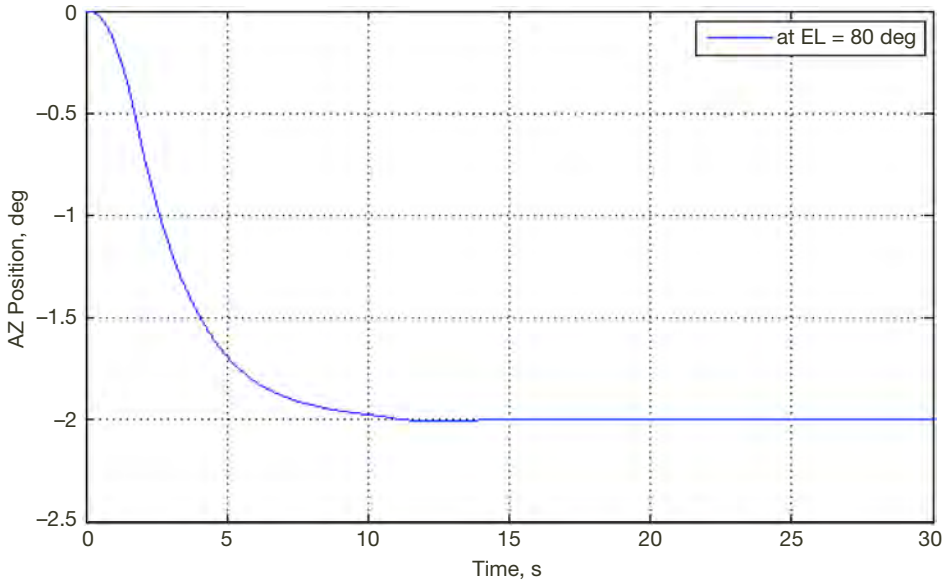

Figure C-6. Overshoot of 4 mdeg, which satisfies the requirements when a negative large position offset of 2 deg is applied to the azimuth drives.

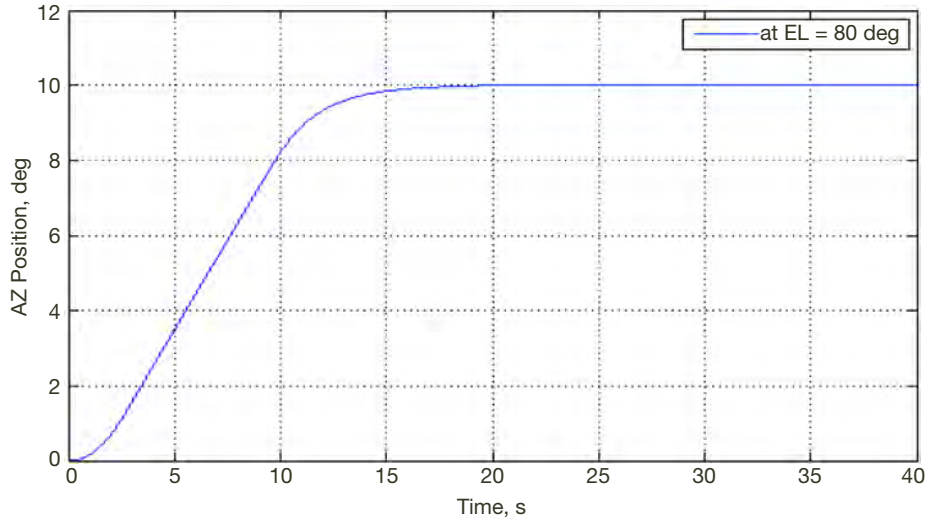

Figure C-7. Overshoot of 4 mdeg, which satisfies the requirements when a positive large position offset of 10 deg is applied to the azimuth drives.

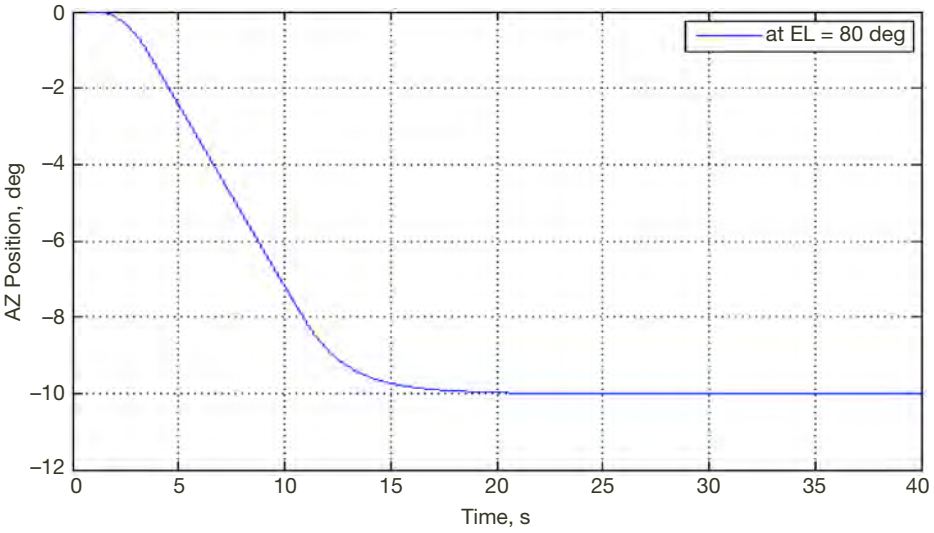

Figure C-8. Overshoot of 4 mdeg, which satisfies the requirements when a negative large position offset of 10 deg is applied to the azimuth drives.

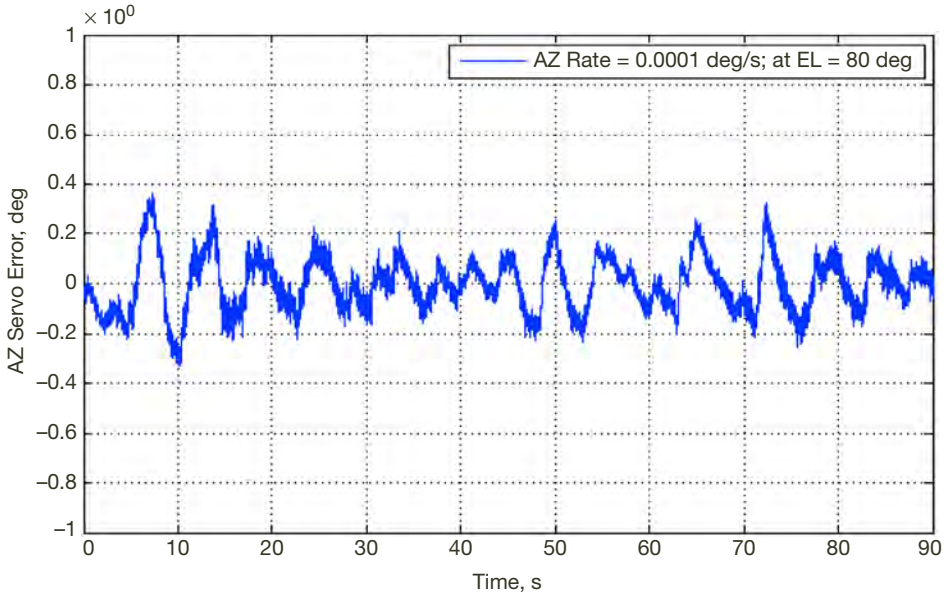

Figure C-9. Azimuth rms mean servo error of 0.1 mdeg when a small positive rate offset of 0.0001 deg/s is applied to the azimuth drives. The mean servo error does meet the requirement of less than 0.001 deg rms.

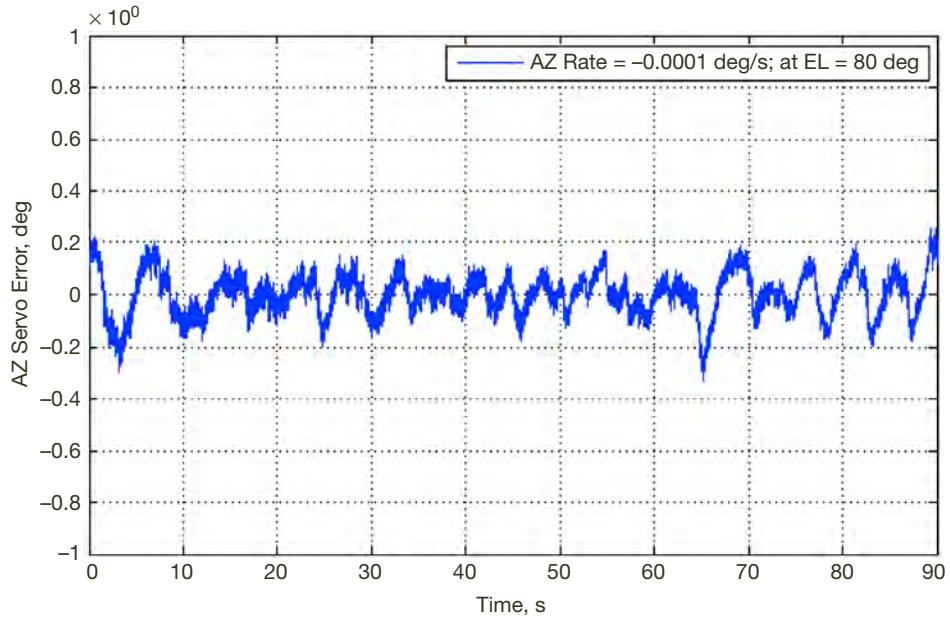

Figure C-10. Azimuth rms mean servo error of 0.1 mdeg when a small negative rate offset of 0.0001 deg/s is applied to the azimuth drives. The mean servo error does meet the requirement of less than 0.001 deg rms.

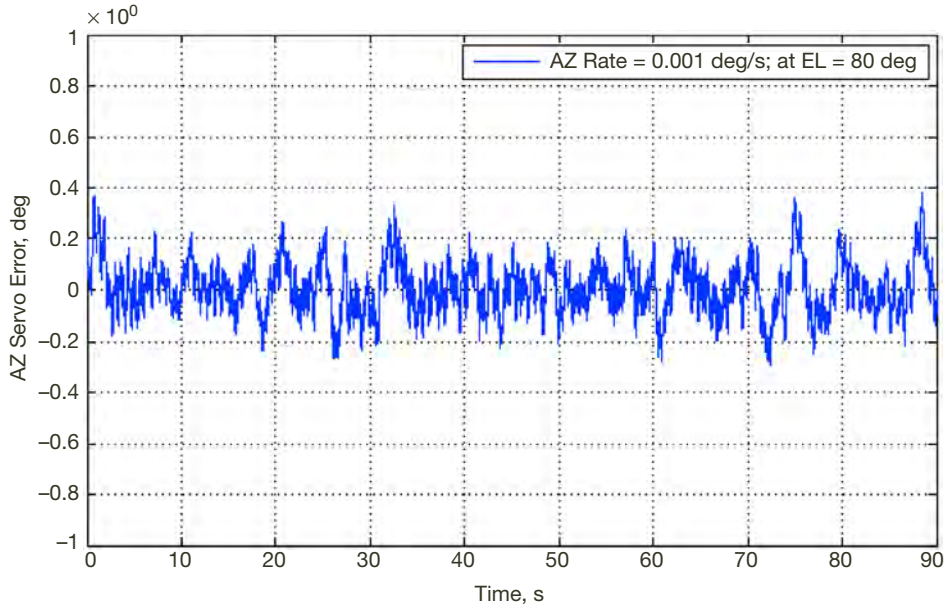

Figure C-11. Azimuth rms mean servo error of 0.1 mdeg when a small positive rate offset of 0.001 deg/s is applied to the azimuth drives. The mean servo error does meet the requirement of less than 0.001 deg rms.

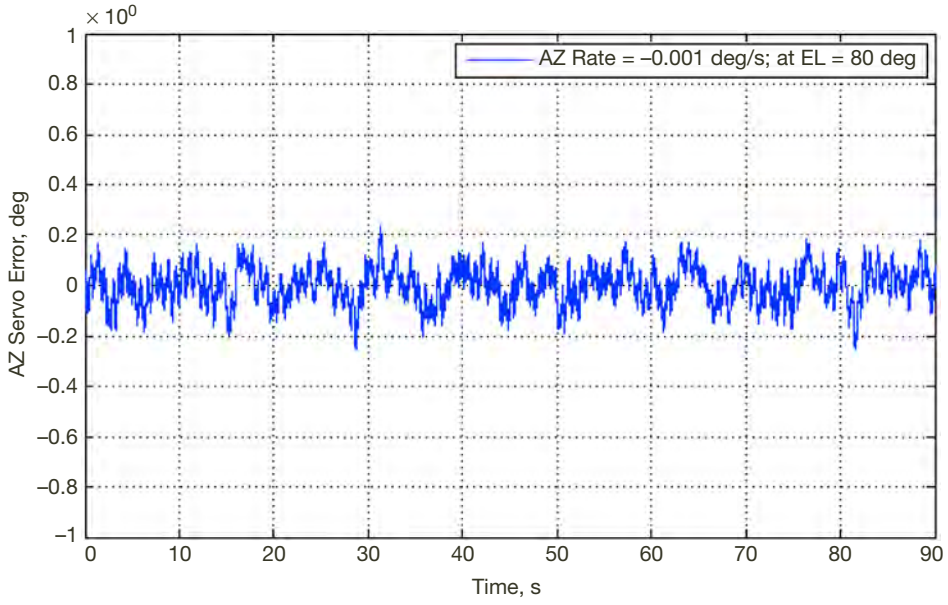

Figure C-12. Azimuth rms mean servo error of 0.1 mdeg when a small negative rate offset of 0.001 deg/s is applied to the azimuth drives. The mean servo error does meet the requirement of less than 0.001 deg rms.

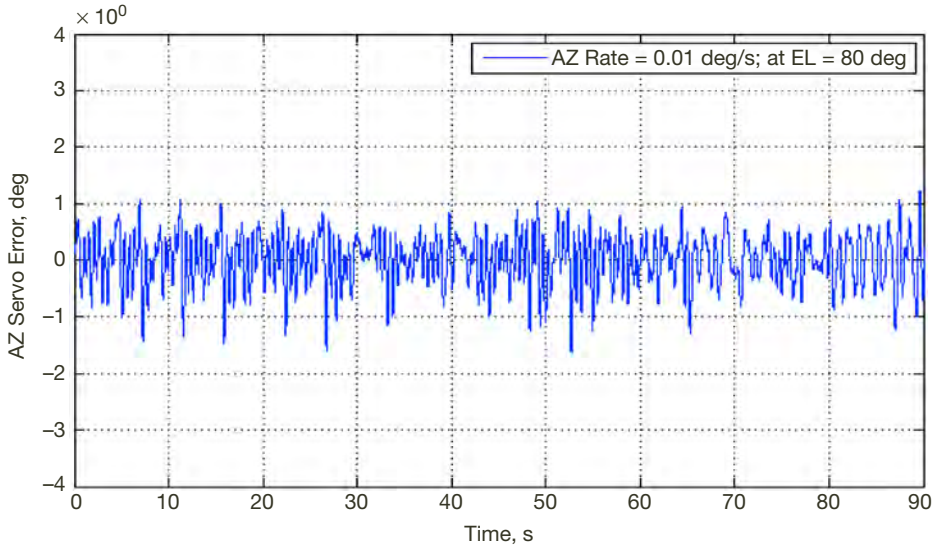

Figure C-13. Azimuth rms mean servo error of 0.4 mdeg when a small positive rate offset of 0.01 deg/s is applied to the azimuth drives. The mean servo error does meet the requirement of less than 0.001 deg rms.

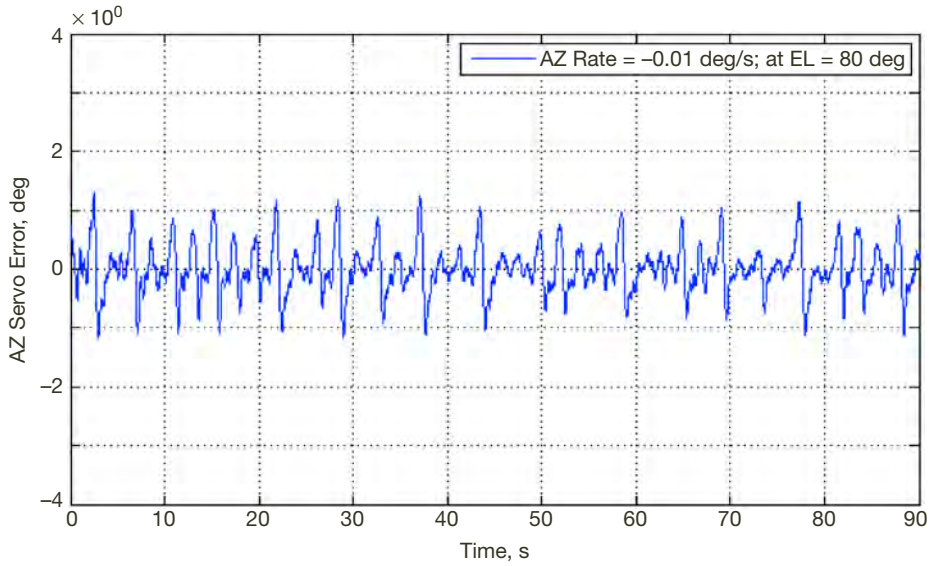

Figure C-14. Azimuth rms mean servo error of 0.4 mdeg when a small negative rate offset of 0.01 deg/s is applied to the azimuth drives. The mean servo error does meet the requirement of less than 0.001 deg rms.

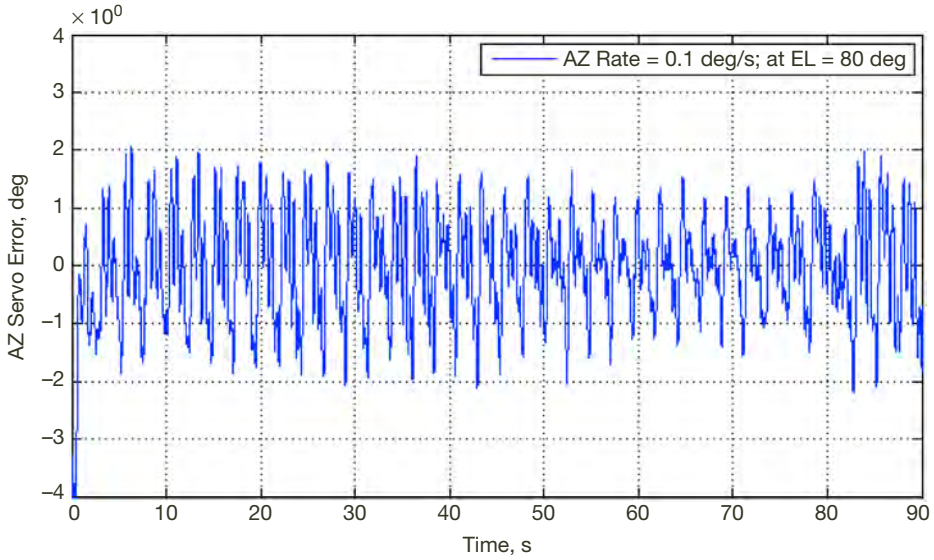

Figure C-15. Azimuth rms mean servo error of 0.8 mdeg when a small positive rate offset of 0.1 deg/s is applied to the azimuth drives. The mean servo error does meet the requirement of less than 0.001 deg rms.

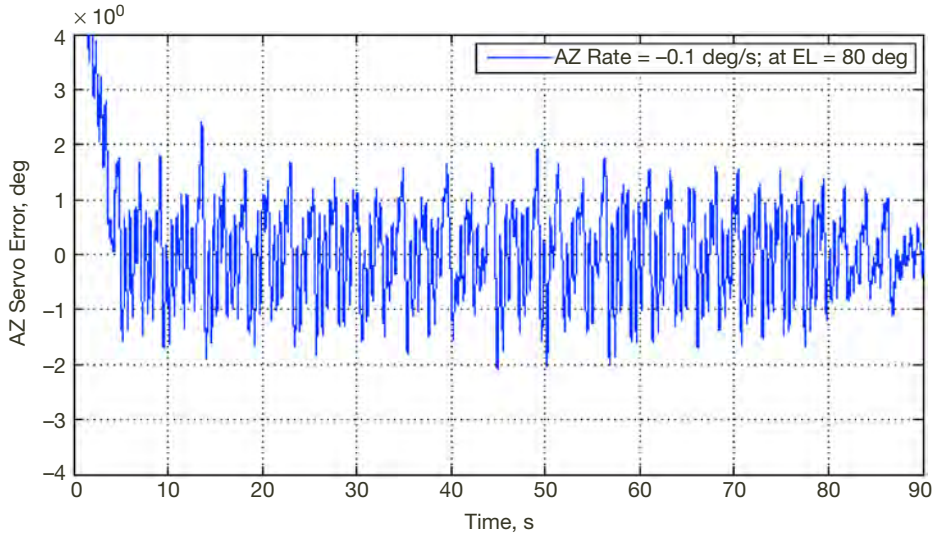

Figure C-16. Azimuth rms mean servo error of 0.8 mdeg when a small negative rate offset of 0.1 deg/s is applied to the azimuth drives. The mean servo error does meet the requirement of less than 0.001 deg rms.

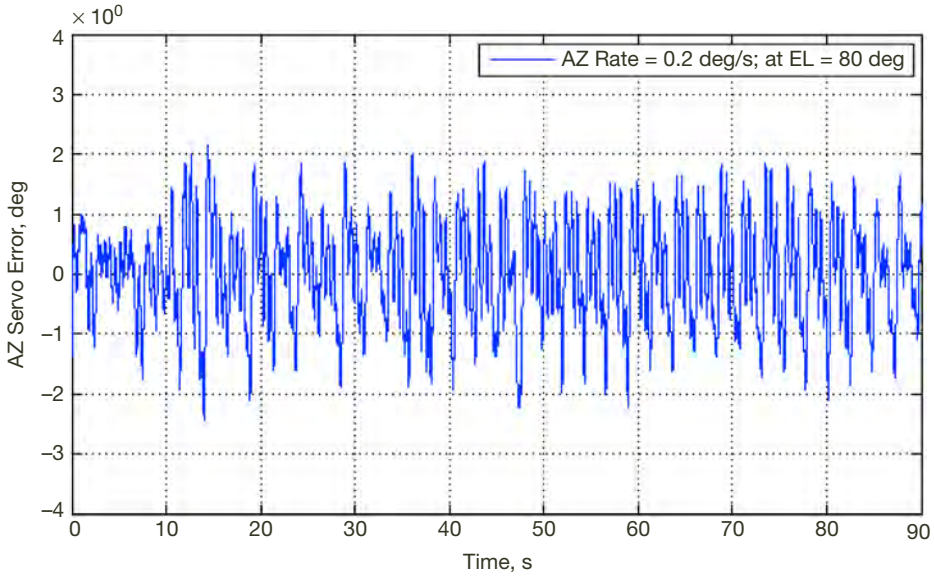

Figure C-17. Azimuth rms mean servo error of 0.9 mdeg when a positive large rate offset of 0.2 deg/s is applied to the azimuth drives. The mean servo error does meet the requirement of less than 0.001 deg rms.

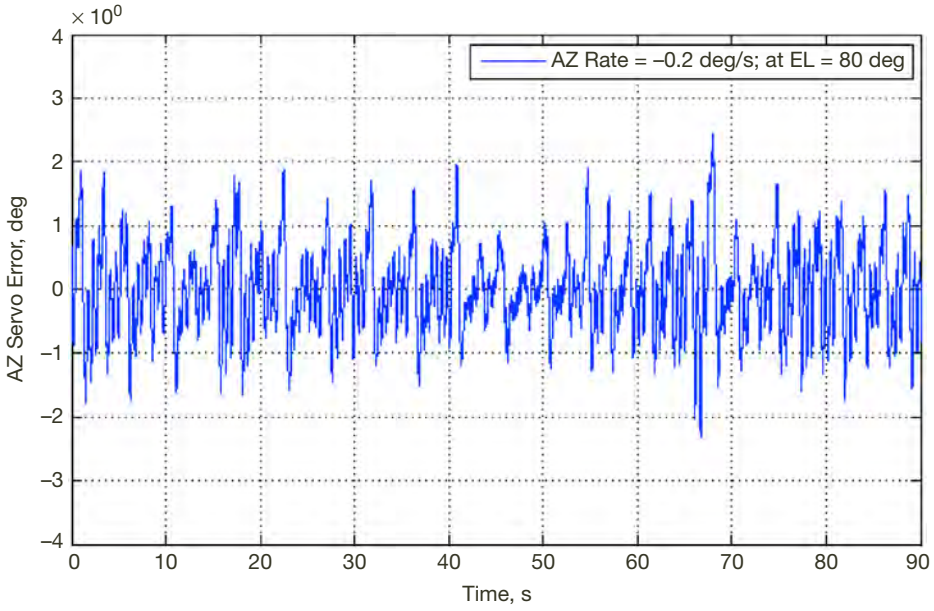

Figure C-18. Azimuth rms mean servo error of 0.7 mdeg when a negative large rate offset of 0.2 deg/s is applied to the azimuth drives. The mean servo error does meet the requirement of less than 0.001 deg rms.

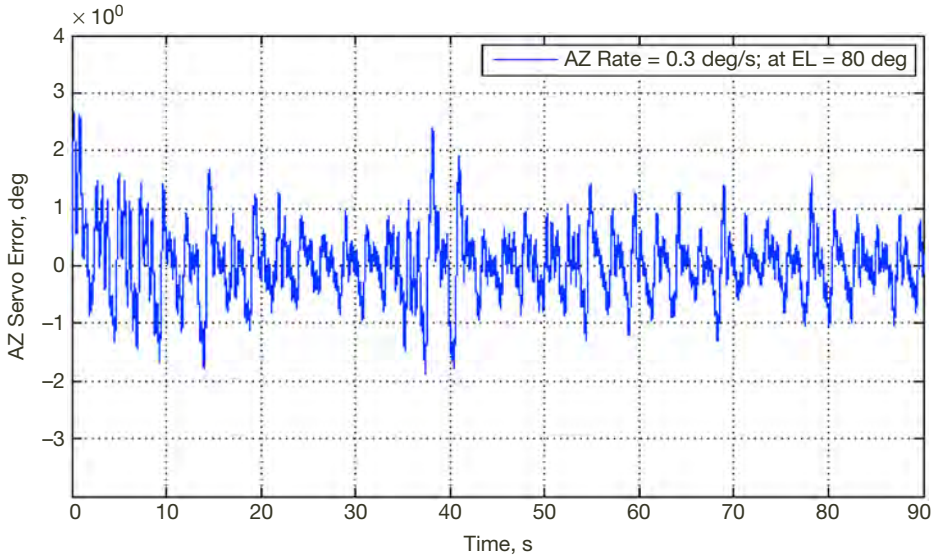

Figure C-19. Azimuth rms mean servo error of 0.5 mdeg when a positive large rate offset of 0.3 deg/s is applied to the azimuth drives. The mean servo error does meet the requirement of less than 0.001 deg rms.

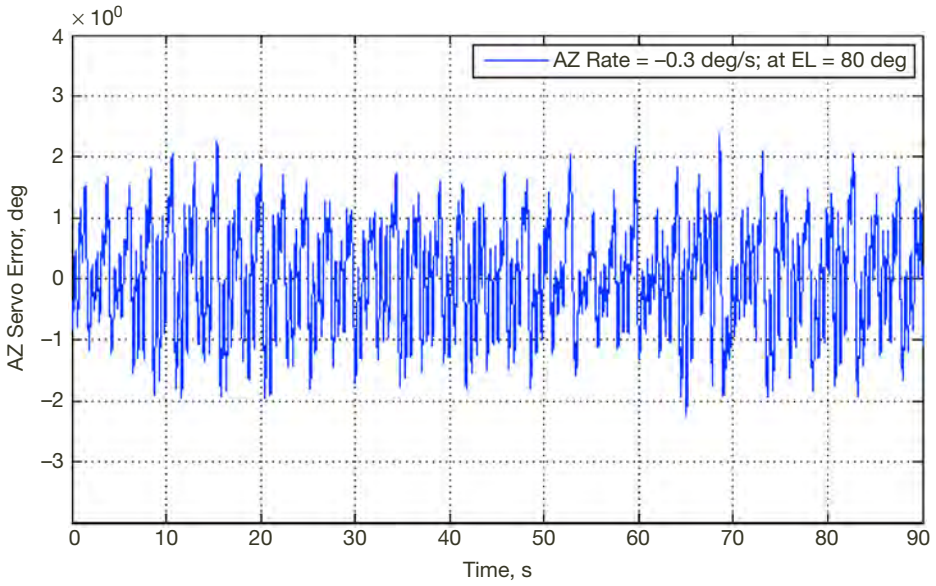

Figure C-20. Azimuth rms mean servo error of 0.9 mdeg when a negative large rate offset of 0.3 deg/s is applied to the azimuth drives. The mean servo error does meet the requirement of less than 0.001 deg rms.

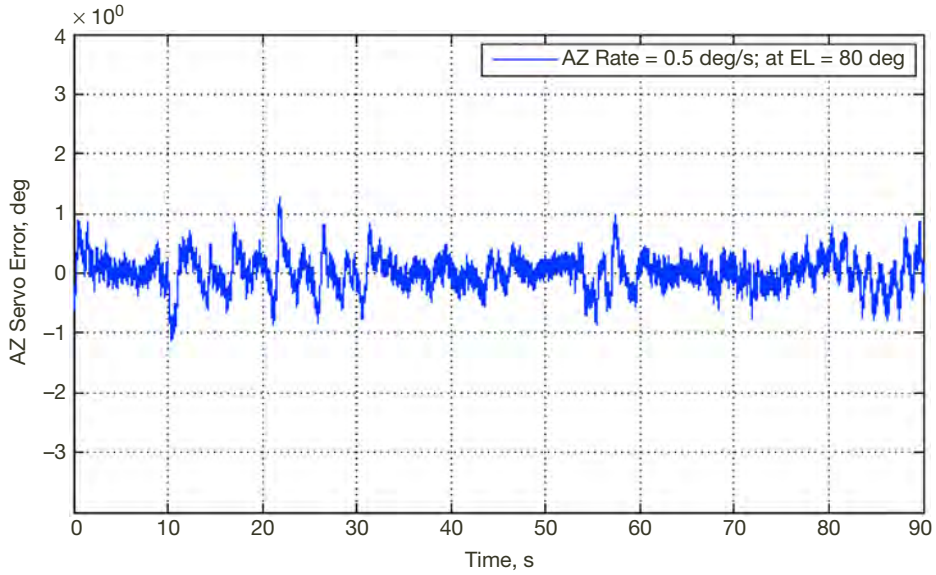

Figure C-21. Azimuth rms mean servo error of 0.3 mdeg when a positive large rate offset of 0.5 deg/s is applied to the azimuth drives. The mean servo error does meet the requirement of less than 0.001 deg rms.

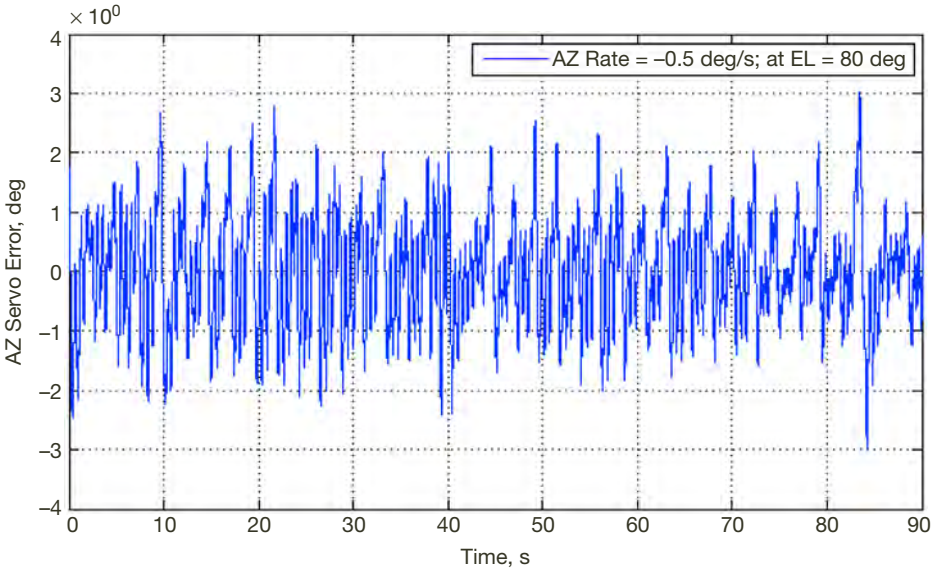

Figure C-22. Azimuth rms mean servo error of 0.9 mdeg when a positive large rate offset of 0.5 deg/s is applied to the azimuth drives. The mean servo error does meet the requirement of less than 0.001 deg rms.

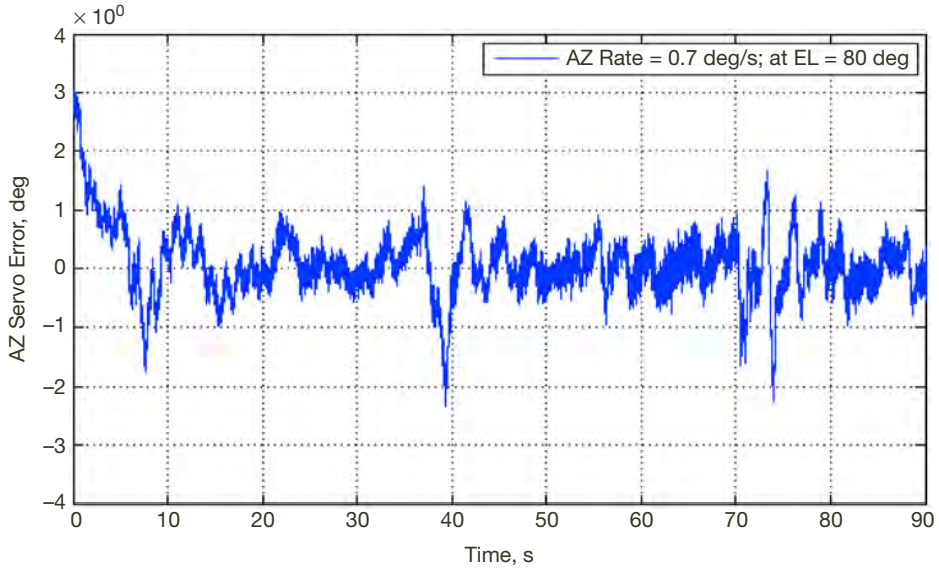

Figure C-23. Azimuth rms mean servo error of 0.4 mdeg when a positive large rate offset of 0.7 deg/s is applied to the azimuth drives. The mean servo error does meet the requirement of less than 0.001 deg rms.

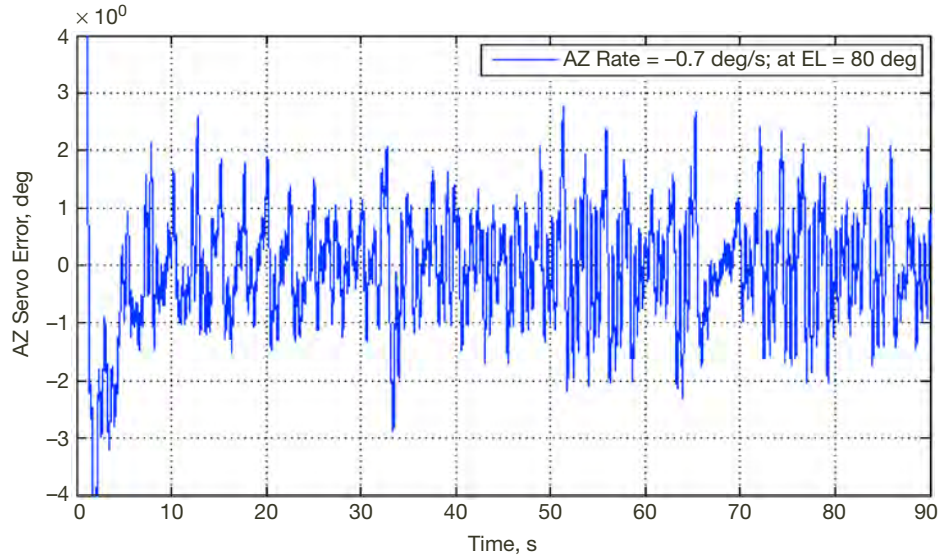

Figure C-24. Azimuth rms mean servo error of 0.9 mdeg when a negative large rate offset of 0.7 deg/s is applied to the azimuth drives. The mean servo error does meet the requirement of less than 0.001 deg rms.

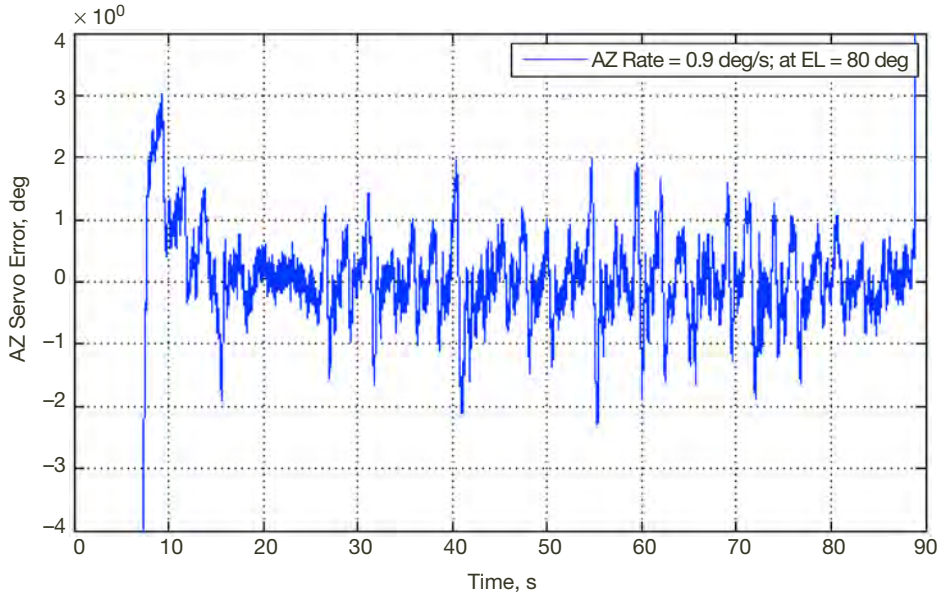

Figure C-25. Azimuth rms mean servo error of 0.6 mdeg when a positive large rate offset of 0.9 deg/s is applied to the azimuth drives. The mean servo error does meet the requirement of less than 0.001 deg rms.

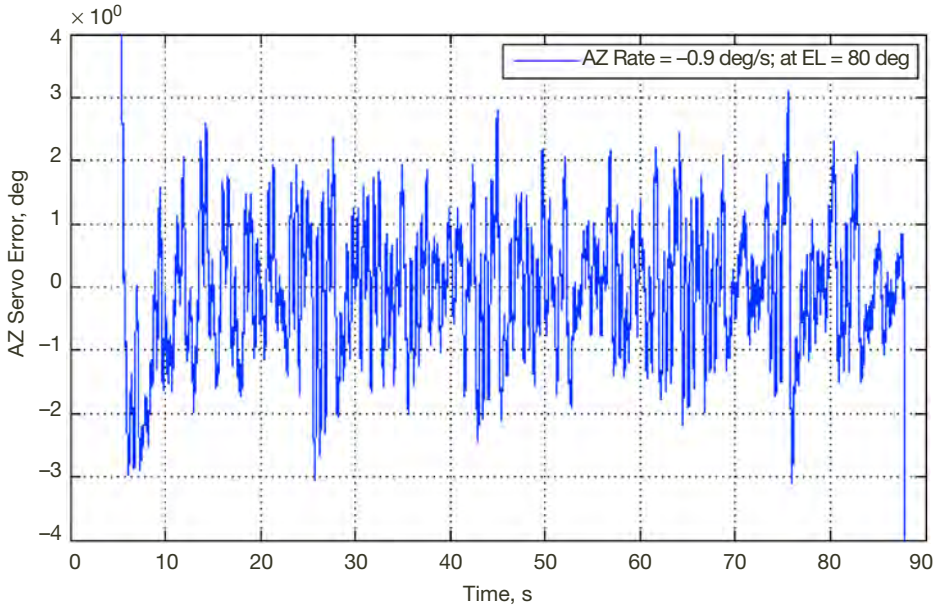

Figure C-26. Azimuth rms mean servo error of 0.96 mdeg when a positive large rate offset of 0.9 deg/s is applied to the azimuth drives. The mean servo error does meet the requirement of less than 0.001 deg rms.

Appendix D

Elevation LQG Closed-Loop Performance

The measurements in Appendix D were all taken at DSS-28 on March 2, 2012.

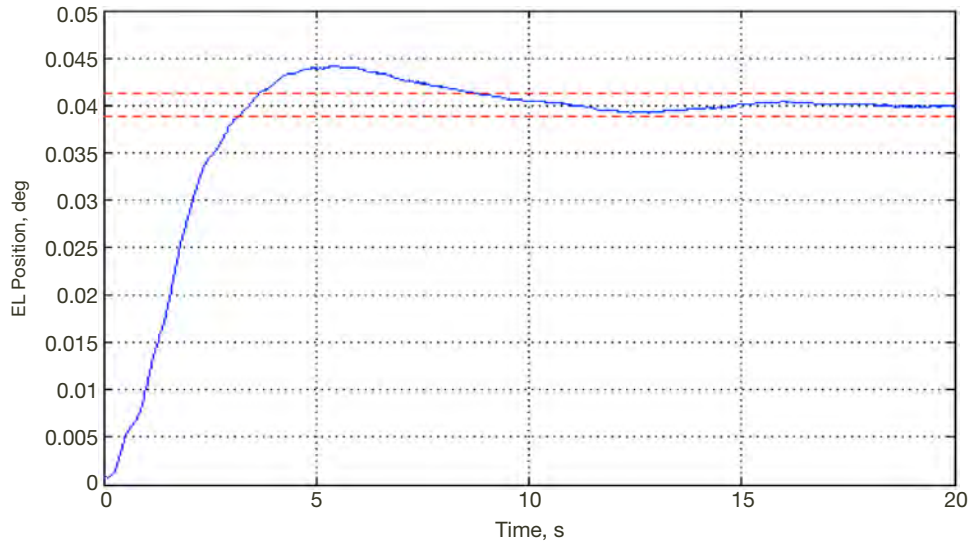

Figure D-1. Overshoot of 11 percent and settling time of 8.8 s response to a positive small position offset of 0.04 deg, which does not satisfy the requirements.

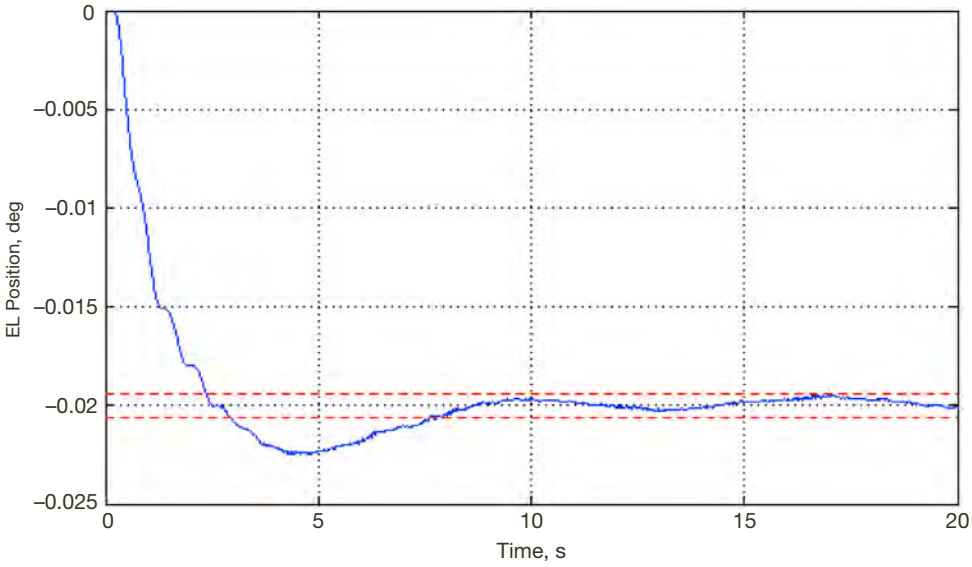

Figure D-2. Overshoot of 11 percent and settling time of 7.6 s response to a negative small position offset of 0.02 deg, which does not satisfy the requirements.

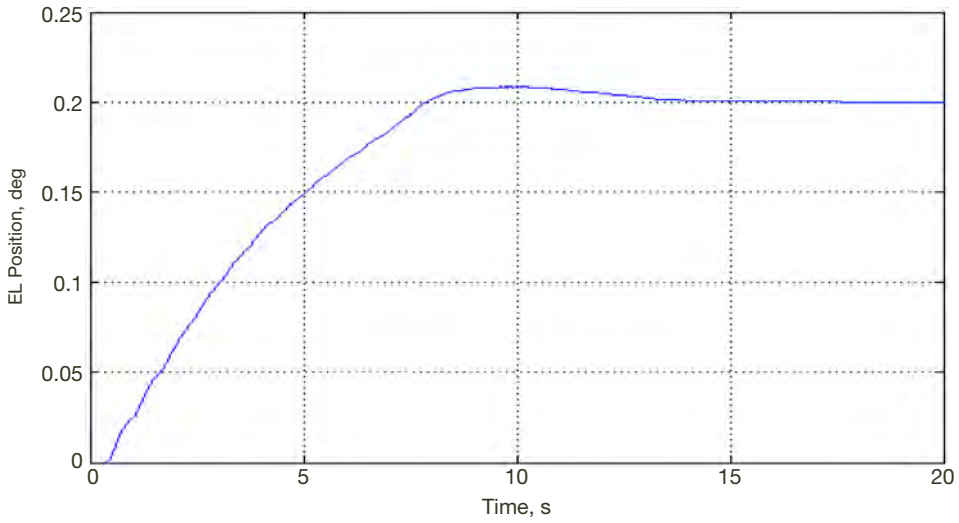

Figure D-3. Overshoot of 8 mdeg, which satisfies the requirements (less than 0.1 deg) when a positive large position offset of 0.2 deg is applied to the elevation drives. The response was attained at maximum speed.

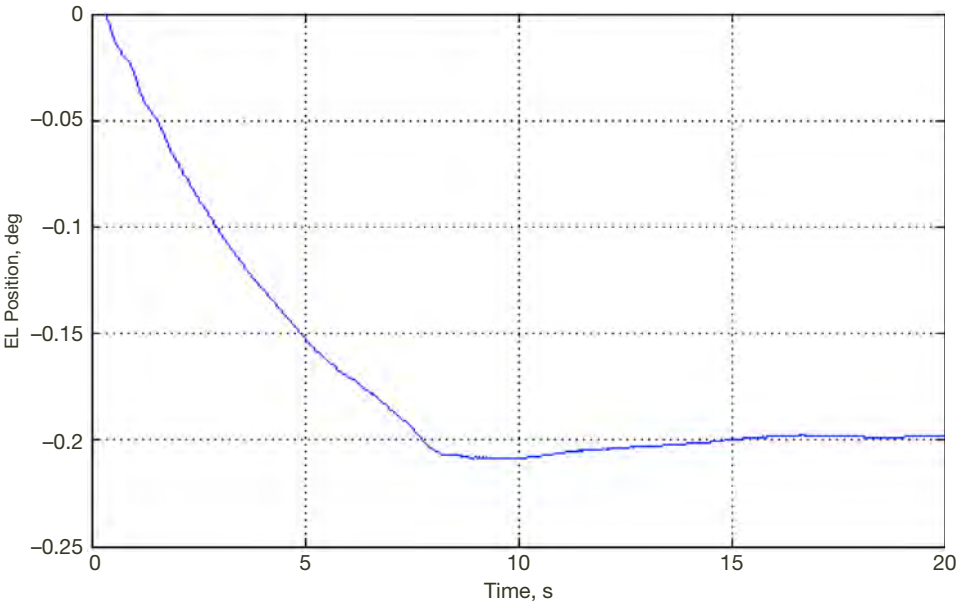

Figure D-4. Overshoot of 8 mdeg, which satisfies the requirements (less than 0.1 deg) when a negative large position offset of 0.2 deg is applied to the elevation drives. The response was attained at maximum speed.

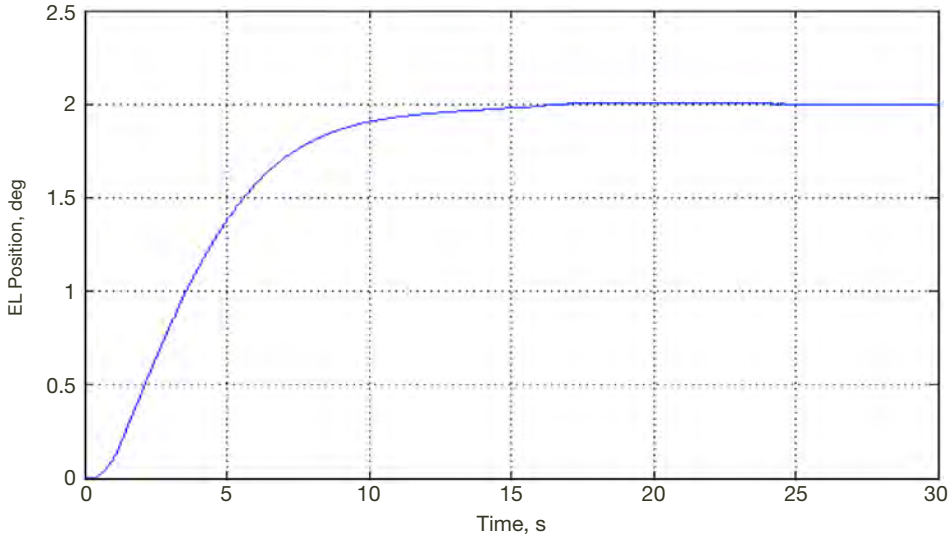

Figure D-5. Overshoot of 6 mdeg, which satisfies the requirements (less than 0.1 deg) when a positive large position offset of 2 deg is applied to the elevation drives. The response was attained at maximum speed.

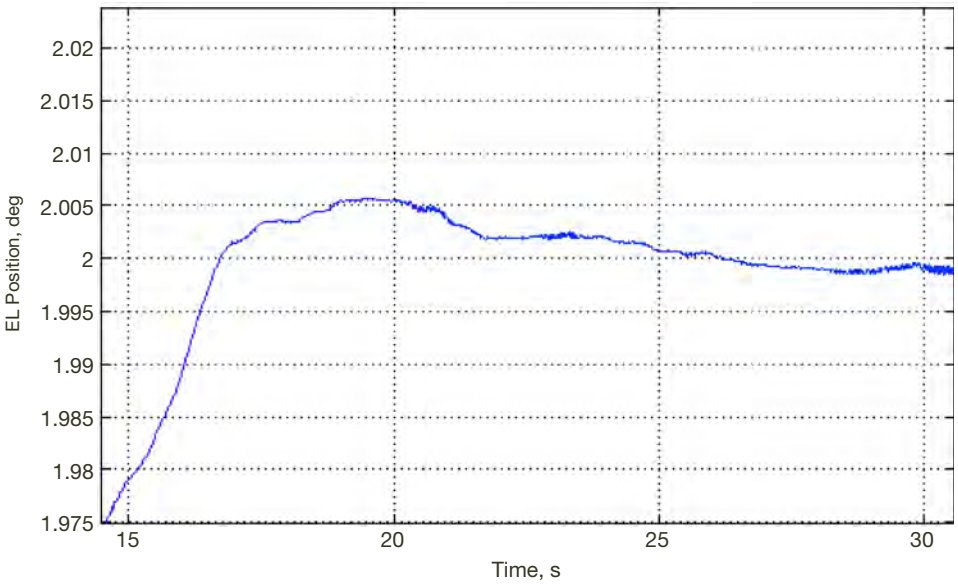

Figure D-6. Zoom of Figure D-5 to show overshoot.

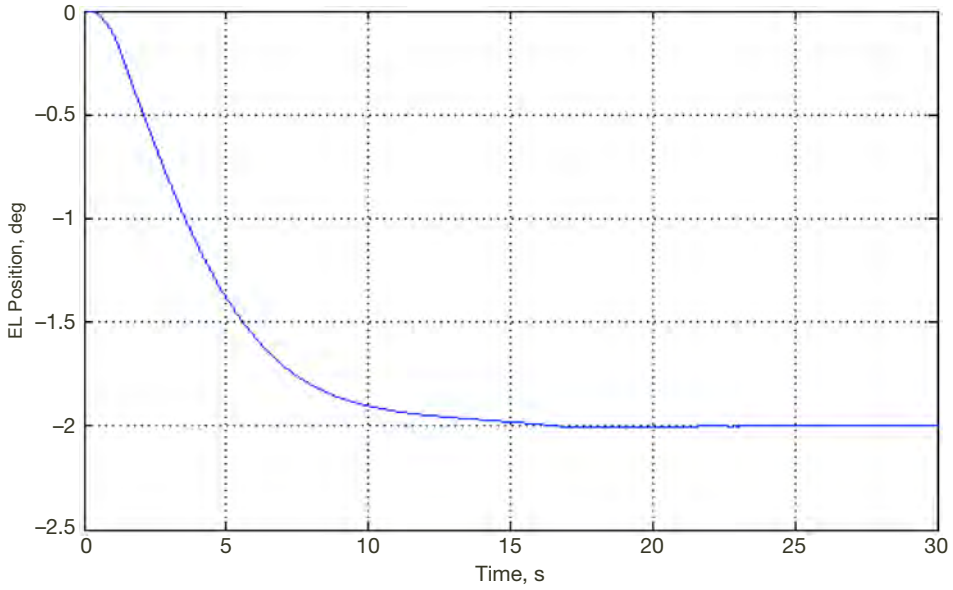

Figure D-7. Overshoot of 7 mdeg, which satisfies the requirements (less than 0.1 deg) when a negative large position offset of 2 deg is applied to the elevation drives. The response was attained at maximum speed.

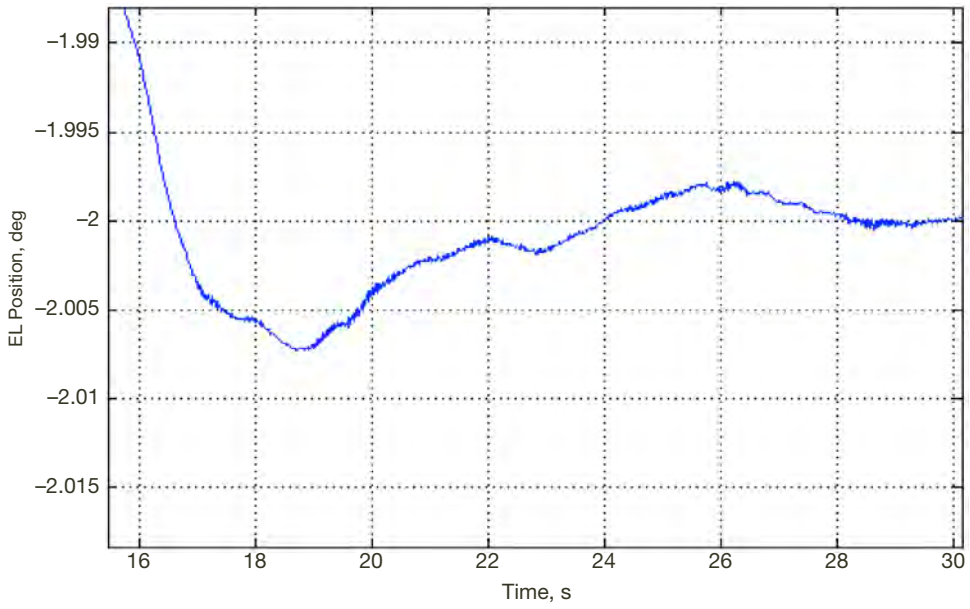

Figure D-8. Zoom of Figure D-7 to show overshoot.

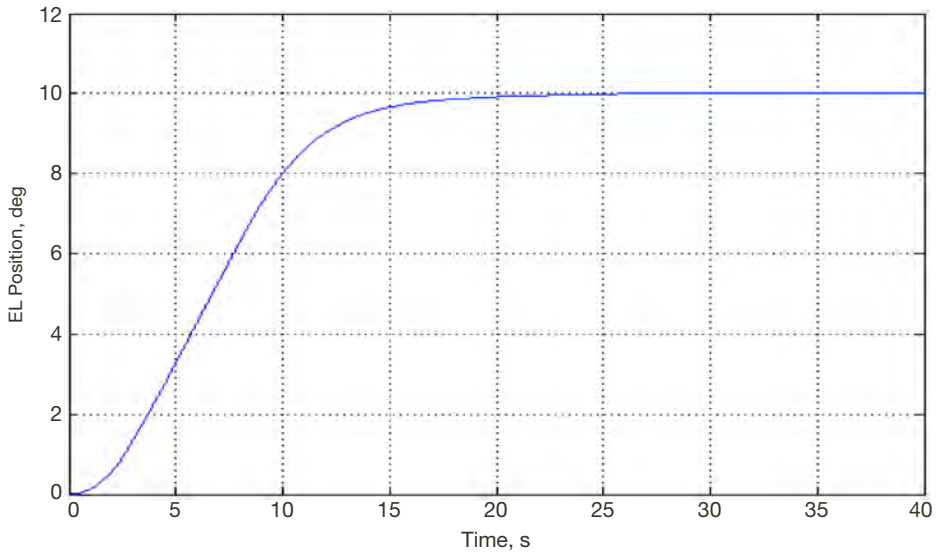

Figure D-9. Overshoot of 7 mdeg, which satisfies the requirements (less than 0.1 deg) when a positive large position offset of 10 deg is applied to the elevation drives. The response was attained at maximum speed.

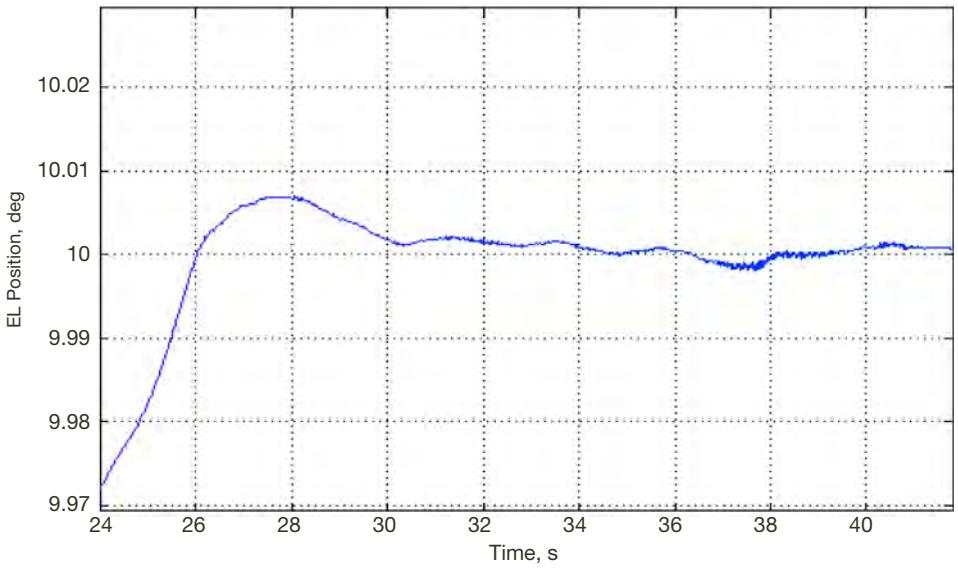

Figure D-10. Zoom of Figure D-9 to show overshoot.

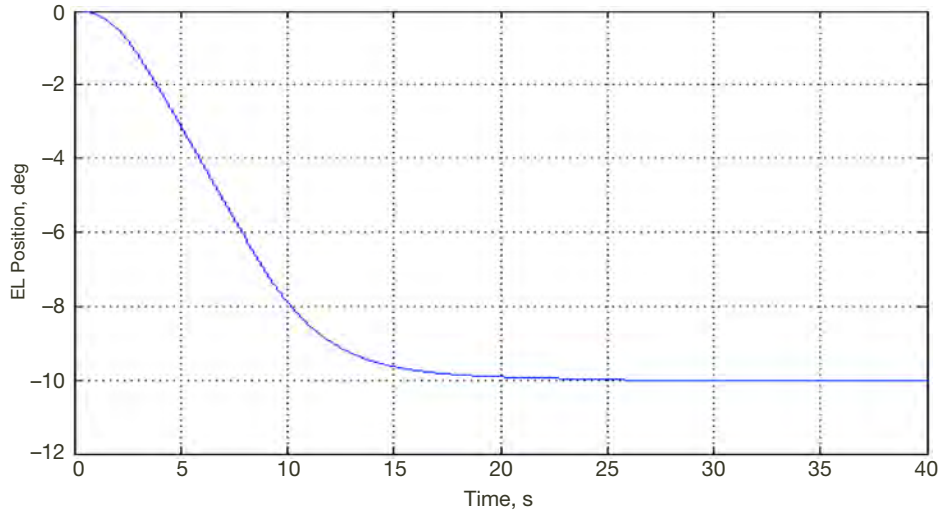

Figure D-11. Overshoot of 7 mdeg, which satisfies the requirements (less than 0.1 deg) when a negative large position offset of 2 deg is applied to the elevation drives. The response was attained at maximum speed.

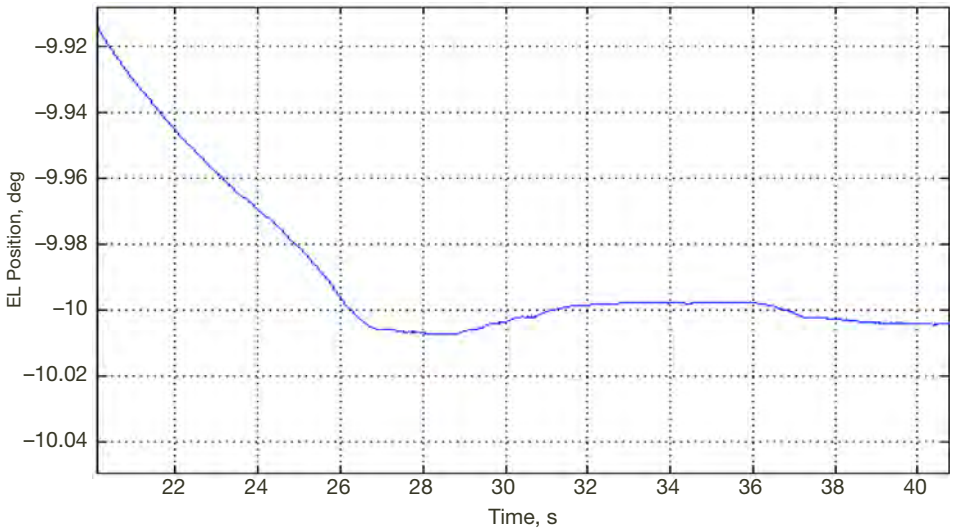

Figure D-12. Zoom of Figure D-11 to show overshoot.

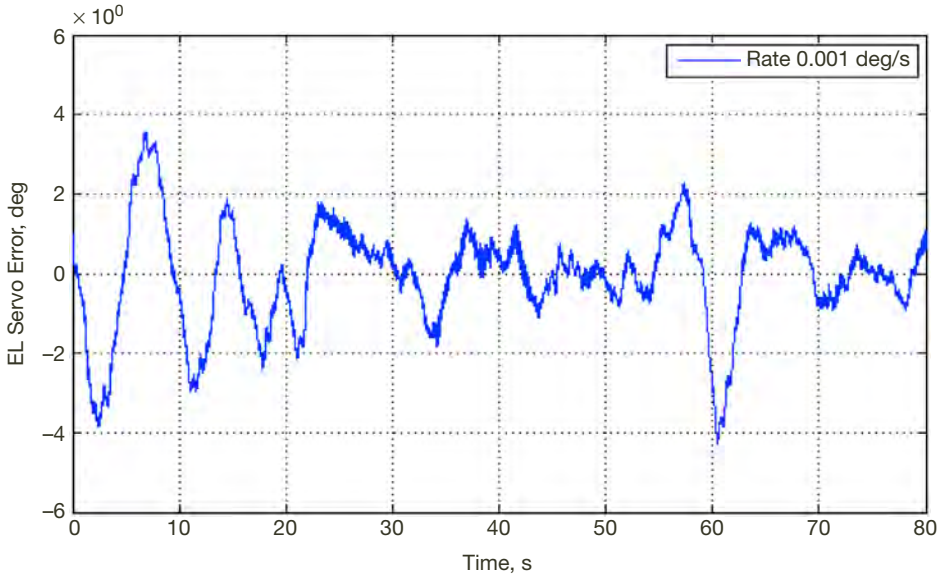

Figure D-13. Elevation rms mean servo error of 1.5 mdeg when a small positive rate offset of 0.001 deg/s is applied to the elevation drives. The mean servo error does meet the requirement of less than 0.001 deg rms. The measurement was performed during high wind of 29 mph.

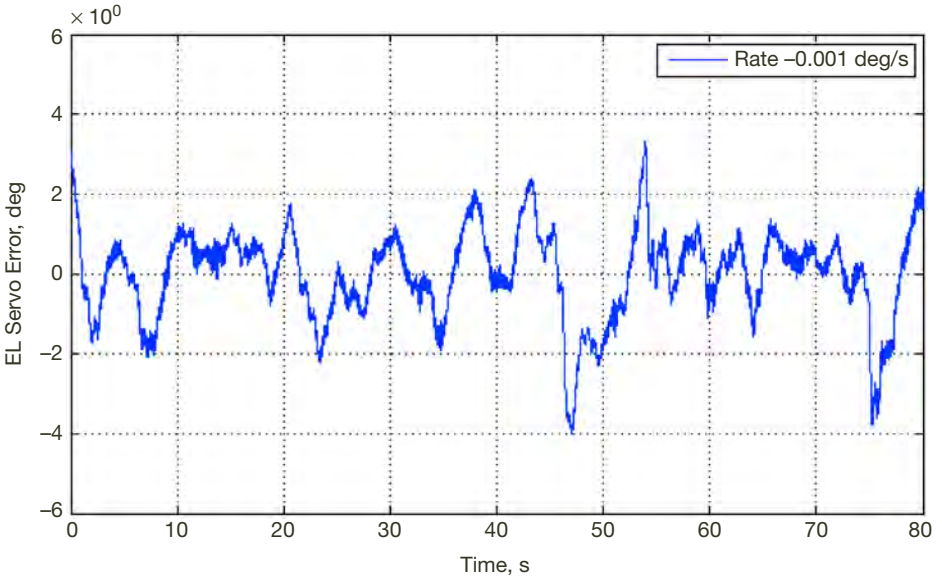

Figure D-14. Elevation rms mean servo error of 1.1 mdeg when a small negative rate offset of 0.001 deg/s is applied to the elevation drives. The mean servo error does meet the requirement of less than 0.001 deg rms. The measurement was performed during high wind of 29 mph.

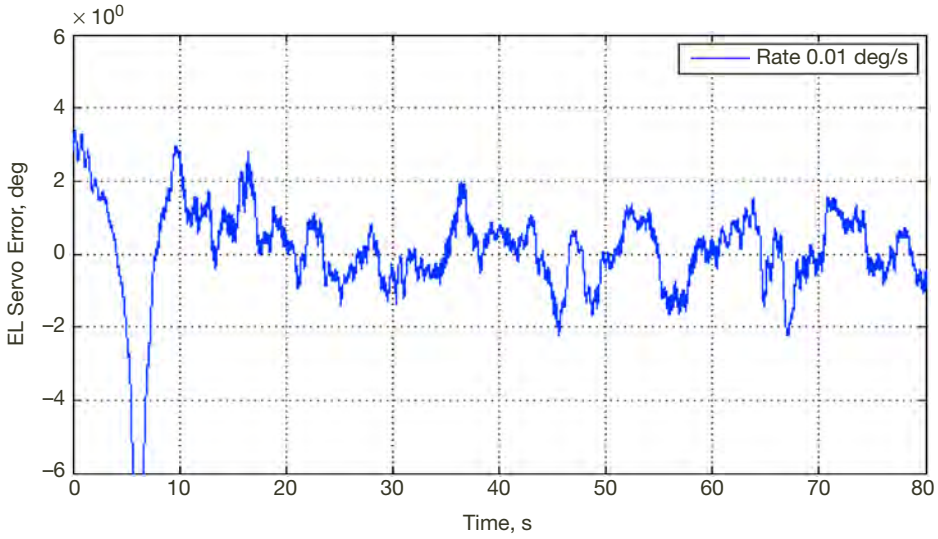

Figure D-15. Elevation rms mean servo error of 0.9 mdeg when a small positive rate offset of 0.01 deg/s is applied to the elevation drives. The mean servo error does meet the requirement of less than 0.001 deg rms. The measurement was performed during high wind of 29 mph.

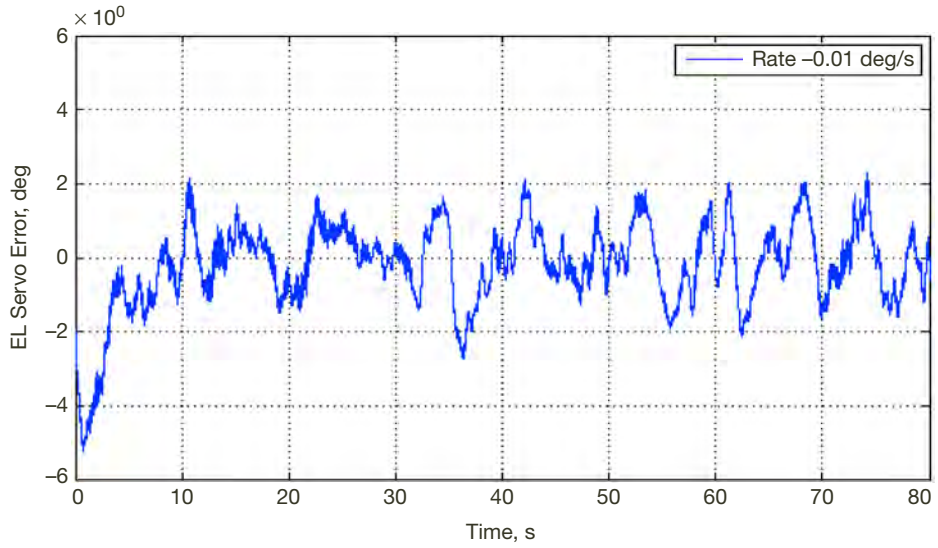

Figure D-16. Elevation rms mean servo error of 0.8 mdeg when a small negative rate offset of 0.01 deg/s is applied to the elevation drives. The mean servo error does meet the requirement of less than 0.001 deg rms. The measurement was performed during high wind of 29 mph.

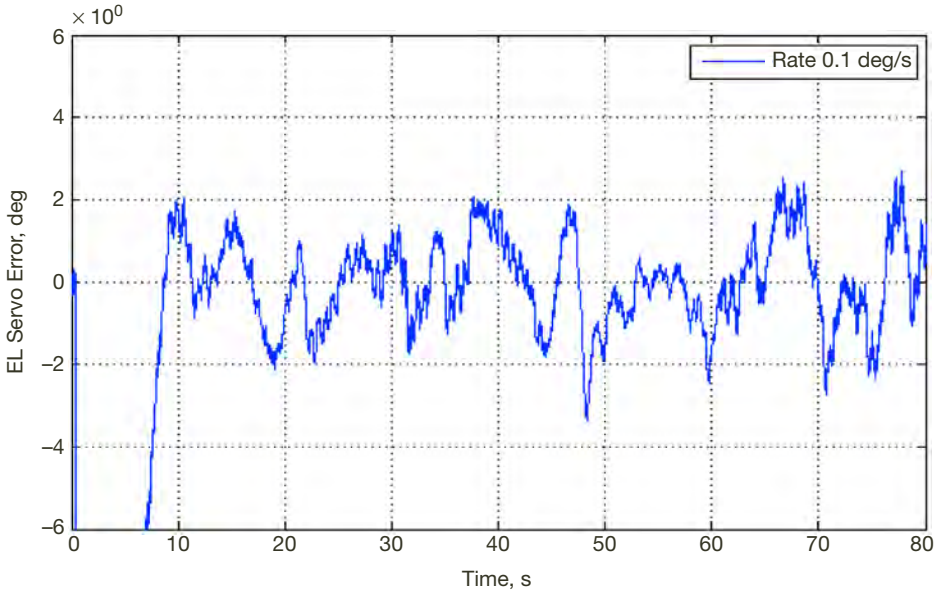

Figure D-17. Elevation rms mean servo error of 1.0 mdeg when a small positive rate offset of 0.01 deg/s is applied to the elevation drives. The mean servo error does meet the requirement of less than 0.001 deg rms. The measurement was performed during high wind of 29 mph.

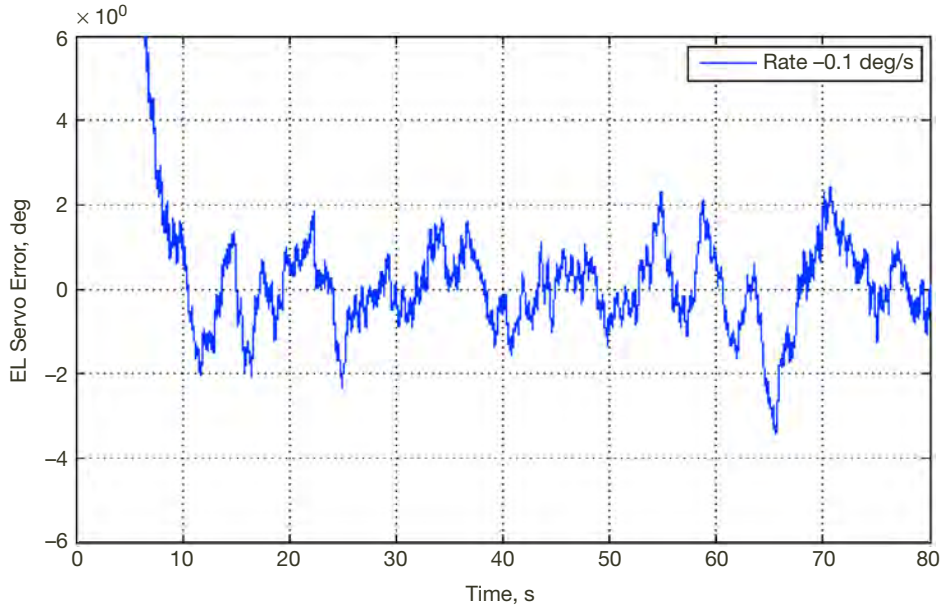

Figure D-18. Elevation rms mean servo error of 0.8 mdeg when a small positive rate offset of 0.01 deg/s is applied to the elevation drives. The mean servo error does meet the requirement of less than 0.001 deg rms. The measurement was performed during high wind of 29 mph.

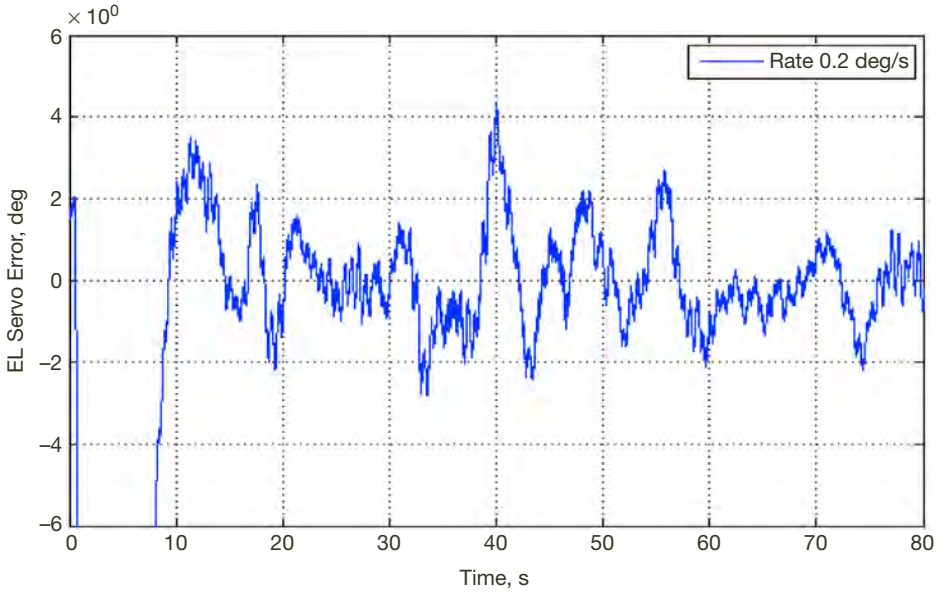

Figure D-19. Elevation rms mean servo error of 1.1 mdeg when a small positive rate offset of 0.2 deg/s is applied to the elevation drives. The mean servo error does meet the requirement of less than 0.001 deg rms. The measurement was performed during high wind of 29 mph.

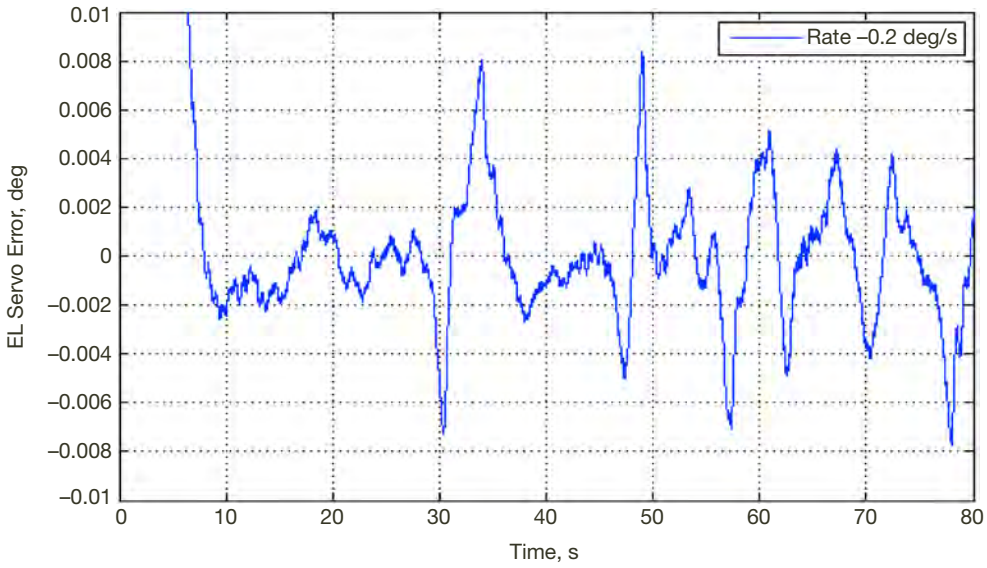

Figure D-20. Elevation rms mean servo error of 1.5 mdeg when a small negative rate offset of 0.2 deg/s is applied to the elevation drives. The mean servo error does meet the requirement of less than 0.001 deg rms. The measurement was performed during high wind of 29 mph.

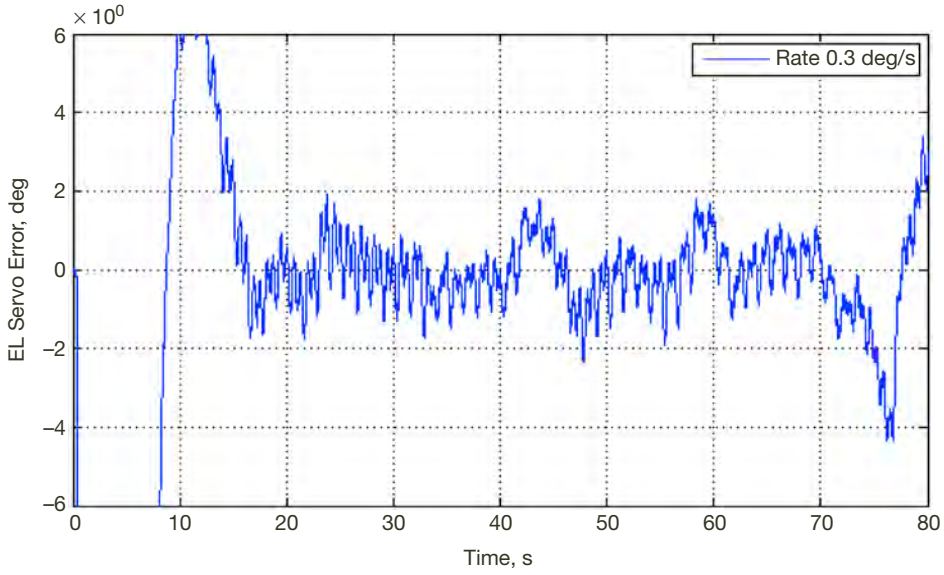

Figure D-21. Elevation rms mean servo error of 0.8 mdeg when a positive rate offset of 0.3 deg/s is applied to the elevation drives. The mean servo error does meet the requirement of less than 0.001 deg rms. The measurement was performed during high wind of 29 mph.

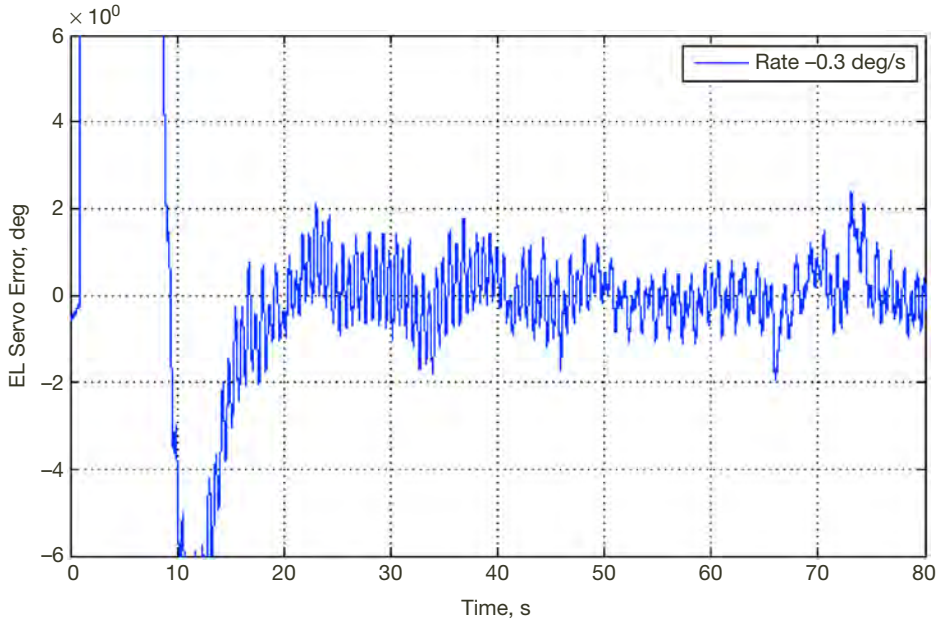

Figure D-22. Elevation rms mean servo error of 0.7 mdeg when a negative rate offset of 0.3 deg/s is applied to elevation drives. The mean servo error does meet the requirement of less than 0.001 deg rms. The measurement was performed during high wind of 29 mph.

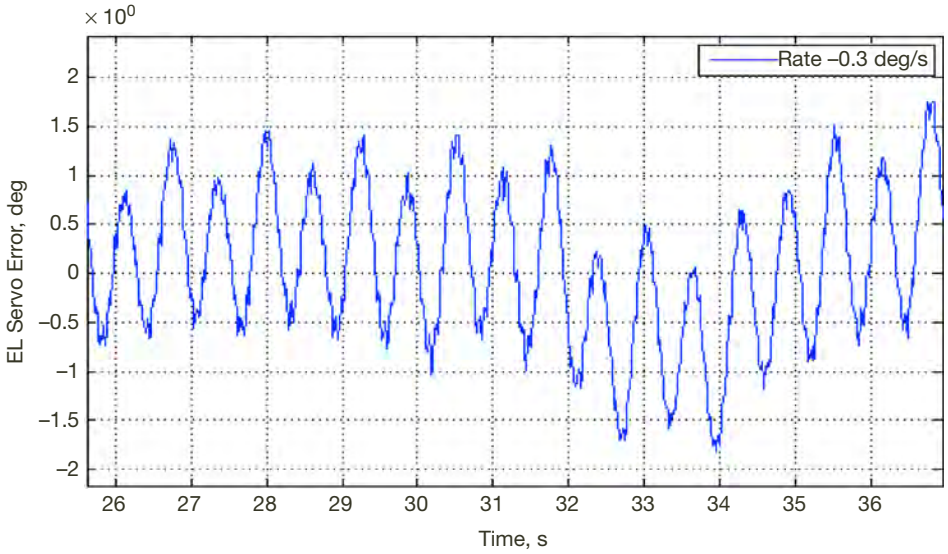

Figure D-23. Zoom of Figure D-22 to show rms servo error of 0.7 deg.

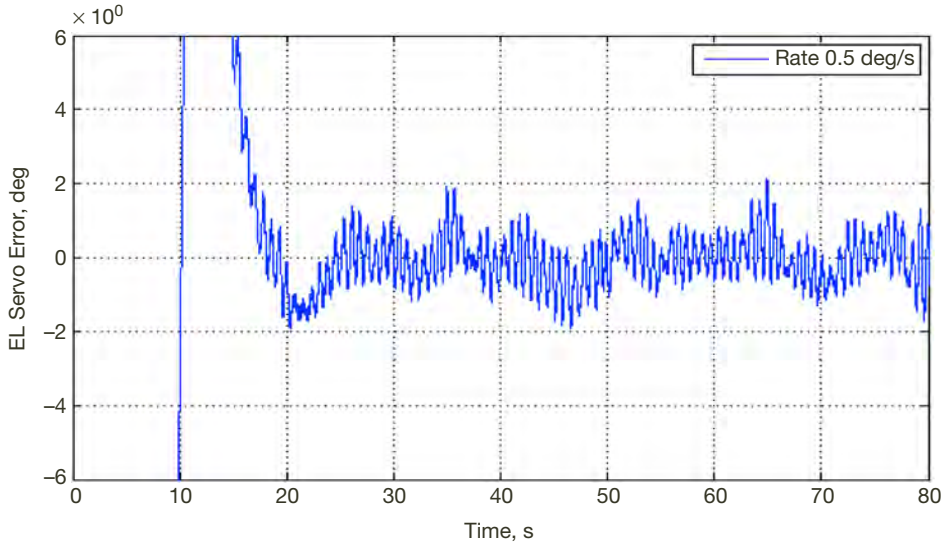

Figure D-24. Elevation rms mean servo error of 0.6 mdeg when a positive large rate offset of 0.5 deg/s is applied to the elevation drives. The mean servo error does meet the requirement of less than 0.001 deg rms. The measurement was performed during high wind of 29 mph.

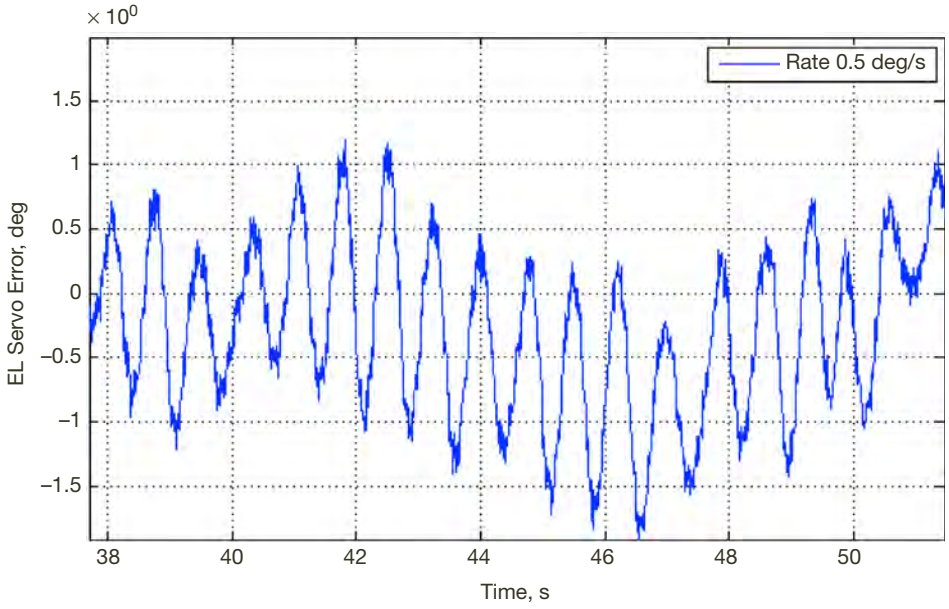

Figure D-25. Zoom of Figure D-24 to show rms servo error of 0.6 deg.

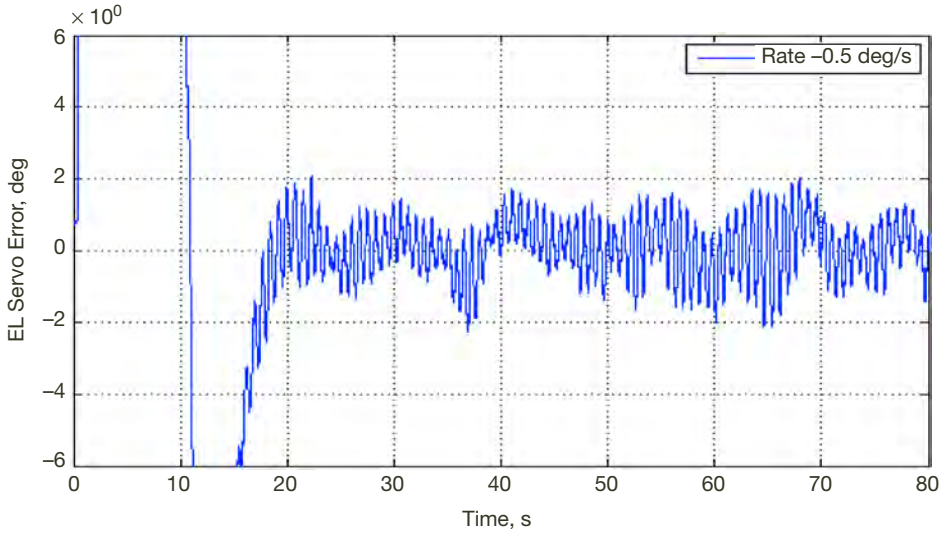

Figure D-26. Elevation rms mean servo error of 0.8 mdeg when a negative large rate offset of 0.5 deg/s is applied to the elevation drives. The mean servo error does meet the requirement of less than 0.001 deg rms. The measurement was performed during high wind of 29 mph.

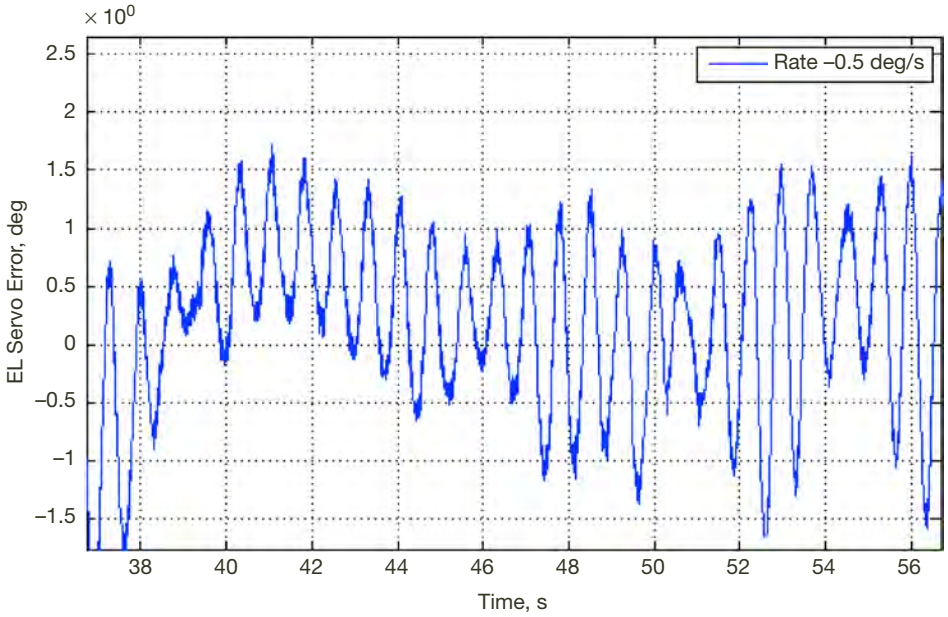

Figure D-27. Zoom of Figure D-26 to show rms servo error of 0.8 deg.

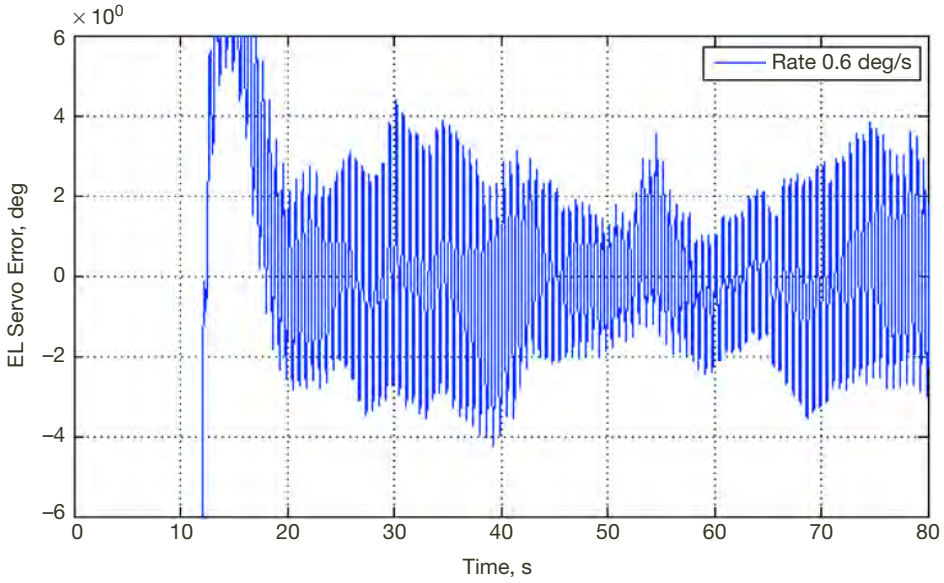

Figure D-28. Elevation rms mean servo error of 1.8 mdeg when a positive large rate offset of 0.6 deg/s is applied to the elevation drives. The mean servo error does not satisfy the requirement of less than 0.001 deg rms. The measurement was performed during high wind of 29 mph.

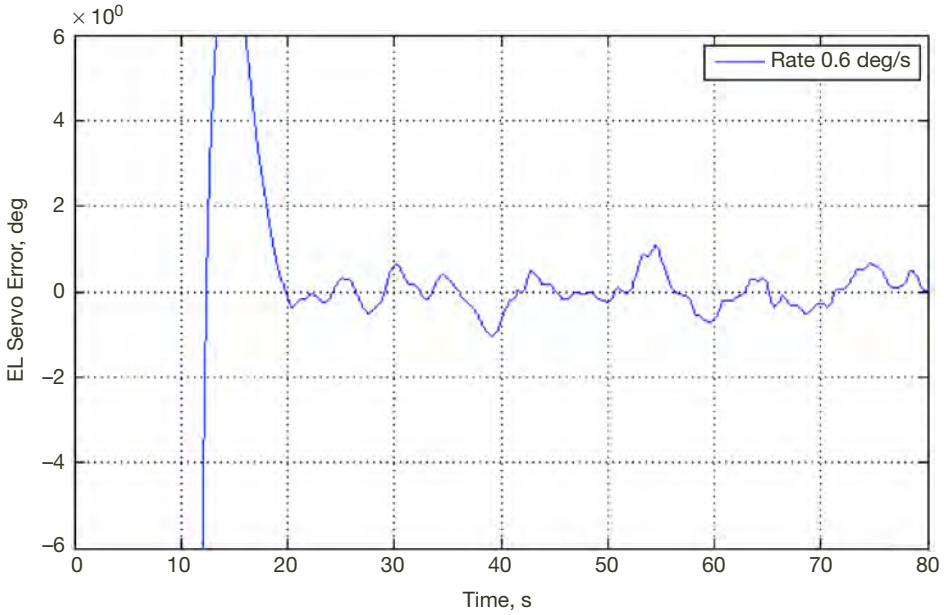

Figure D-29. Zoom of Figure D-28 to show rms servo error of 1.8 deg.

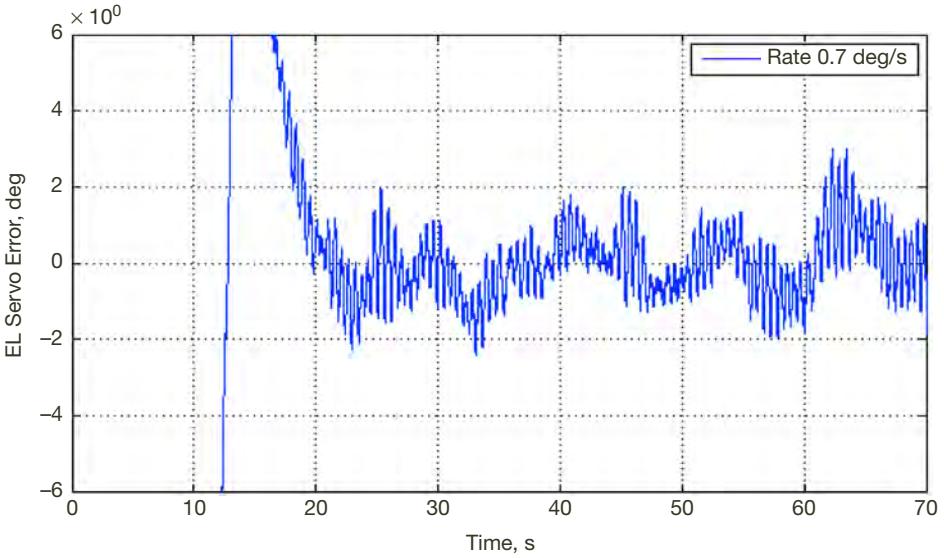

Figure D-30. Elevation rms mean servo error of 0.9 mdeg when a positive large rate offset of 0.7 deg/s is applied to the elevation drives. The mean servo error does meet the requirement of less than 0.001 deg rms. The measurement was performed during high wind of 29 mph.

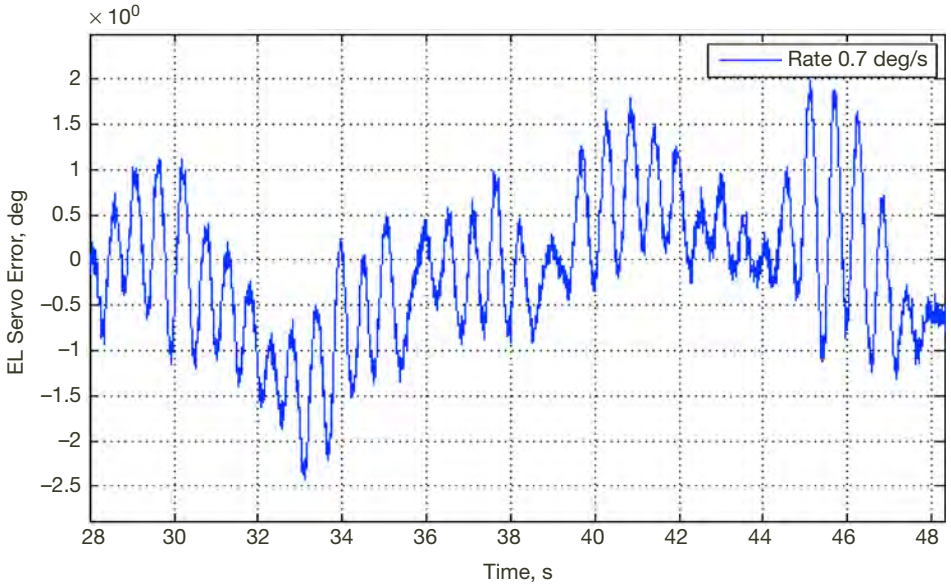

Figure D-31. Zoom of Figure D-30 to show rms servo error of 0.9 deg.

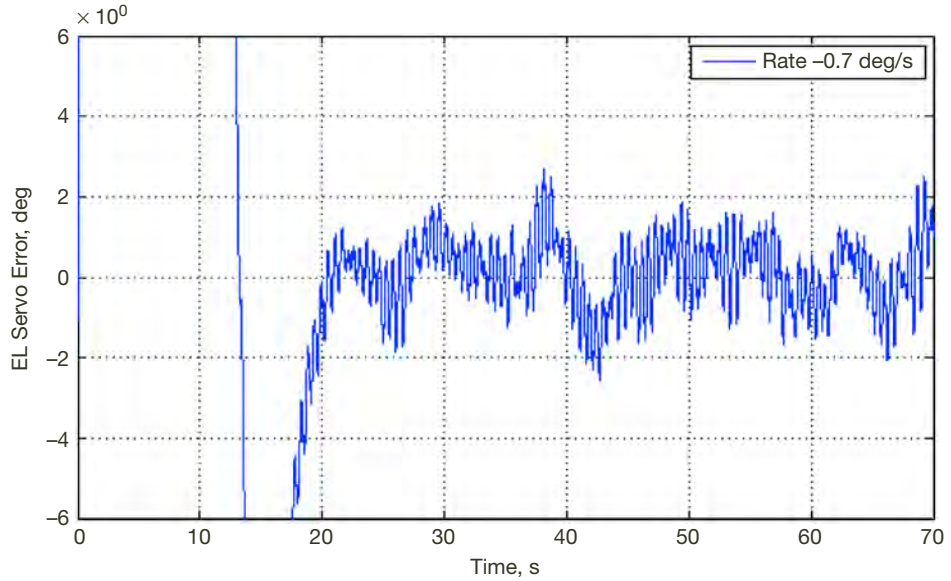

Figure D-32. Elevation rms mean servo error of 0.8 mdeg when a negative large rate offset of 0.7 deg/s is applied to the elevation drives. The mean servo error does meet the requirement of less than 0.001 deg rms. The measurement was performed during high wind of 29 mph.

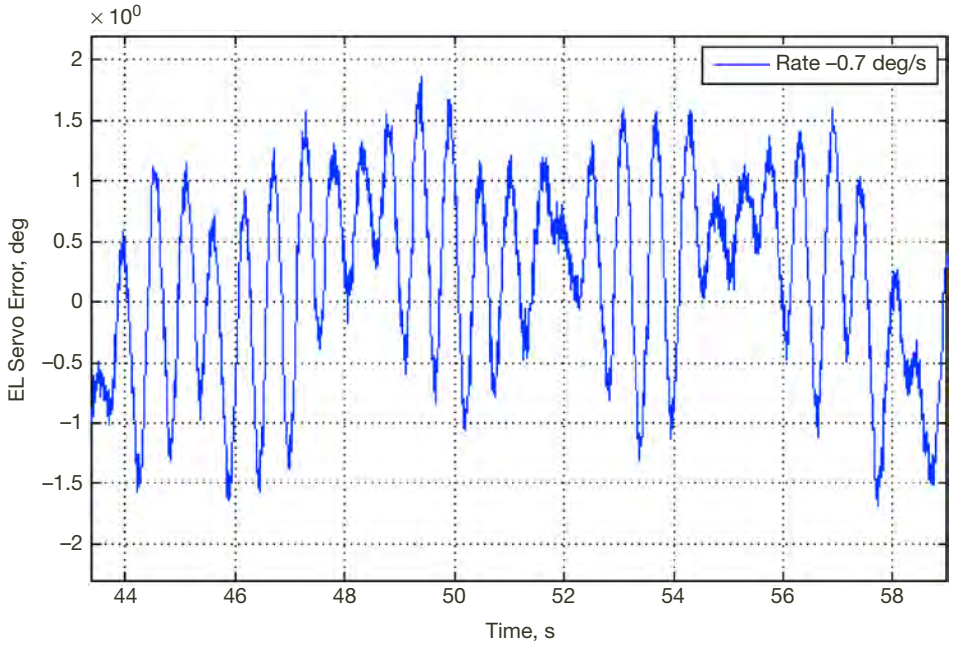

Figure D-33. Zoom of Figure D-32 to show rms servo error of 0.8 deg.

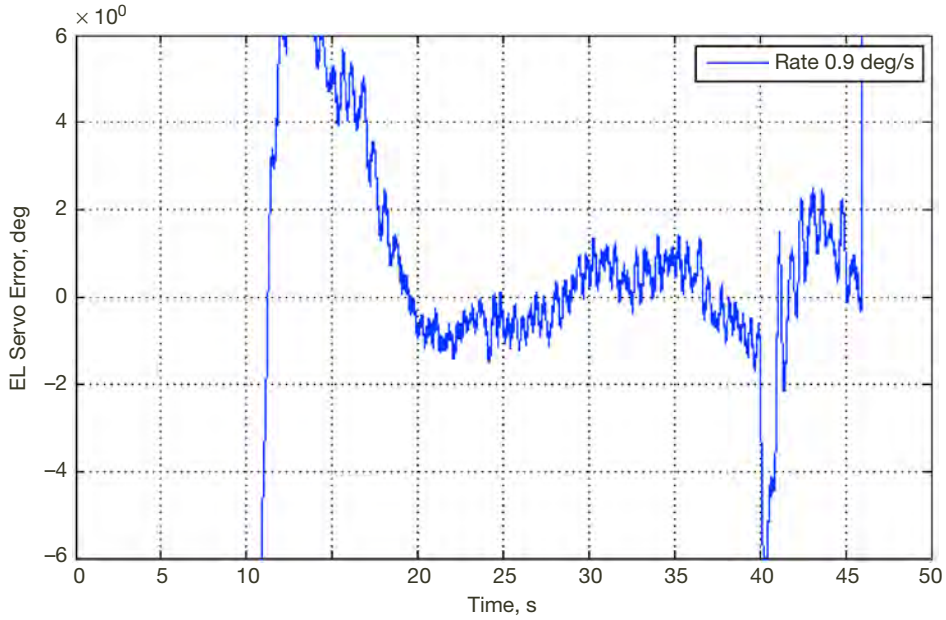

Figure D-34. Elevation rms mean servo error of 0.7 mdeg when a positive large rate offset of 0.9 deg/s is applied to the elevation drives. The mean servo error does meet the requirement of less than 0.001 deg rms. The measurement was performed during high wind of 29 mph.

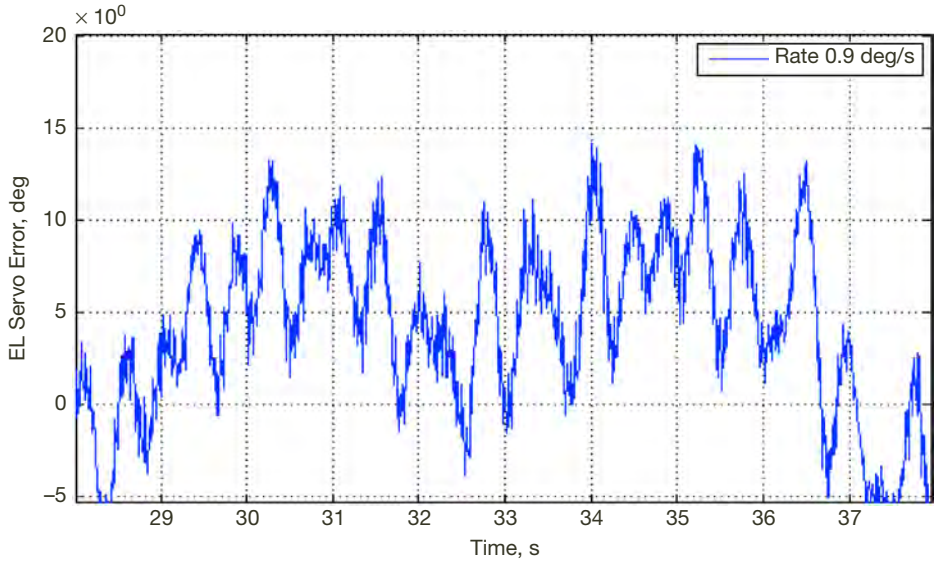

Figure D-35. Zoom of Figure D-34 to show rms servo error of 0.7 deg.

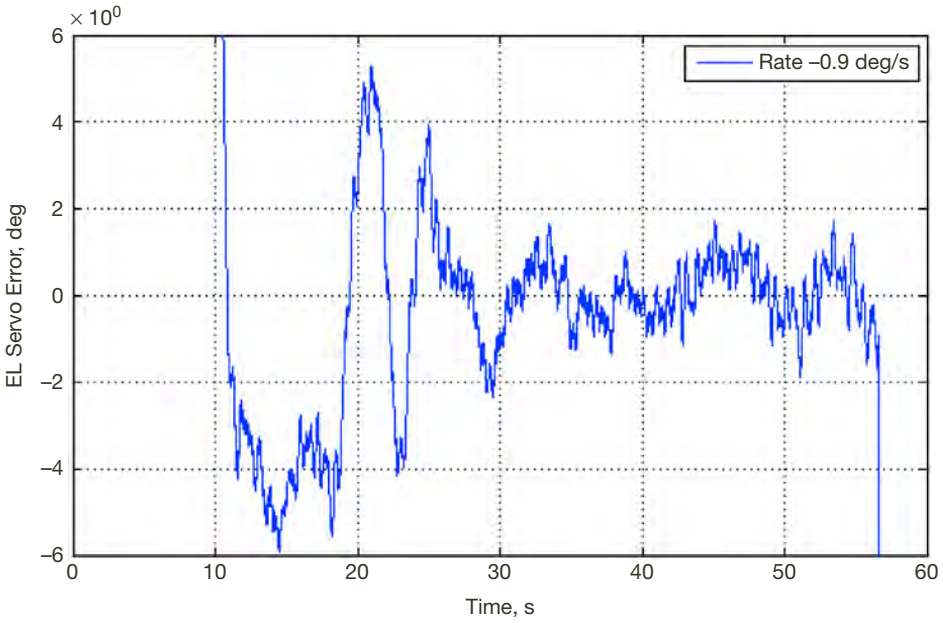

Figure D-36. Elevation rms mean servo error of 0.6 mdeg when a negative large rate offset of 0.9 deg/s is applied to the elevation drives. The mean servo error does meet the requirement of less than 0.001 deg rms. The measurement was performed during high wind of 29 mph.

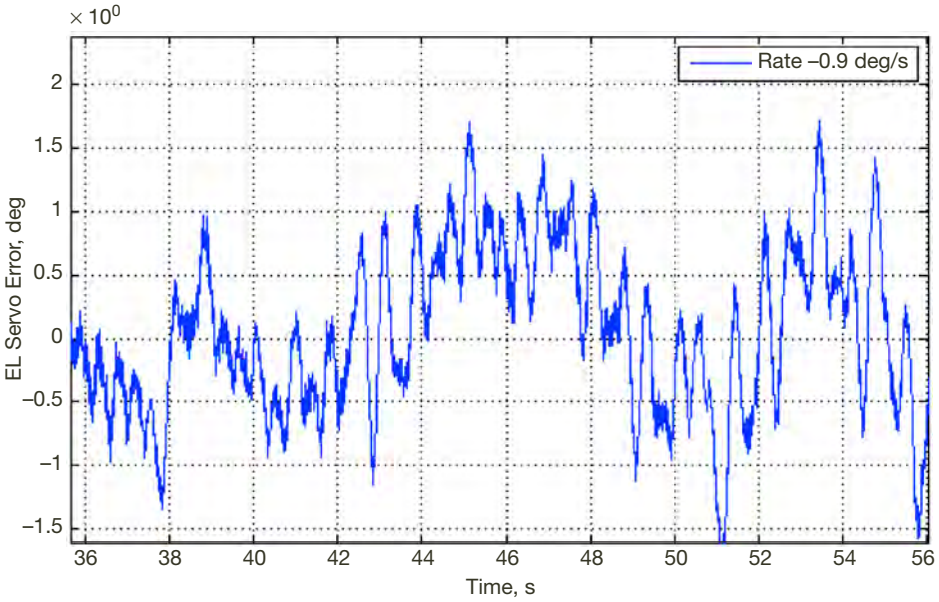

Figure D-37. Zoom of Figure D-36 to show rms servo error of 0.6 deg.

Appendix E

Azimuth Open-Loop Performance and Comparison with DSS-27

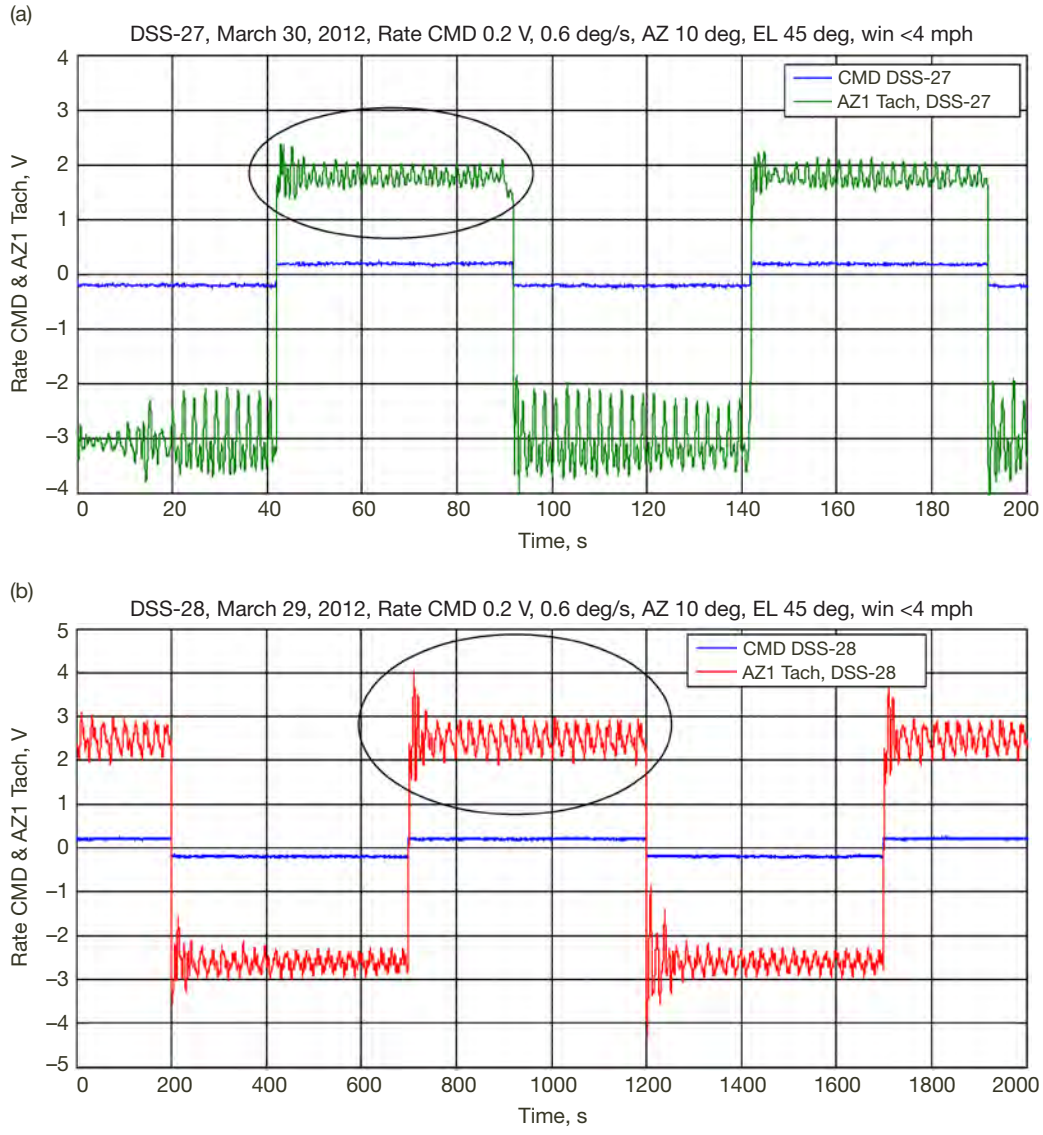

Figure E-1. AZ1 tachometer step responses for (a) DSS-27 and (b) DSS-28. Frequency (timescale) 0.01 Hz (T=100 s) and 0.001 Hz (T=1000 s) for DSS-27 and DSS-28, respectively. DSS-27 has 0.03 V offset and shows asymmetric amplitude oscillation performance on clockwise (0.4 V p–p) and counterclockwise (1.4 V p–p) directions. See Figure E-2 for detailed oscillations as indicated by ellipse.

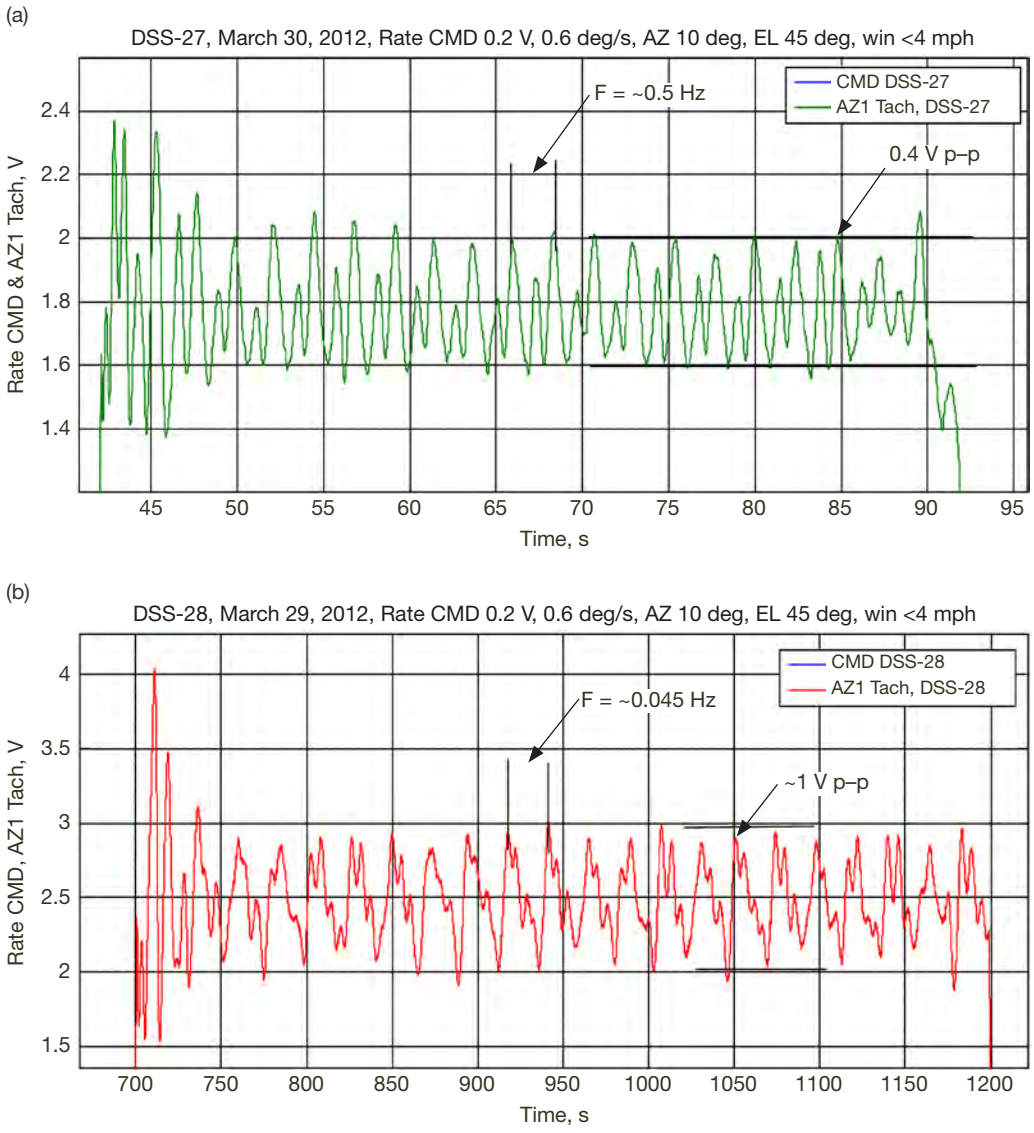

Figure E-2. AZ1 tachometer zoomed at clockwise direction from Figure E-1 to show amplitude and frequency of oscillations for (a) DSS-27 and (b) DSS-28. DSS-28 has much lower oscillation than DSS-27 by a factor of 10 and amplitude of oscillation is twice that of DSS-27.

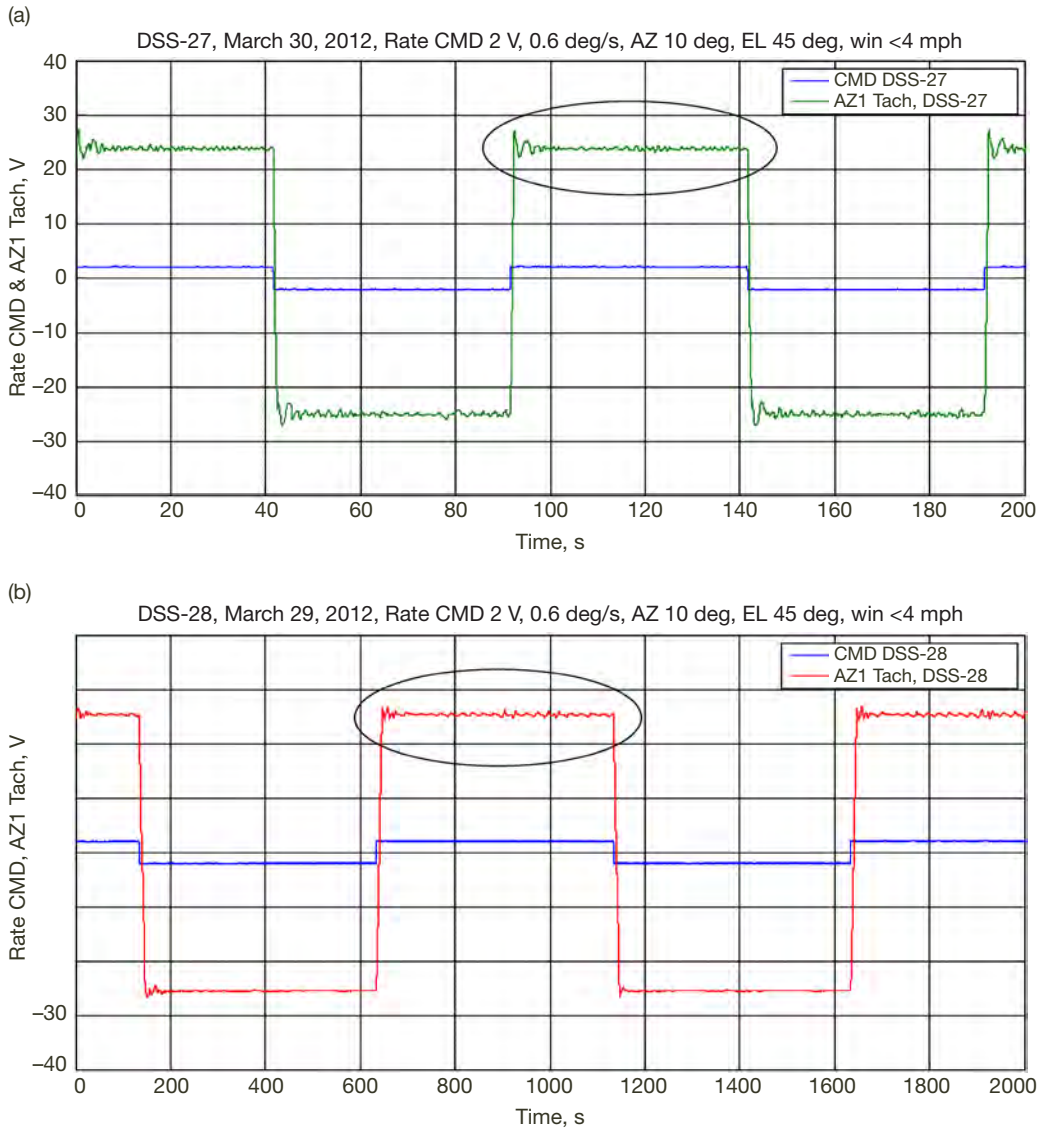

Figure E-3. AZ1 tachometer responses of (a) DSS-27 and (b) DSS-28 to 0.6 deg/s rate command. Frequency (timescale) 0.01 Hz (T=100 s) and 0.001 Hz (T=1000 s) for DSS-27 and DSS-28, respectively. See Figure E-4 for oscillations detail.

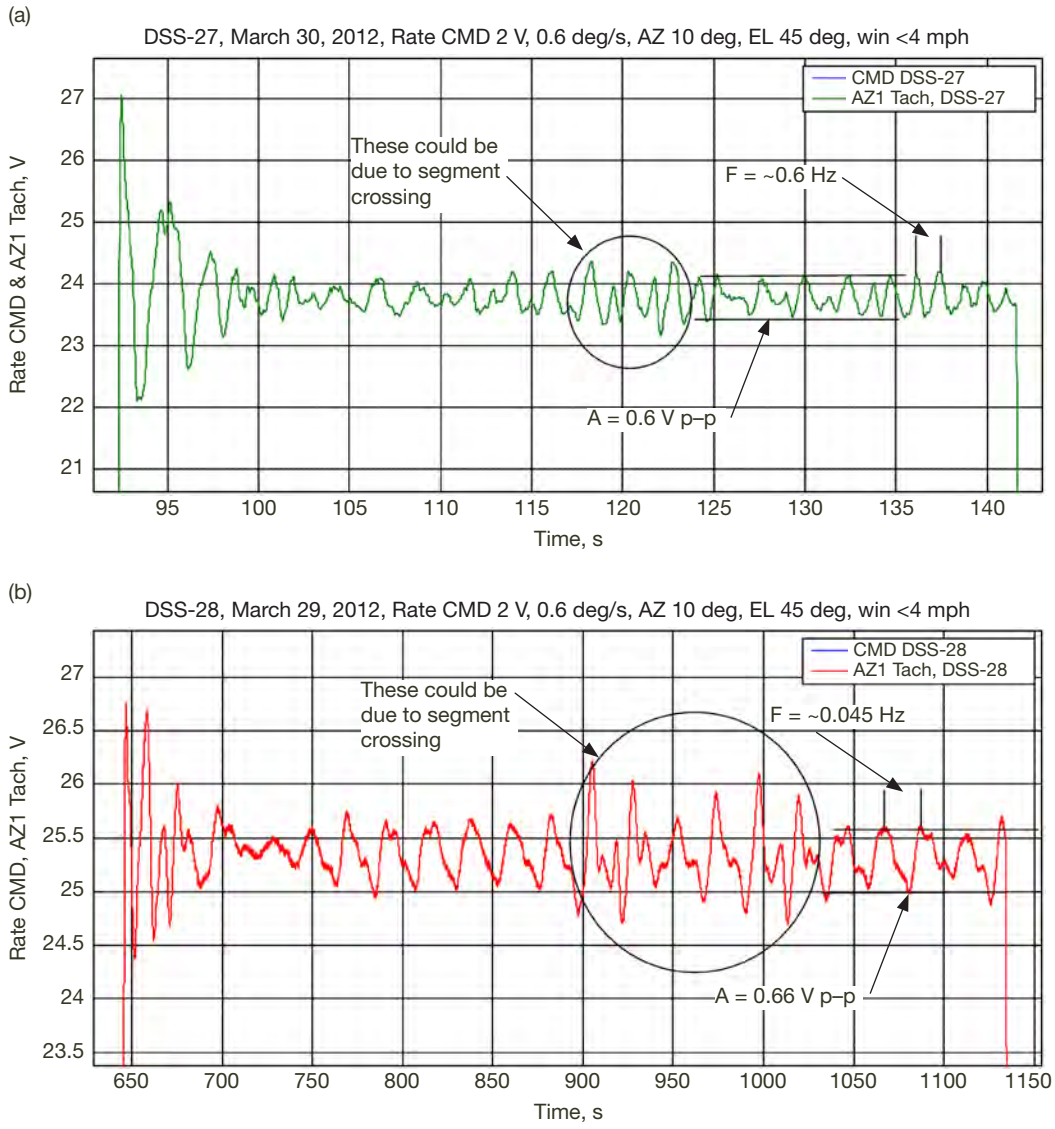

Figure E-4. AZ1 tachometer responses of (a) DSS-27 and (b) DSS-28 zoomed from Figure E-3 at clockwise direction to show amplitude and frequency of oscillations. High amplitude for both antennas as circled may be due to the runner segment crossing.

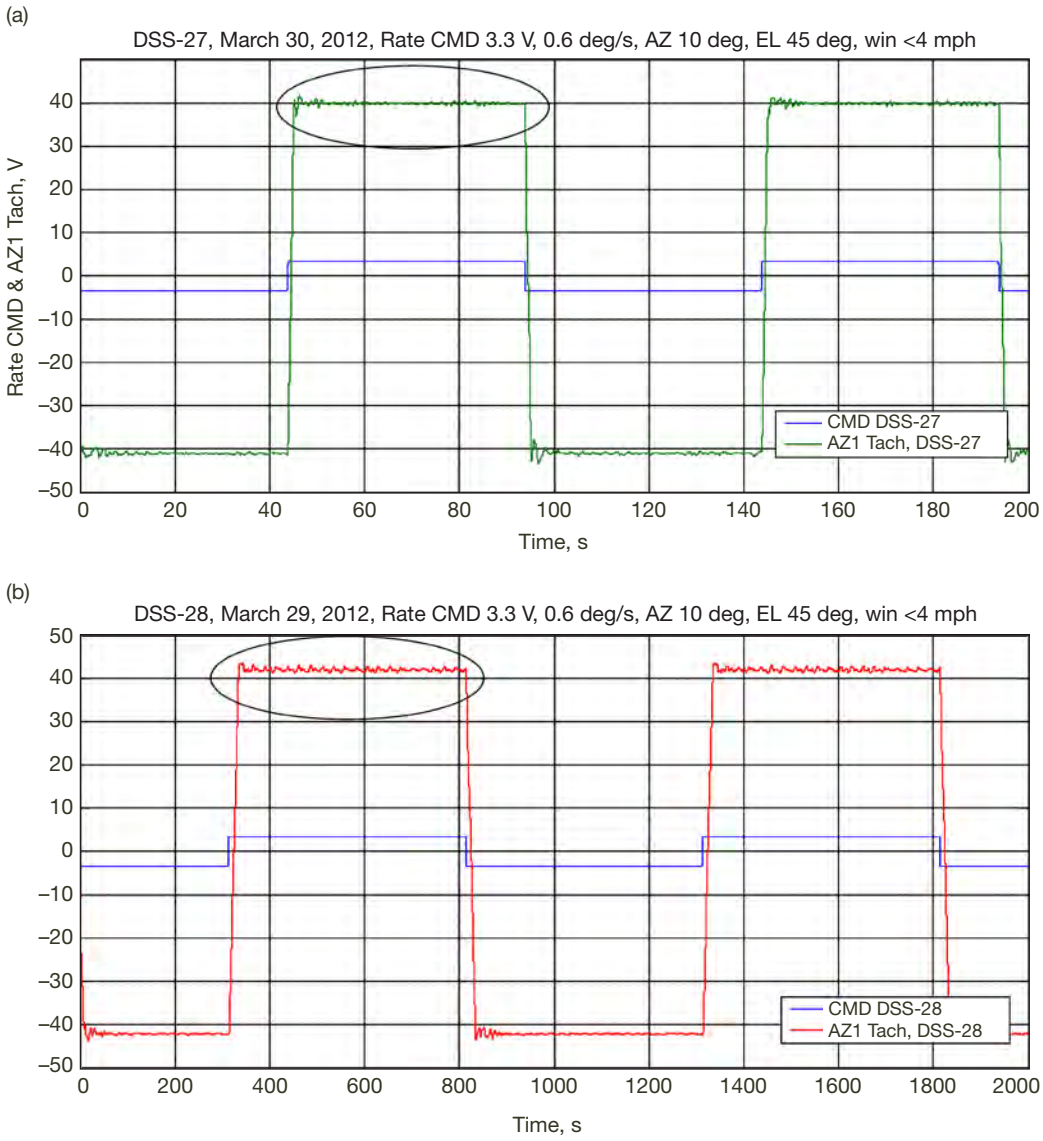

Figure E-5. AZ1 tachometer responses of (a) DSS-27 and (b) DSS-28 to 1 deg/s rate command. Frequency (timescale) 0.01 Hz (T=100 s) and 0.001 Hz (T=1000 s) for DSS-27 and DSS-28, respectively. See Figure E-6 for oscillation detail.

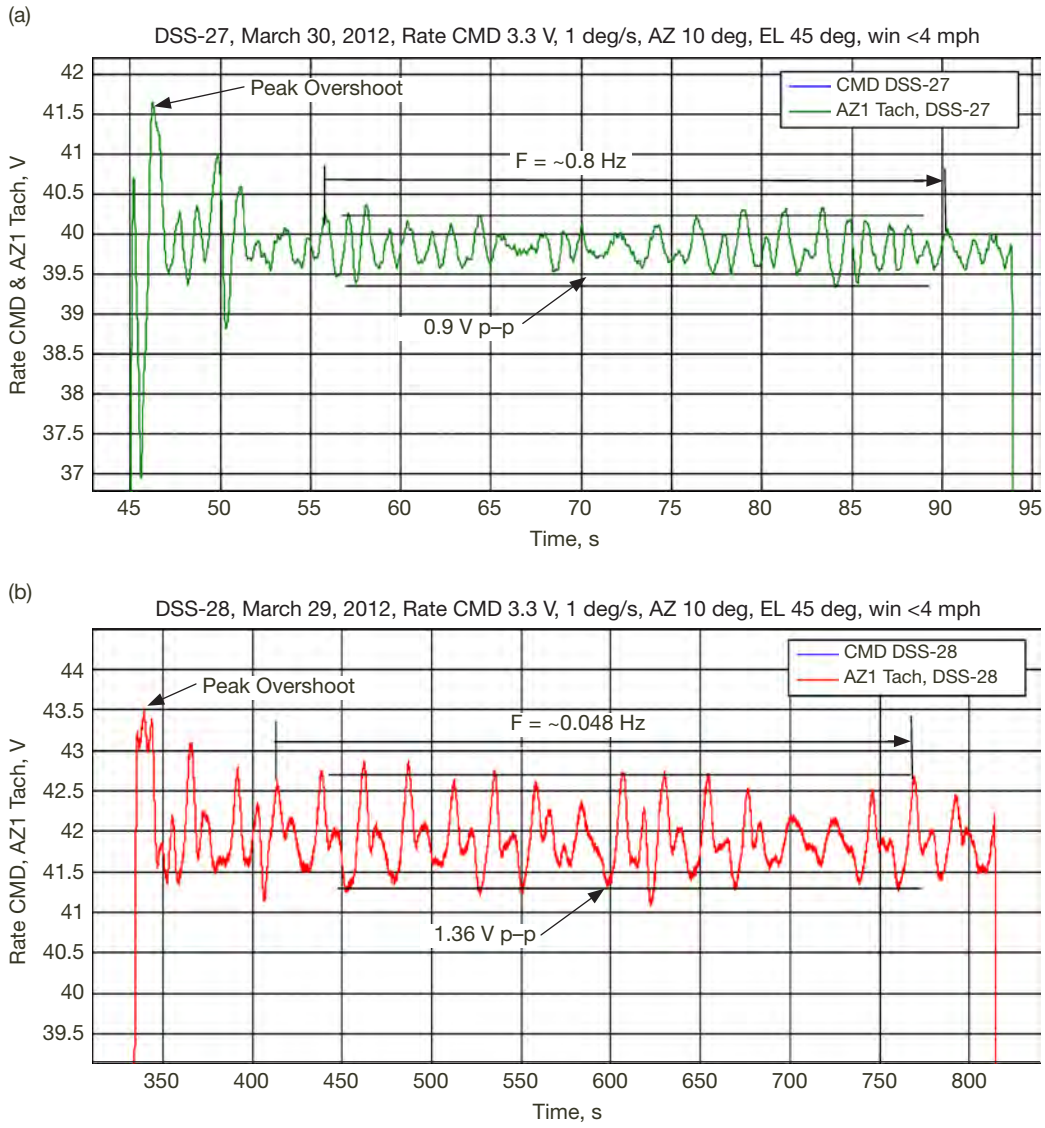

Figure E-6. AZ1 tachometer responses of (a) DSS-27 and (b) DSS-28 zoomed from Figure E-5 as indicated by ellipse to show amplitude and frequency of oscillations. The frequency of oscillation is determined by taking the number of pulses divided by duration of the pulses. DSS-28 has lower frequency oscillation than DSS-27. The amplitude of oscillations is very close. However, they both have undamped oscillation.

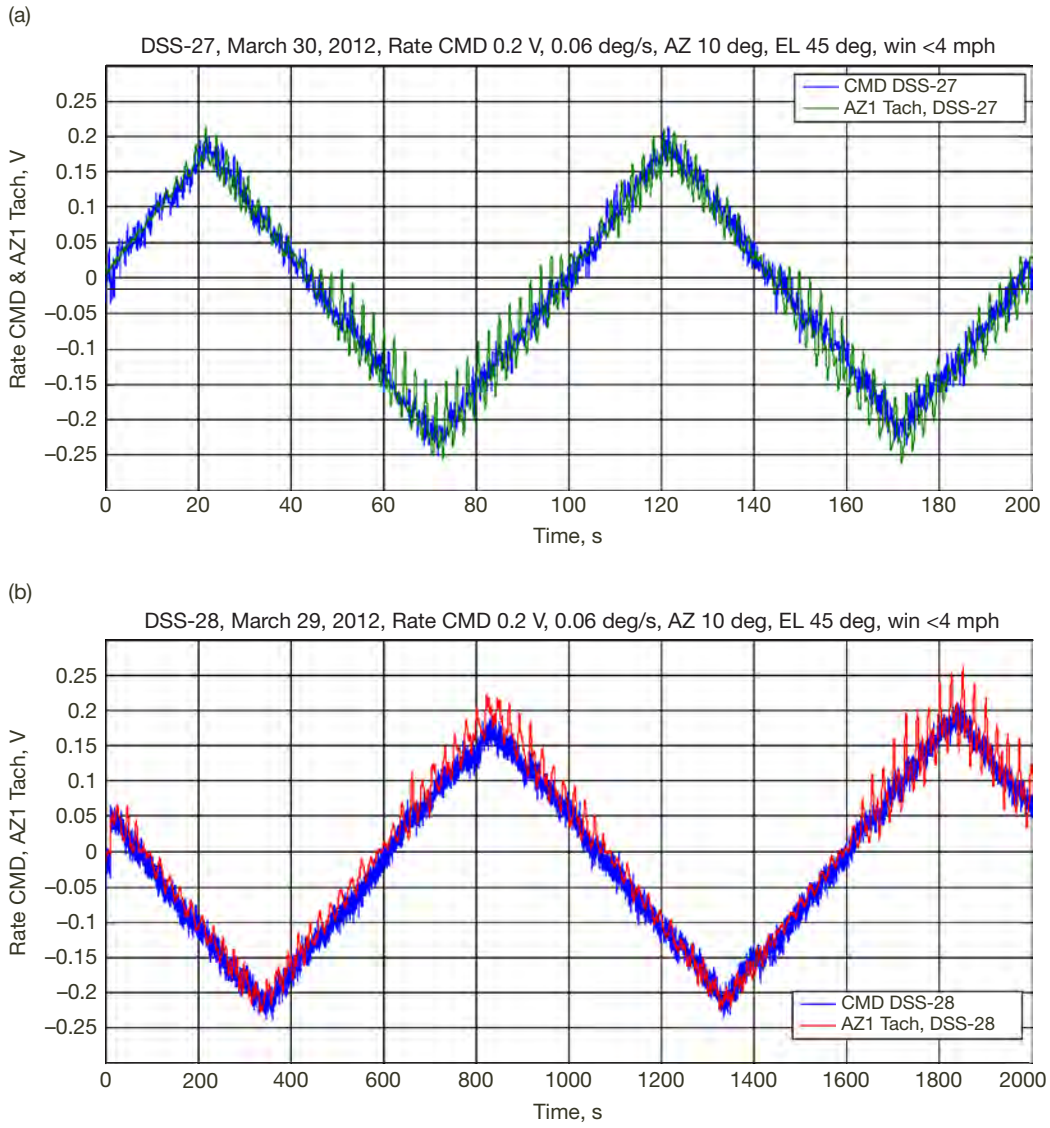

Figure E-7. AZ1 tachometer responses for (a) DSS-27 and (b) DSS-28. Tachometer signals are scaled by 12 to show linearity as well as symmetry. DSS-27 tachometer response has very low (0.03 V) offset. Input signal frequency for DSS-27 is 0.01 Hz (T=100 s) and 0.001 Hz (T=1000 s) for DSS-28.

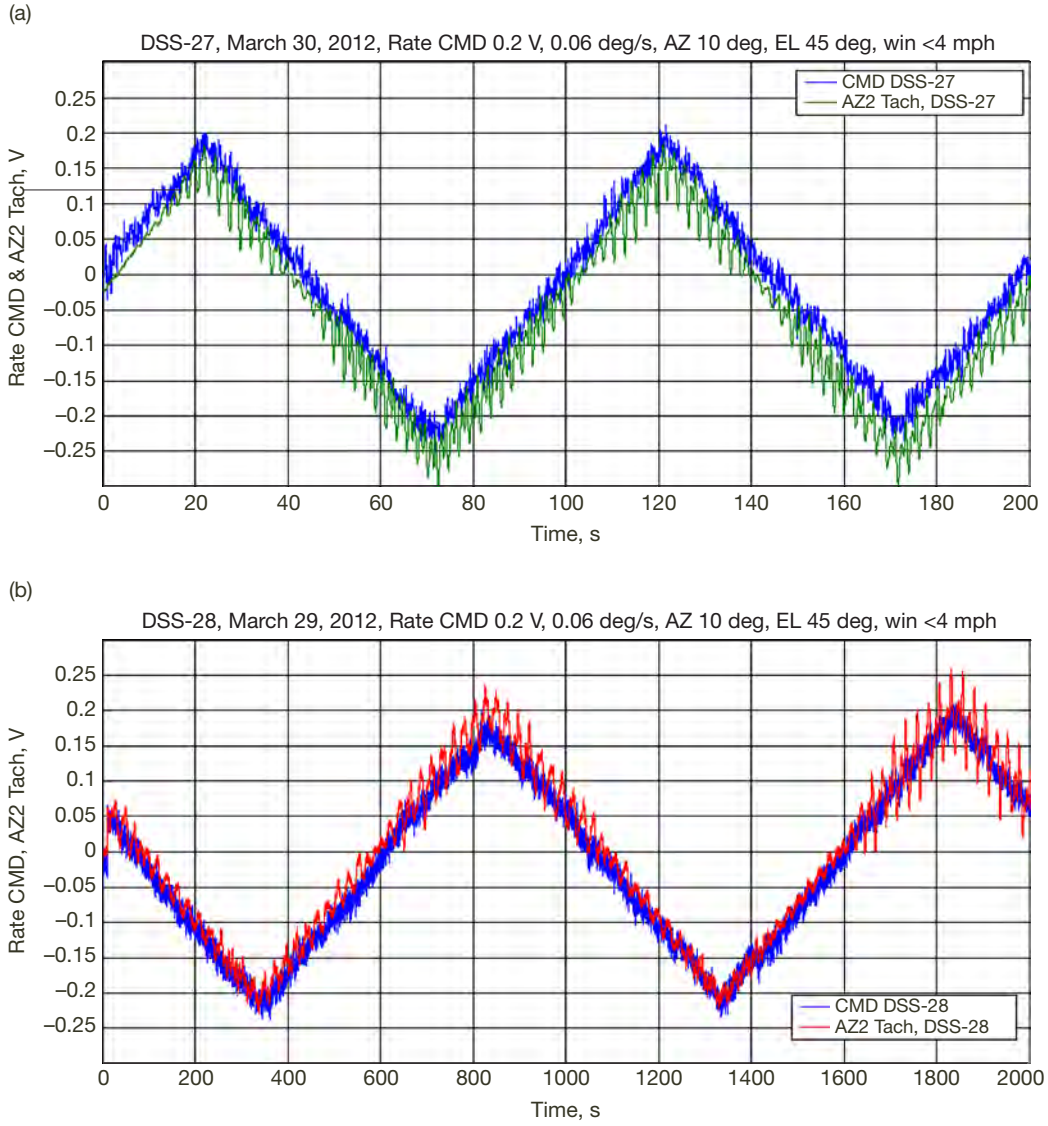

Figure E-8. AZ2 tachometer responses for (a) DSS-27 and (b) DSS-28. Tachometer signals are inverted and scaled by 12 to show linearity as well as symmetry. DSS-27 tachometer response has very low (0.03 V) offset. Input signal frequency for DSS-27 is 0.01 Hz (T=100 s) and 0.001 Hz (T=1000 s) for DSS-28.

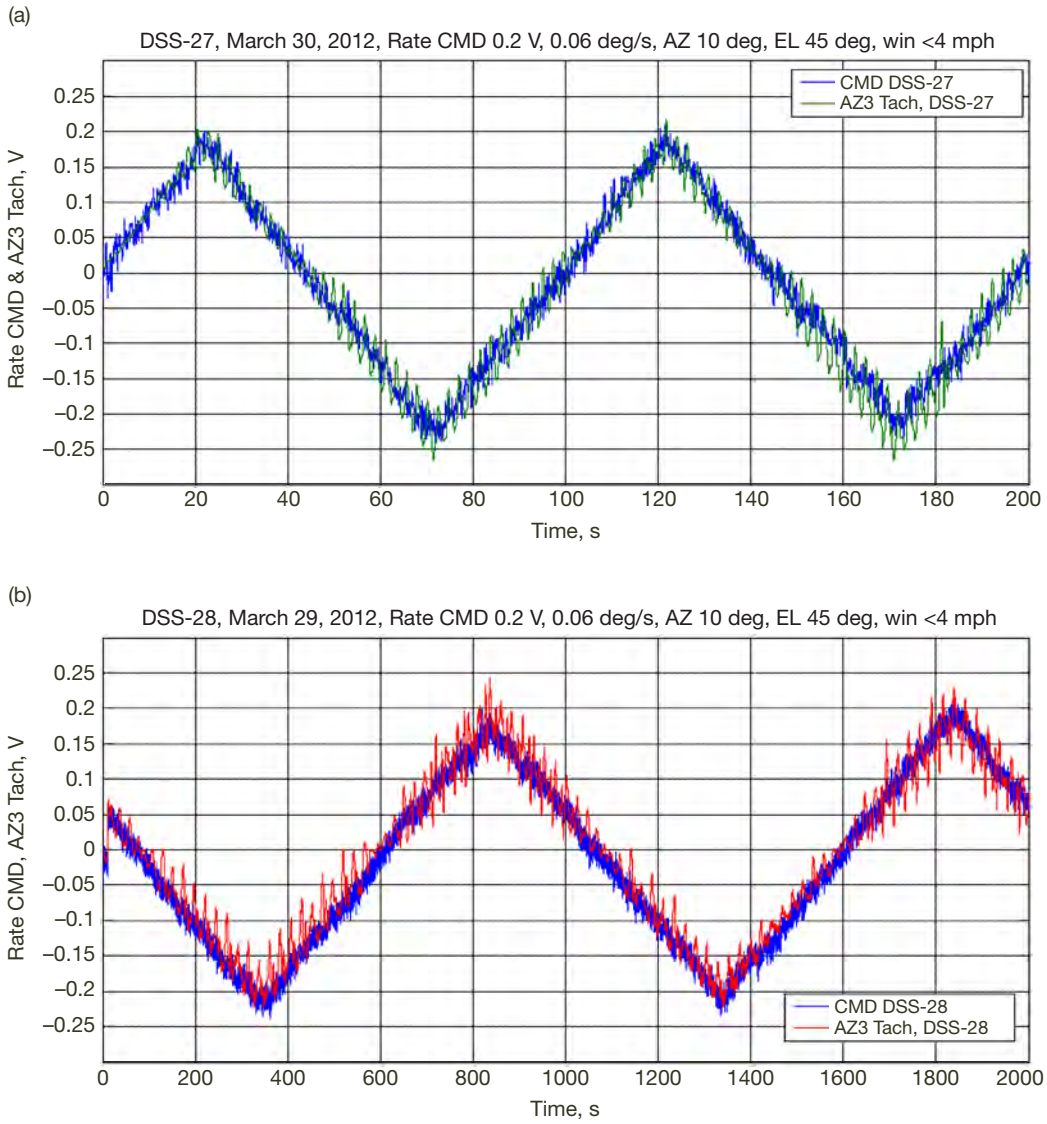

Figure E-9. AZ3 tachometer responses for (a) DSS-27 and (b) DSS-28. Tachometer signals are scaled by 12 to show linearity as well as symmetry. DSS-27 tachometer response has very low (0.03 V) offset. Input signal frequency for DSS-27 is 0.01 Hz (T=100 s) and 0.001 Hz (T=1000 s) for DSS-28.

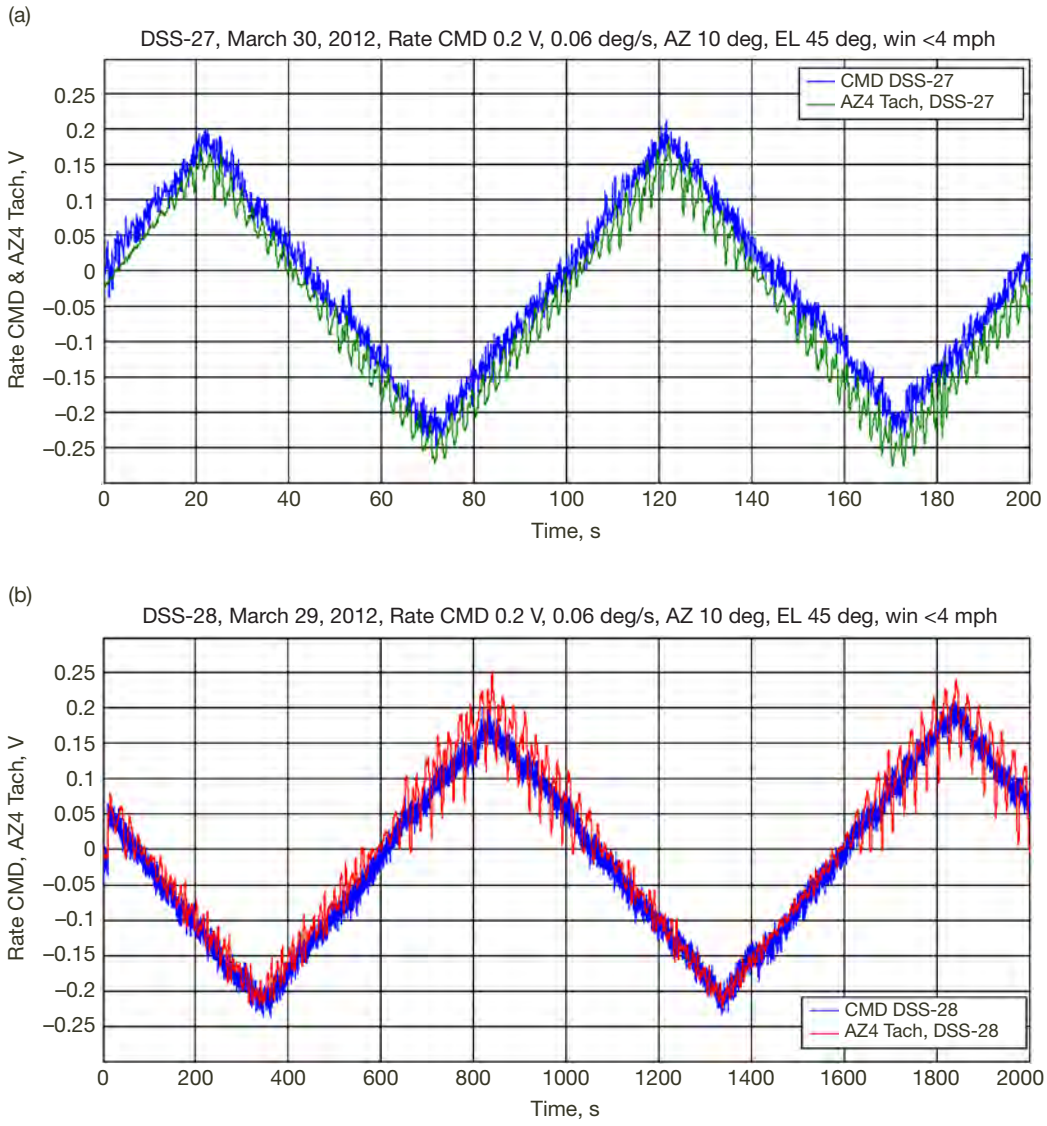

Figure E-10. AZ4 tachometer responses for (a) DSS-27 and (b) DSS-28. Tachometer signals are inverted and scaled by 12 to show linearity as well as symmetry. DSS-27 tachometer response has very low (0.03 V) offset. Input signal frequency for DSS-27 is 0.01 Hz (T=100 s) and 0.001 Hz (T=1000 s) for DSS-28.

Appendix F

Elevation Open-Loop Performance and Comparison with DSS-27

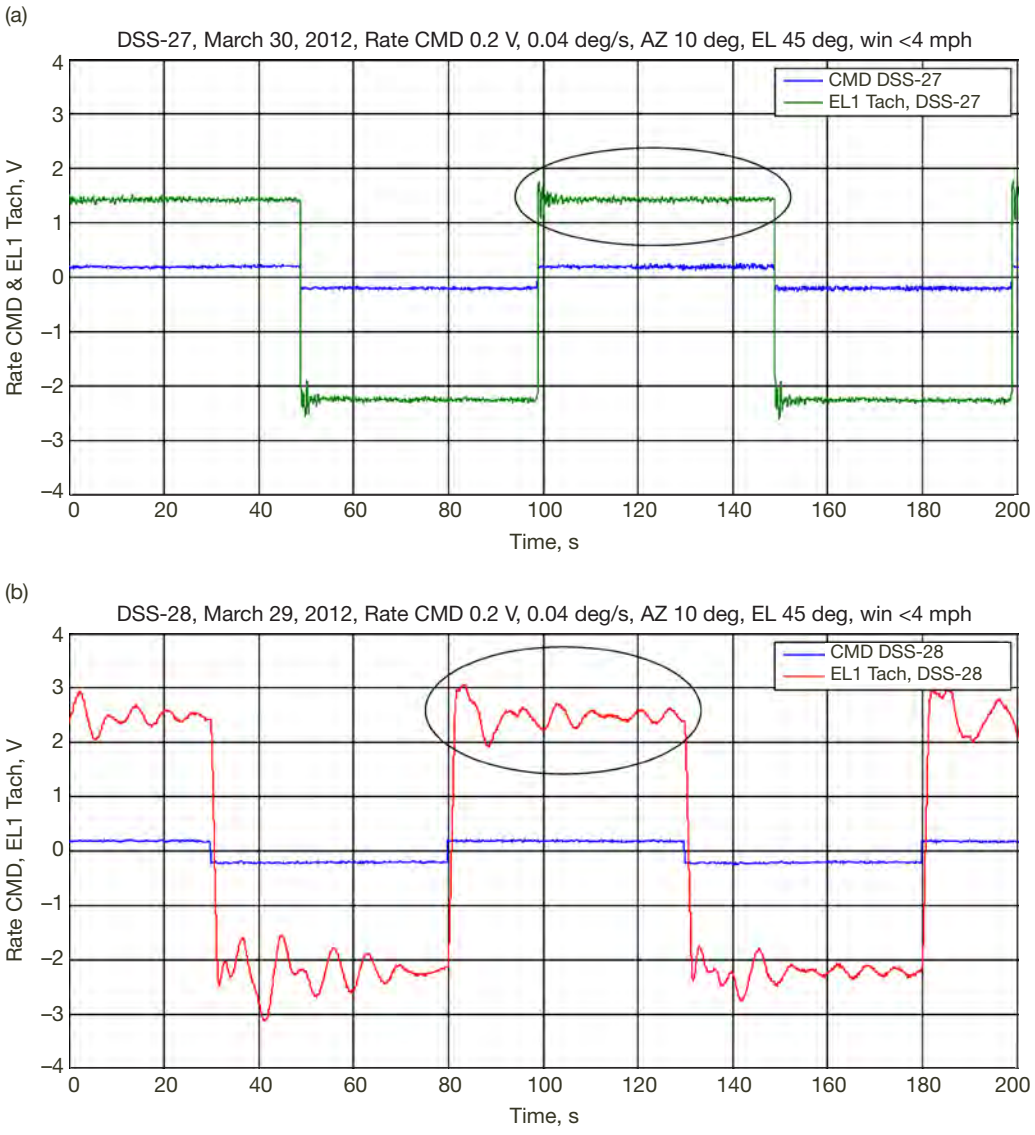

Figure F-1. EL1 tachometer responses of (a) DSS-27 and (b) DSS-28. Frequency (time cale) 0.01 Hz (T=100 s). See Figure F-2 for oscillation detail. Rise time for DSS-27 is 0.2 s compared to DSS-28 at 1 s. DSS-27 has faster time (by a factor of 5) than DSS-28.

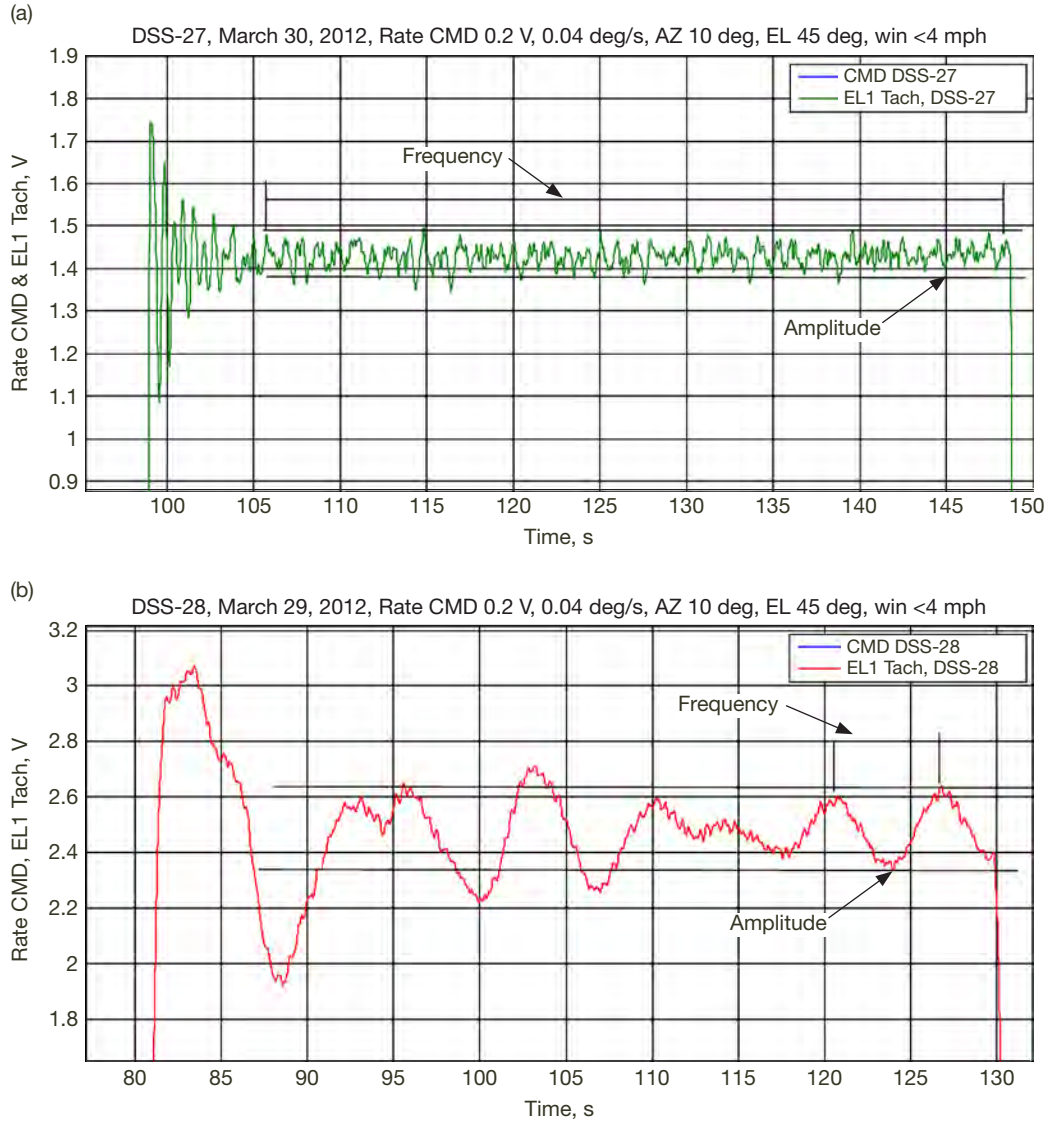

Figure F-2. EL1 tachometer responses of (a) DSS-27 and (b) DSS-28 zoomed from Figure F-1 as indicated by ellipse to show amplitude and frequency of oscillations. The frequency of oscillation (0.15 Hz) is determined by taking the number of pulses divided by duration of the pulses for DSS-27. DSS-28 has a lower frequency oscillation (1.2 Hz) than DSS-27. The amplitude of oscillations of DSS-28 (0.3 V p–p) is higher than DSS-27 (0.1 V p–p).

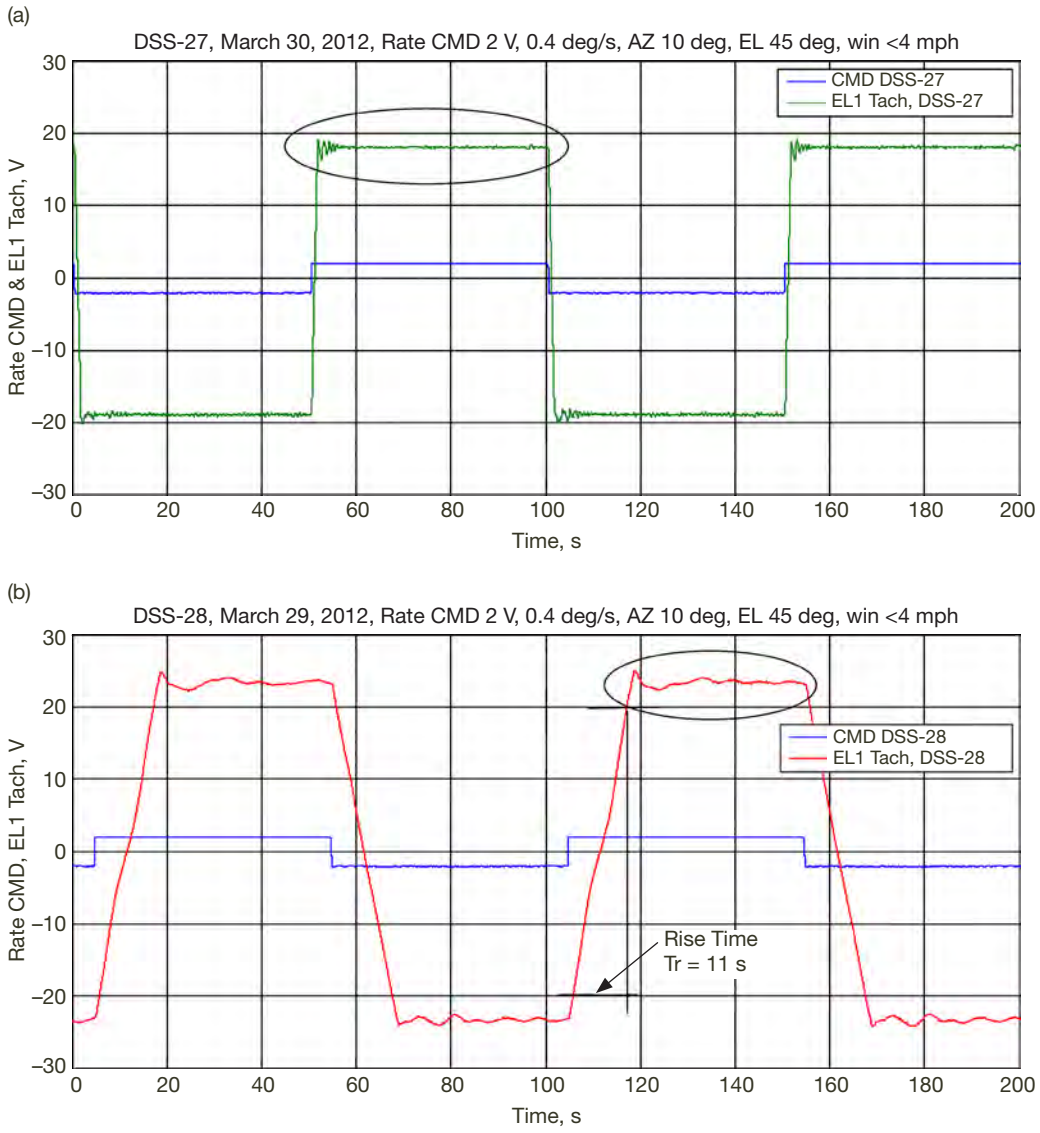

Figure F-3. EL1 tachometer responses for (a) DSS-27 and (b) DSS-28. The rise time of DSS-27 (1 s) is over 10 times faster than DSS-28 rise time (11 s). See Figure F-4 for oscillations detail.

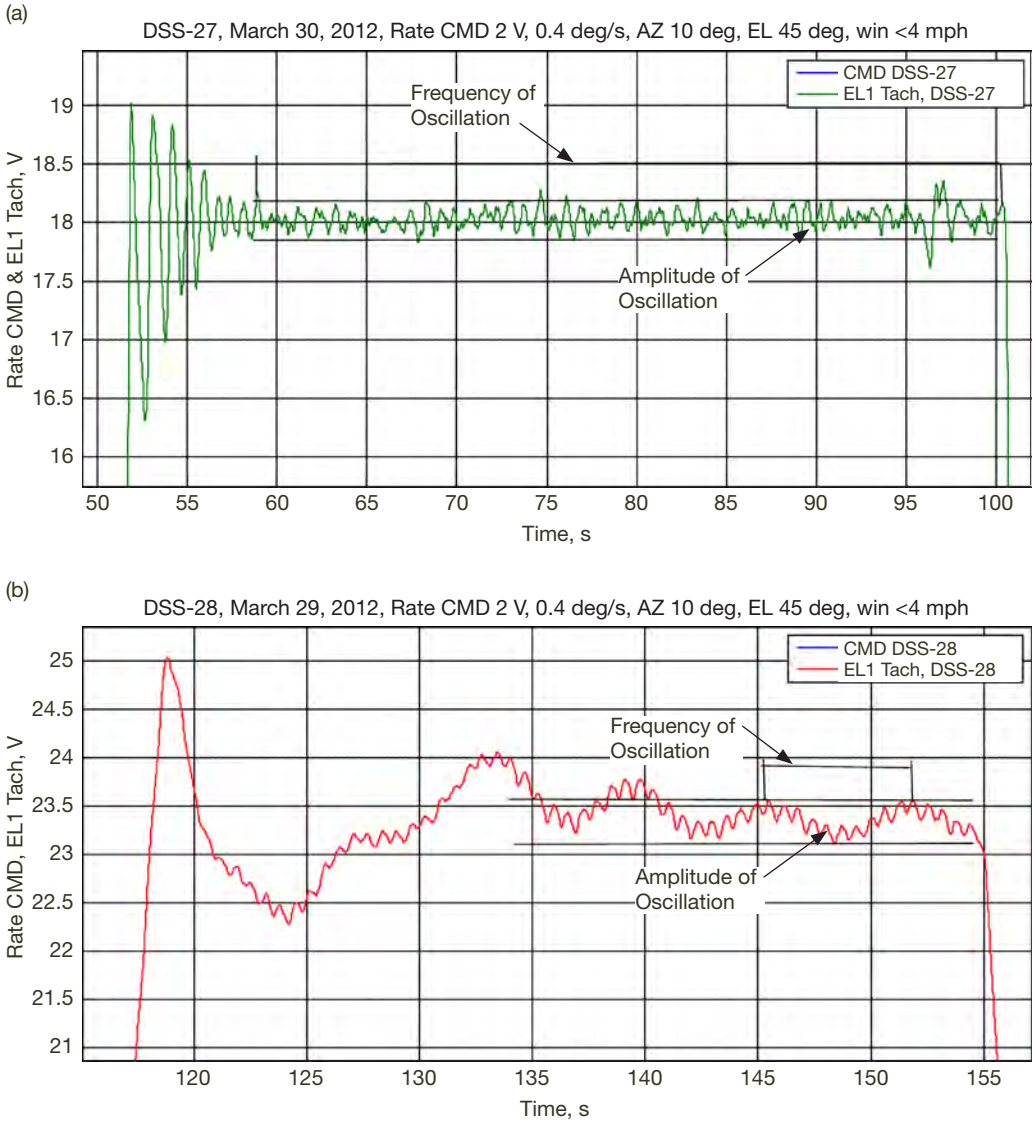

Figure F-4. EL1 tachometer responses of (a) DSS-27 and (b) DSS-28 zoomed from Figure F-3 as indicated by ellipse to show amplitude and frequency of oscillations. The frequency of oscillation (0.15 Hz) is determined by taking the number of pulses divided by duration of the pulses for DSS-27. DSS-28 has a lower frequency oscillation (1.2 Hz) than DSS-27. The amplitude of oscillations of DSS-28 (0.6 V p–p) is higher than DSS-27 (0.19 V p–p).

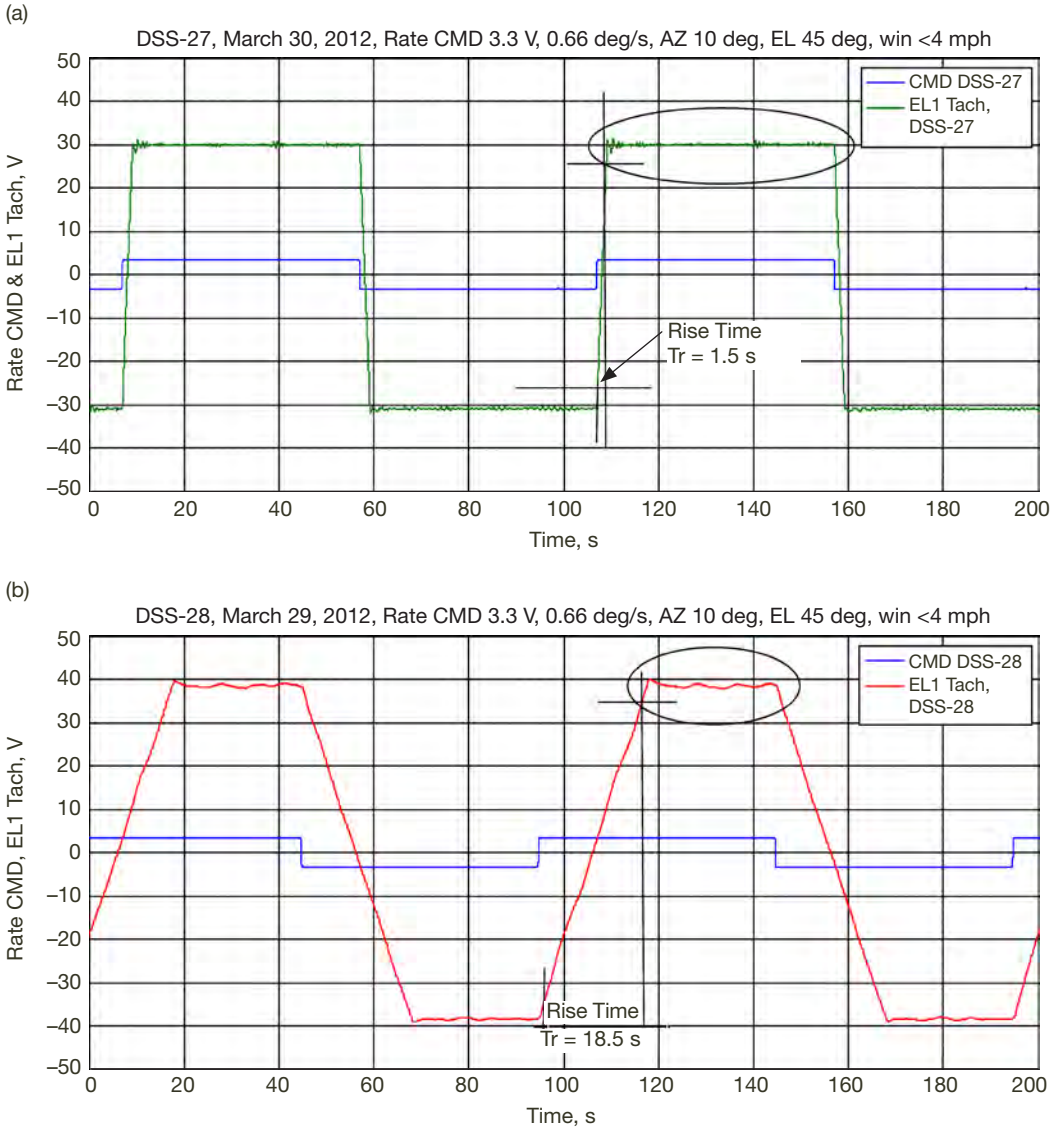

Figure F-5. EL1 tachometer responses for (a) DSS-27 and (b) DSS-28. The rise time of DSS-27 (1.6 s) is over 10 times faster than DSS-28 rise time (18.5 s). See Figure F-6 for oscillation detail.

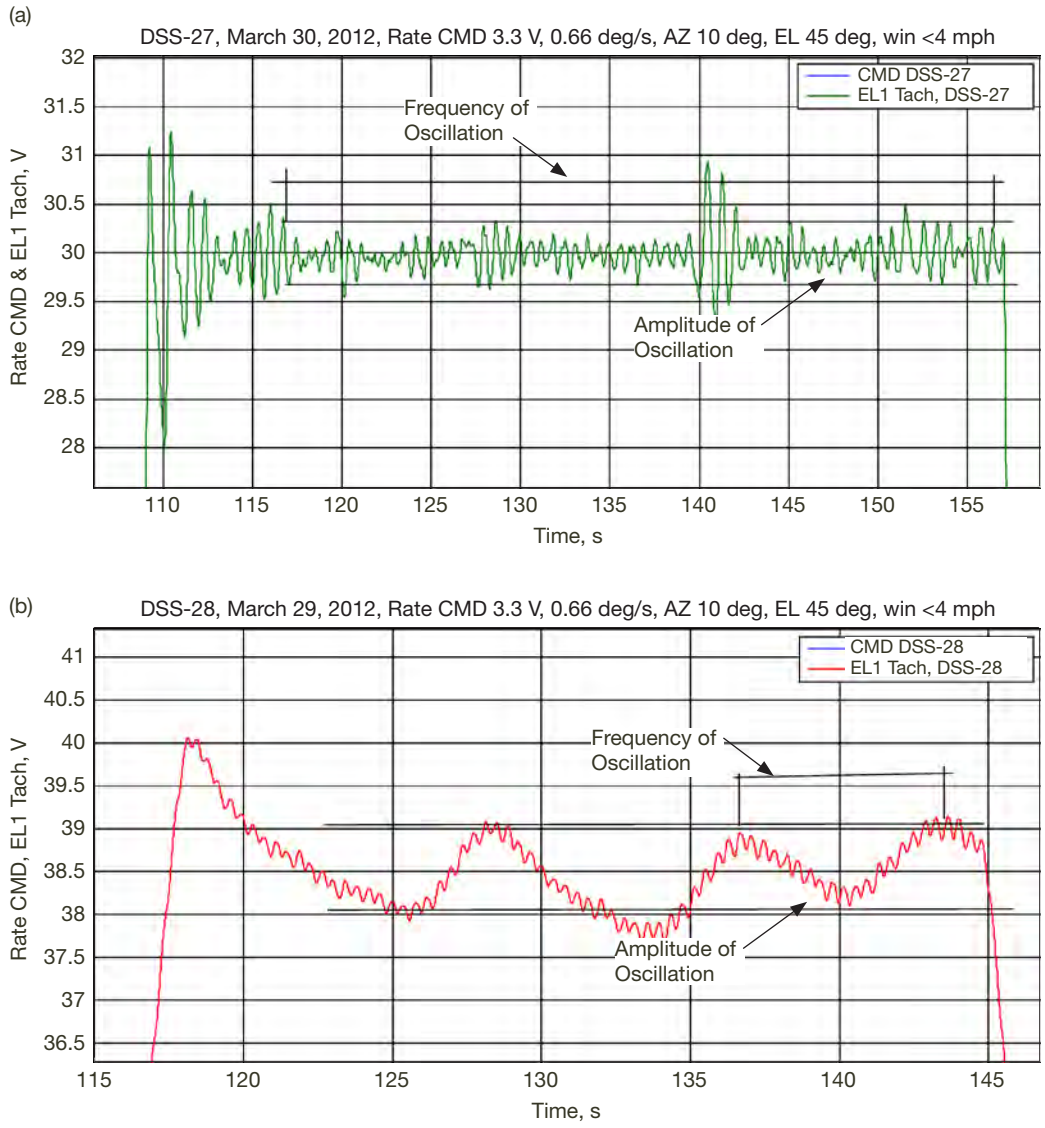

Figure F-6. EL1 tachometer step responses for (a) DSS-27 and (b) DSS-28 to 0.66 deg/s rate command zoomed from Figure F-5 as indicated by ellipse. The frequency of oscillation of DSS-27 is 0.8 Hz; DSS-28 has a lower frequency of 0.2 Hz. The amplitude of oscillations for DSS-27 and DSS-28 are 0.5 V p–p and 1.0 V p–p, respectively.

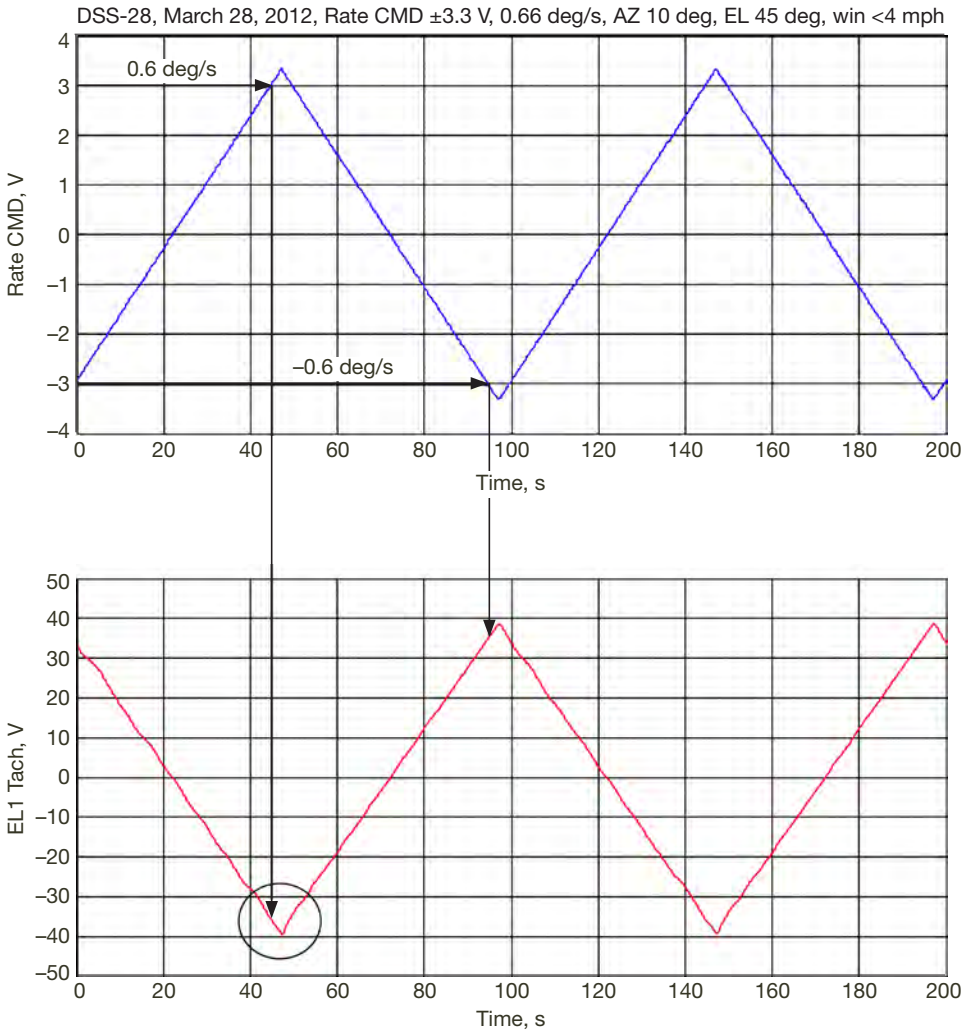

Figure F-7. EL1 tachometer response for DSS-28 as rate crosses ±0.6 deg/s (3 VDC) corresponds to ±35 VDC tachometer response. The response does not show discontinuity at 0.6 deg/s. See Figure F-8 for zoomed area.

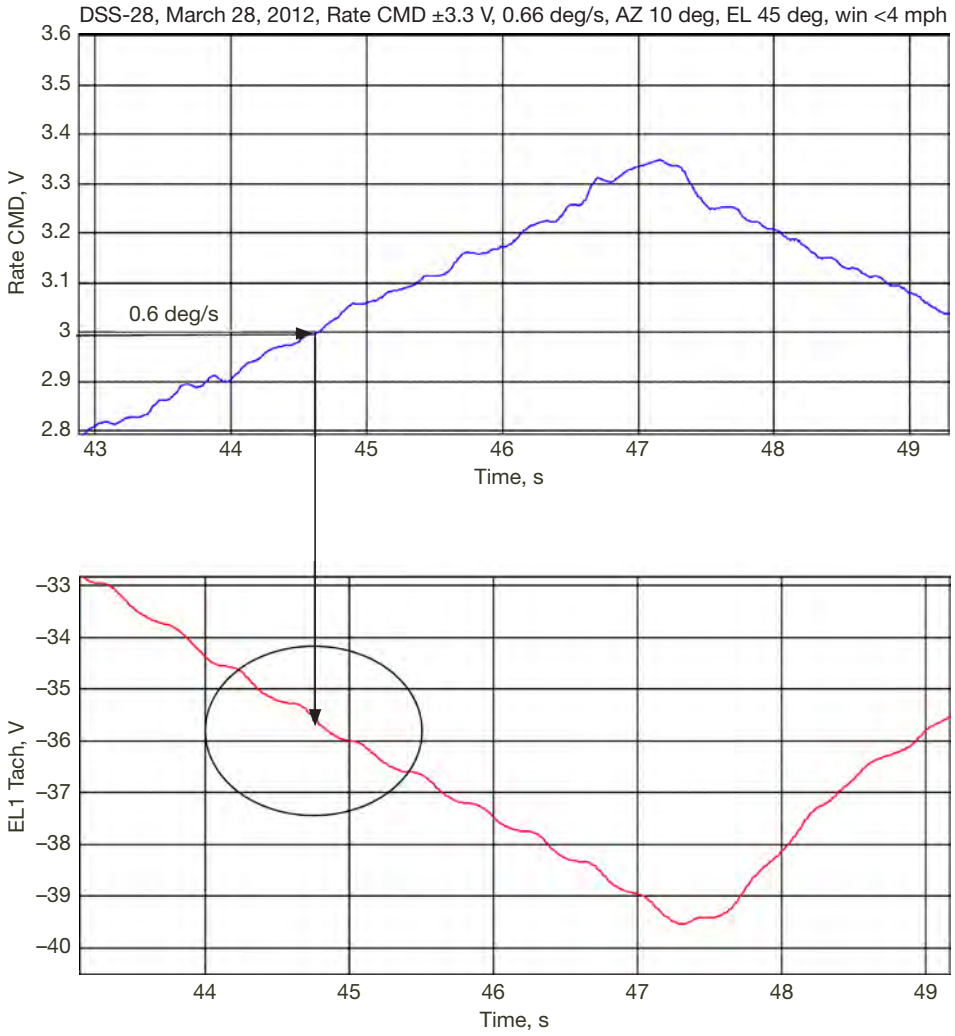

Figure F-8. EL1 tachometer response for DSS-28 zoomed from Figure F-7 at rate 0.6 deg/s (3 VDC) corresponds to ~–35 VDC tachometer voltage. There is no discontinuity around this area other than undamped oscillations, which may contribute to oscillation reported in position-loop analysis.

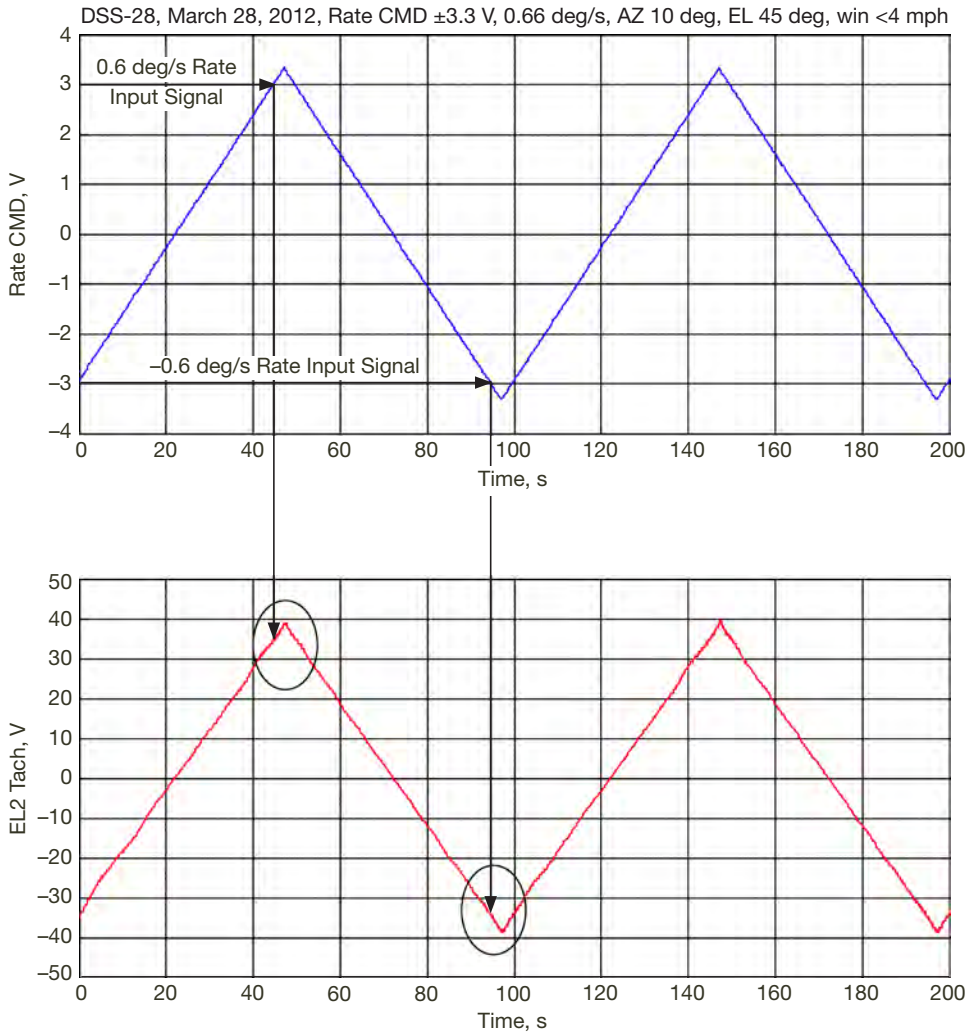

Figure F-9. A ±3.3 V input triangle signal is applied at DSS-28 to determine if there is discontinuity as the rate crosses 3 V (0.6 deg/s) in both directions. Tachometer response for ± 0.6 deg/s corresponds to ±35V EL2 tachometer voltage. See Figure F-10 for zoomed area.

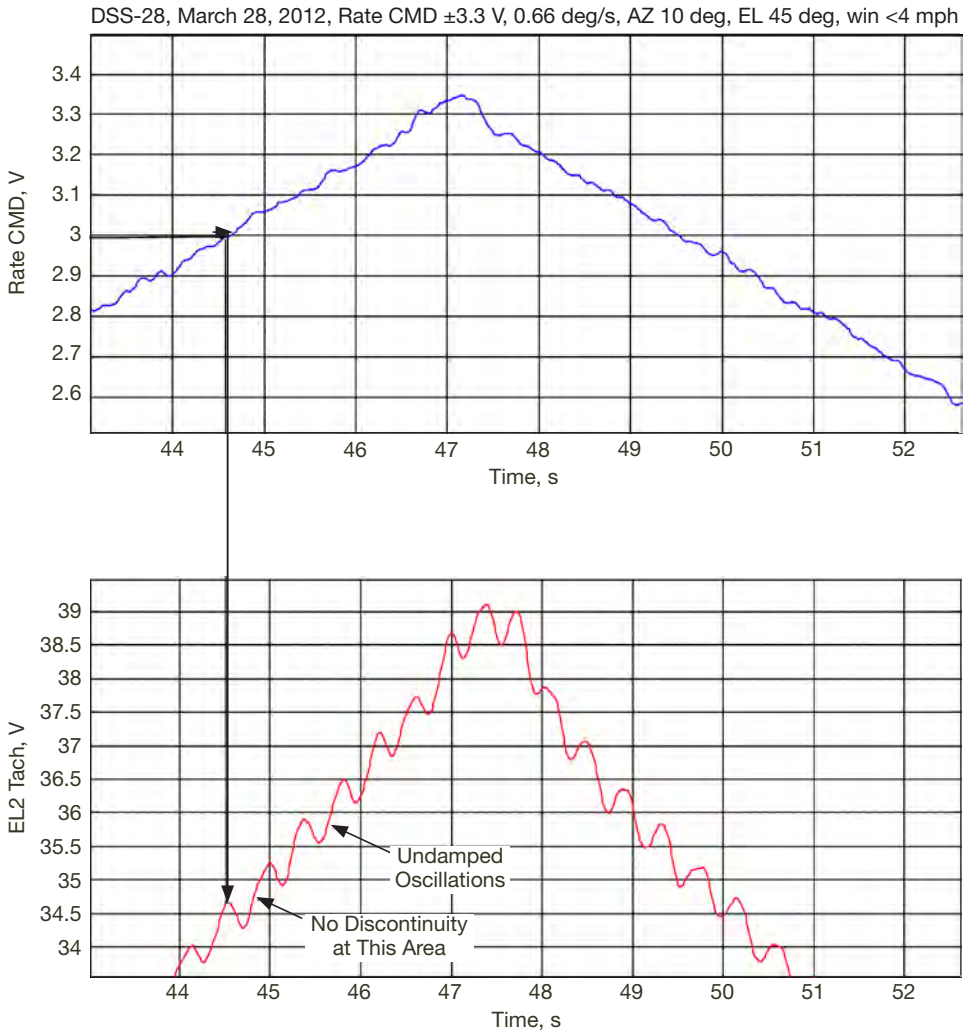

Figure F-10. EL2 tachometer response for DSS-28 zoomed from Figure F-9 at rate 0.6 deg/s (3 VDC) corresponds to ~35 VDC tachometer voltage. There is no discontinuity around this area other than undamped oscillations, which may contribute to oscillation reported in position-loop analysis.

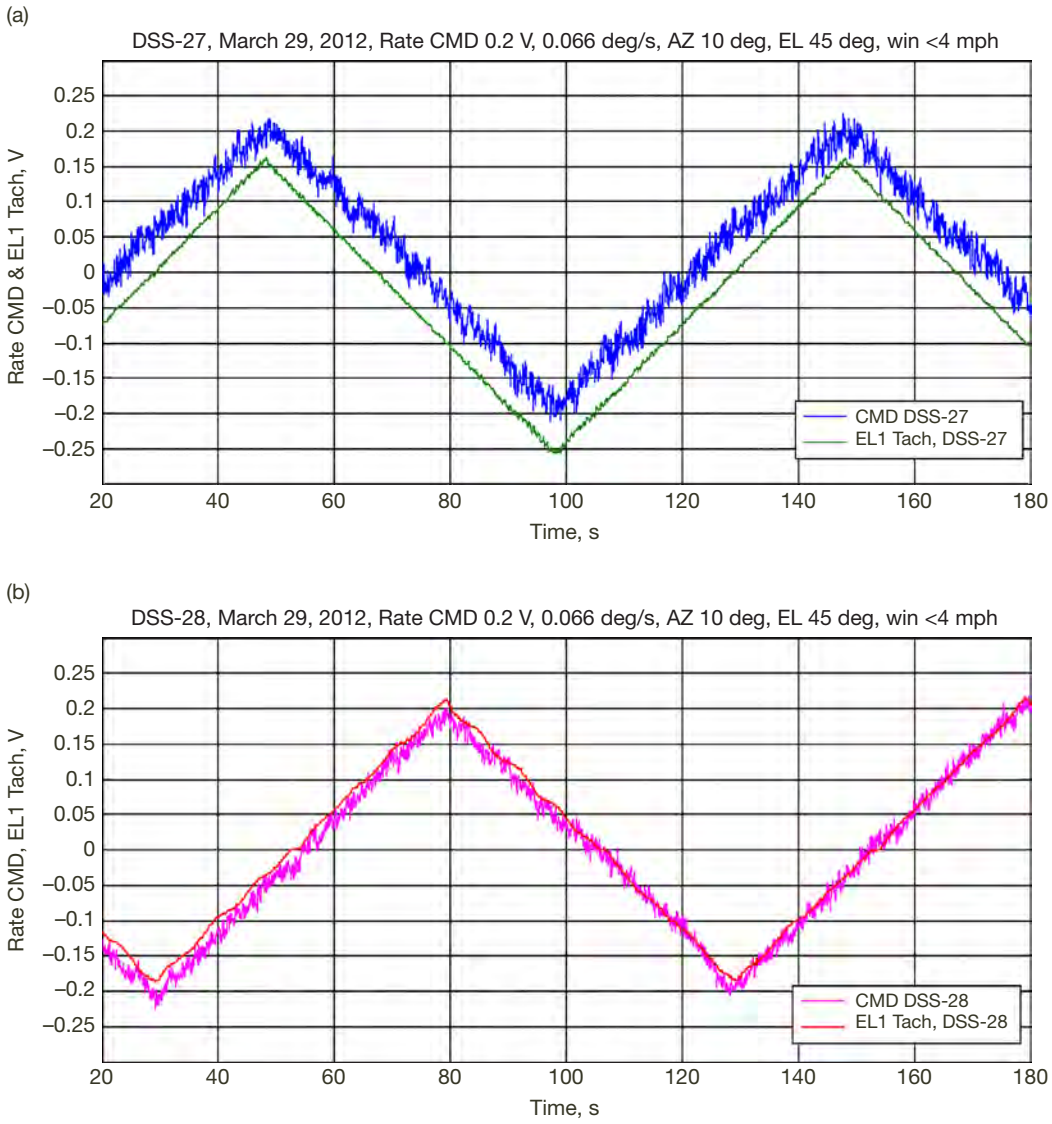

Figure F-11. EL1 tachometer response for (a) DSS-27 and (b) DSS-28. Tachometer signals are inverted and scaled by 9 for DSS-27, and by 12 for DSS-28 to overlap the input command. The output response of DSS-27 and DSS-28 generally follows the input signal. DSS-27 shows 0.05 V offset. DSS-28 shows 1.5 s discontinuity at zero crossing the same behavior as EL2.

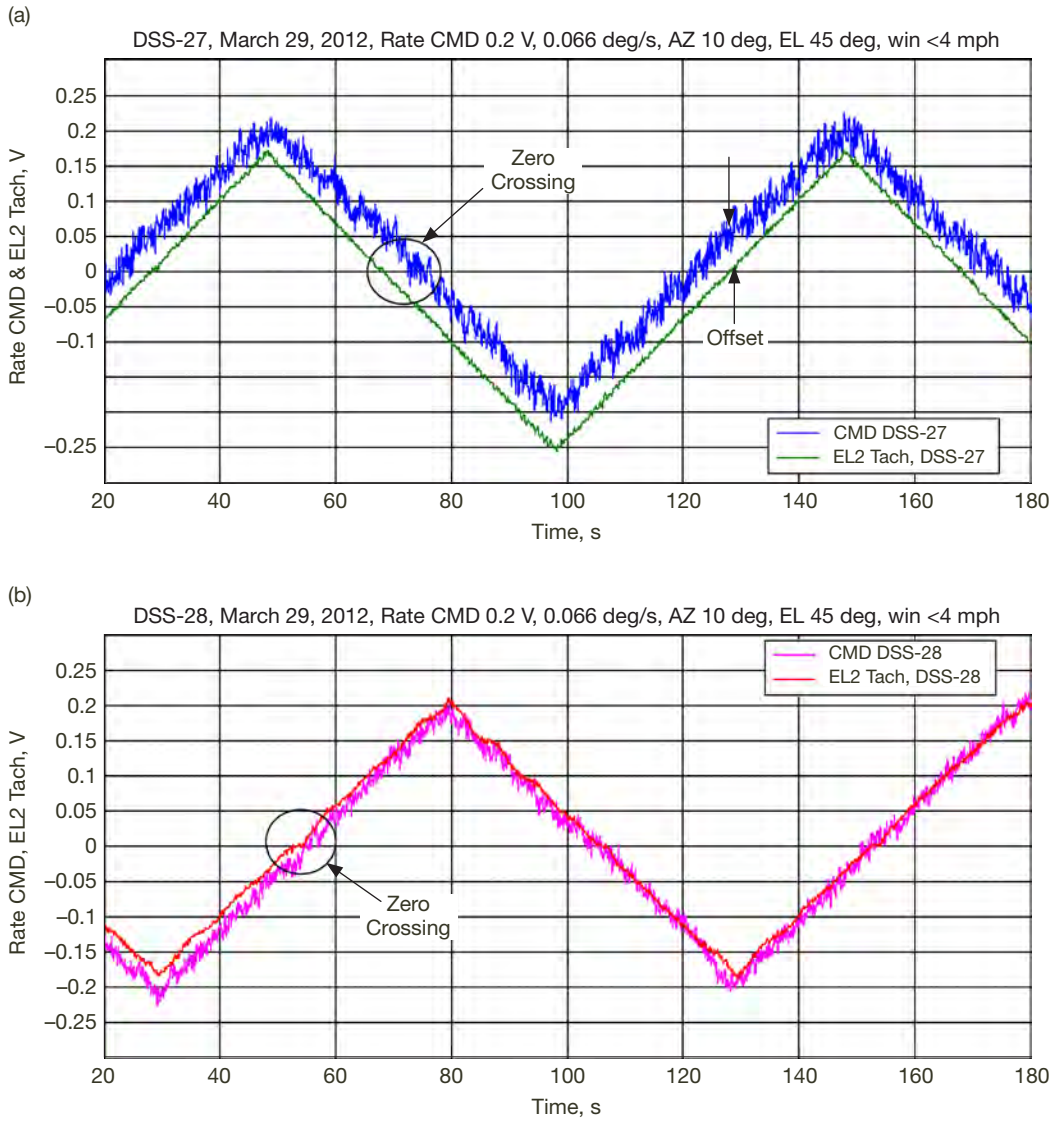

Figure F-12. EL2 tachometer response for (a) DSS-27 and (b) DSS-28. Tachometer signals are scaled by 9 for DSS-27, and by 12 for DSS-28 to overlap the input command. The output response of DSS-27 and DSS-28 generally follows the input signal. DSS-27 shows 0.05 V offset.
See Figure F-13 for detail of the zero crossing.

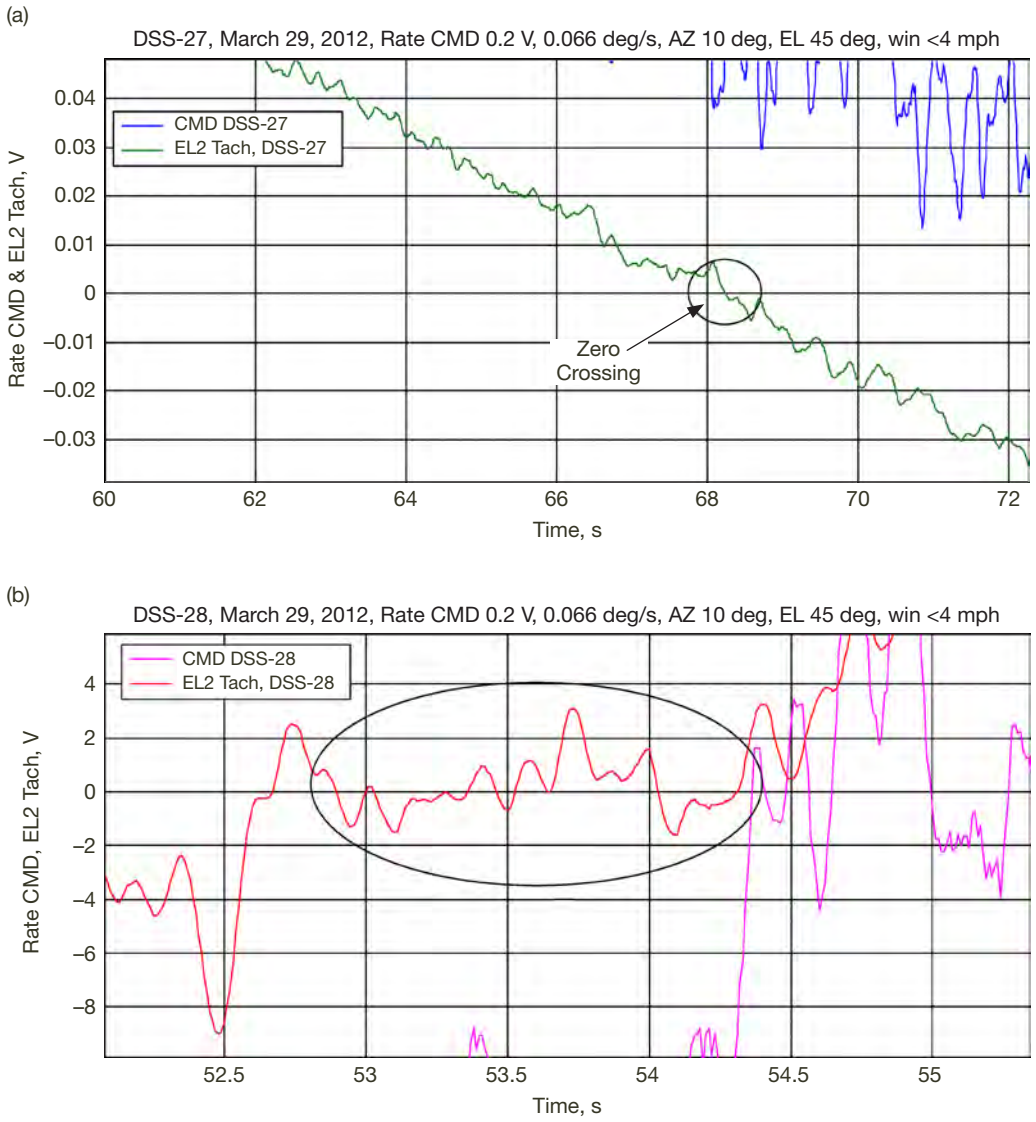

Figure F-13. EL2 tachometer response for (a) DSS-27 and (b) DSS-28 zoomed from Figure F-12. There is no discontinuity at DSS-27 zero crossing. DSS-28 has ~1 s discontinuity at zero crossing. However, this value is low and will not affect the position loop.

Appendix G

LQG Controller Coefficients

Created by Wodek Gawronski on January 19, 2012 for DSS-28 antenna.
Version 4 — more modal damping than in Version 3 EL coefficients.

The order of coefficients for AZ and EL is as follows:

n	(1×1)	— Dimension of the estimator
ei_max	(1×1)	— Maximal allowable value of the integral error
kp	(1×1)	— Proportional gain
ki	(1×1)	— Integral gain
kff	(1×1)	— Rate feedforward gain
kf	(1×n-1)	— Flexible mode gain vector
ke	(1×n)	— Estimator gain vector
a	(nun)	— Estimator state matrix
b	(n×1)	— Estimator input matrix
cp	(1×n)	— Estimator encoder output matrix
cf	(n-1×n)	— Estimator state output matrix

***

10
0.4
2.0784216
0.96031057
1.0

1.7175087e-01 –1.3897309e+00 2.9239597e-01 1.5230338e-01 –3.3133340e-01
–2.0250574e-01 –1.6256507e-02 –5.3959851e-02 1.3710873e-01

7.4098928e-01 1.1786821e-02 1.1638980e-01 3.0060985e-01 –1.9832101e-02
–1.1606039e-02 3.7352351e-09 –5.7628494e-10 5.0783600e-09 5.5184196e-10

1.0000000e+00 1.2440371e-02 1.1351463e-02 6.8640004e-02 –3.1283744e-02
–5.7101921e-02 –4.1450671e-02 6.4088293e-02 3.9533818e-02 6.4717223e-02
0.0000000e+00 8.4907464e-01 0.0000000e+00 0.0000000e+00 0.0000000e+00
0.0000000e+00 0.0000000e+00 0.0000000e+00 0.0000000e+00 0.0000000e+00
0.0000000e+00 0.0000000e+00 9.5443910e-01 1.7727563e-01 0.0000000e+00
0.0000000e+00 0.0000000e+00 0.0000000e+00 0.0000000e+00 0.0000000e+00
0.0000000e+00 0.0000000e+00 –1.7727563e-01 9.5443910e-01 0.0000000e+00
0.0000000e+00 0.0000000e+00 0.0000000e+00 0.0000000e+00 0.0000000e+00
0.0000000e+00 0.0000000e+00 0.0000000e+00 0.0000000e+00 7.9343877e-01
3.4043327e-01 0.0000000e+00 0.0000000e+00 0.0000000e+00 0.0000000e+00
0.0000000e+00 0.0000000e+00 0.0000000e+00 0.0000000e+00 –3.4043327e-01
7.9343877e-01 0.0000000e+00 0.0000000e+00 0.0000000e+00 0.0000000e+00

0.0000000e+00 0.0000000e+00 0.0000000e+00 0.0000000e+00 0.0000000e+00
0.0000000e+00 6.3957496e-01 6.8753853e-01 0.0000000e+00 0.0000000e+00
0.0000000e+00 0.0000000e+00 0.0000000e+00 0.0000000e+00 0.0000000e+00
0.0000000e+00 –6.8753853e-01 6.3957496e-01 0.0000000e+00 0.0000000e+00
0.0000000e+00 0.0000000e+00 0.0000000e+00 0.0000000e+00 0.0000000e+00
0.0000000e+00 0.0000000e+00 0.0000000e+00 3.6165089e-01 8.6025800e-01
0.0000000e+00 0.0000000e+00 0.0000000e+00 0.0000000e+00 0.0000000e+00
0.0000000e+00 0.0000000e+00 0.0000000e+00 –8.6025800e-01 3.6165089e-01

–2.1548489e-05 6.7652790e-03 –5.4117147e-02 –1.2142177e-02 –5.3800864e-03
–2.6115921e-02 1.2430159e-02 –5.9836353e-03 7.6583906e-03 6.2027549e-03

1.0000000e+00 0.0000000e+00 0.0000000e+00 0.0000000e+00 0.0000000e+00
0.0000000e+00 0.0000000e+00 0.0000000e+00 0.0000000e+00 0.0000000e+00
0.0000000e+00 1.0000000e+00 0.0000000e+00 0.0000000e+00 0.0000000e+00
0.0000000e+00 0.0000000e+00 0.0000000e+00 0.0000000e+00 0.0000000e+00
0.0000000e+00 0.0000000e+00 1.0000000e+00 0.0000000e+00 0.0000000e+00
0.0000000e+00 0.0000000e+00 0.0000000e+00 0.0000000e+00 0.0000000e+00
0.0000000e+00 0.0000000e+00 0.0000000e+00 1.0000000e+00 0.0000000e+00
0.0000000e+00 0.0000000e+00 0.0000000e+00 0.0000000e+00 0.0000000e+00
0.0000000e+00 0.0000000e+00 0.0000000e+00 0.0000000e+00 1.0000000e+00
0.0000000e+00 0.0000000e+00 0.0000000e+00 0.0000000e+00 0.0000000e+00
0.0000000e+00 0.0000000e+00 0.0000000e+00 0.0000000e+00 0.0000000e+00
1.0000000e+00 0.0000000e+00 0.0000000e+00 0.0000000e+00 0.0000000e+00
0.0000000e+00 0.0000000e+00 0.0000000e+00 0.0000000e+00 0.0000000e+00
0.0000000e+00 1.0000000e+00 0.0000000e+00 0.0000000e+00 0.0000000e+00
0.0000000e+00 0.0000000e+00 0.0000000e+00 0.0000000e+00 0.0000000e+00
0.0000000e+00 0.0000000e+00 1.0000000e+00 0.0000000e+00 0.0000000e+00
0.0000000e+00 0.0000000e+00 0.0000000e+00 0.0000000e+00 0.0000000e+00
0.0000000e+00 0.0000000e+00 0.0000000e+00 1.0000000e+00 0.0000000e+00
0.0000000e+00 0.0000000e+00 0.0000000e+00 0.0000000e+00 0.0000000e+00
0.0000000e+00 0.0000000e+00 0.0000000e+00 0.0000000e+00 1.0000000e+00

6
0.4
1.3923225
0.4877038
1.0

3.0284142e-01 2.2266368e+00 1.8250816e-01 –2.2913010e-01 –5.7161235e-01
6.0239627e-01 5.5242802e-10 –5.3042493e-01 –1.2541278e+00 –3.7265092e-02
–4.3115858e-01

1.0000000e+00 1.5823805e-02 –2.1247191e-02 –6.4416910e-02 –1.6613658e-03
–5.2672104e-02
0.0000000e+00 9.3675824e-01 0.0000000e+00 0.0000000e+00 0.0000000e+00
0.0000000e+00
0.0000000e+00 0.0000000e+00 9.6062648e-01 1.8356930e-01 0.0000000e+00
0.0000000e+00
0.0000000e+00 0.0000000e+00 –1.8356930e-01 9.6062648e-01 0.0000000e+00
0.0000000e+00
0.0000000e+00 0.0000000e+00 0.0000000e+00 0.0000000e+00 9.0114194e-01
1.8449435e-01
0.0000000e+00 0.0000000e+00 0.0000000e+00 0.0000000e+00 –1.8449435e-01
9.0114194e-01

–2.8564196e-05 3.1720676e-02 7.0386618e-02 2.7557312e-02 –4.7682502e-02
–4.6156796e-02

1.0000000e+00 0.0000000e+00 0.0000000e+00 0.0000000e+00 2.7755576e-17
0.0000000e+00
0.0000000e+00 1.0000000e+00 0.0000000e+00 0.0000000e+00 0.0000000e+00
0.0000000e+00
0.0000000e+00 0.0000000e+00 1.0000000e+00 0.0000000e+00 0.0000000e+00
0.0000000e+00
0.0000000e+00 0.0000000e+00 0.0000000e+00 1.0000000e+00 0.0000000e+00
0.0000000e+00
0.0000000e+00 0.0000000e+00 0.0000000e+00 0.0000000e+00 1.0000000e+00
0.0000000e+00
0.0000000e+00 0.0000000e+00 0.0000000e+00 0.0000000e+00 0.0000000e+00
1.0000000e+00

Appendix H

DSS-28 and DSS-27 Controller Parameter Configuration Measurement

On January 27, 2012, the antenna servo drive system (amplifier configuration and percent torque bias) measurement and recording of both DSS-27 and DSS-28 were performed by station personnel Fred Soria, Karen Portillo, Seymore Unpingco, and JPL cognizant development engineer, Farrokh Baher. Recording was conducted using a Baldor amplifier tester model 800, digital voltmeter, and drive cabinet meter observation (countertorque).

Table H-1 shows the ±15 VDC on each amplifier.

Table H-2 and Table H-3 summarize the result of the measurement of the controllers' parameter configuration for AZ and EL axes.

Table H-4 and Table H-5 illustrate the countertorque measurement as the antenna was in motion.

The results of the amplifier parameters configuration for both DSS-27 and DSS-28 were similar except the value of the gain for DSS-27 AZ3 shows lower than (about half) gain setting of 0.75.

Note: The gain value shown with (*) in Table H -2 and Table H-3 does not reflect the actual gain setting of (0.75). This is due to the change in other parameters after the initial gain setting. Also, there is lower percent countertorque for E1/EL2 for DSS-28 as compared to DSS-27.

Table H-1. ±15 VDC verification, EL=89.95, AZ=10, wind speed approximately 20–25 mph.

Controller	Recommended +15 VDC Value, Range	+ 15 VDC		Recommended –15 VDC Value, Range	–15 VDC	
		DSS-27	DSS-28		DSS-27	DSS-28
AZ1	15, (14.8 to 15.2)	14.98	15.0	15, (14.8 to 15.2)	–14.96	–15.0
AZ2	15, (14.8 to 15.2)	15.0	15.0	15, (14.8 to 15.2)	–14.95	–15.0
AZ3	15, (14.8 to 15.2)	14.99	15.0	15, (14.8 to 15.2)	–14.96	–15.0
AZ4	15, (14.8 to 15.2)	15.08	15.0	15, (14.8 to 15.2)	–15.04	–15.0
EL1	15, (14.8 to 15.2)	15.0	15.0	15, (14.8 to 15.2)	–15.0	–15.0
EL2	15, (14.8 to 15.2)	15.0	15.0	15, (14.8 to 15.2)	–15.02	–15.0

Table H-2. AZ1–AZ4 controller configuration parameters for DSS-27 and DSS-28, wind speed approximately 20–25 mph.

	AMP POT Adjustment	Tester Set Position	Tester Output DVM Reading Recommended Manufacturer Setting, VDC	AZ1, VDC		AZ2, VDC		AZ3, VDC		AZ4, VDC	
				DSS-27	DSS-28	DSS-27	DSS-28	DSS-27	DSS-28	DSS-27	DSS-28
1	Over Speed	OSPD Trip	9.0	9.05	9.02	9.02	8.96	9.28	9.08	9.00	9.11
2(a)	Rate (Gain) Set Current Limit	Current Limit	+1.0	N/A	N/A	N/A	N/A	N/A	N/A	N/A	N/A
2(b)	Then Rate Gain	Gain Set with G/F Set Pushed	0.75	3.32*	3.12*	3.26*	3.22*	1.74*	3.10*	3.22*	3.29*
3(a)	Null Forcing Set Current Limit	Current Limit Null Force with G/F	+3.20	N/A	N/A	N/A	N/A	N/A	N/A	N/A	N/A
3(b)	Then Null Forcing	Set Pushed	–8.00	–11.56	–9.47	–11.41	–9.54	–11.58	–9.84	–11.33	–9.86
4	Current Limit	Current Limit	+6.20	6.23	6.24	6.24	6.23	6.26	6.23	6.22	6.23
5	IOC	IOC Trip	+7.50	7.52	7.54	7.55	7.52	7.54	7.52	7.51	7.59
6	Max Field Current	FIELD/IR COPM	–2.20	–0.074	0.00	0.00	0.00	0.00	0.00	0.00	0.00

*See note on page 104.

Table H-3. EL1 and EL2 controller configuration parameters for DSS-27 and DSS-28.

	AMP POT Adjustment	Tester Set Position	Tester Output DVM Reading Recommended Manufacturer Setting, VDC	EL1, VDC		EL2, VDC	
				DSS-27	DSS-28	DSS-27	DSS-28
1	Over Speed	OSPD Trip	9.0	9.07	9.06	9.09	9.07
2(a)	Rate (Gain) Set Current Limit	Current Limit	+1.0	N/A	N/A	N/A	N/A
2(b)	Then Rate Gain	Gain Set with G/F Set Pushed	0.75	3.30*	3.25*	3.29*	2.96*
3(a)	Null Forcing Set Current Limit	Current Limit Null Force with G/F	+3.20	N/A	N/A	N/A	N/A
3(b)	Then Null Forcing	Set Pushed	–8.00	–0.02 –11.43	–0.82 –9.42	–0.883 –11.46	–1.18 –9.47
4	Current Limit	Current Limit	+6.20	6.23	6.24	6.32	6.28
5	IOC	IOC Trip	+7.50	7.51	7.49	7.56	7.59
6	Max Field Current	FIELD/IR COPM	–2.20	0.00	0.00	0.00	0.00

*See note on page 104.

Table H-4. AZ1–AZ4 percent countertorque for DSS-27 and DSS-28, rate 0.5 deg/s, wind speed approximately 20–25 mph.

Direction	Recommended Manufacturer Value	AZ1/AZ2, VDC, A20 Pot		AZ1/AZ2, %, Countertorque Meter		AZ3/AZ4, VDC, B20 Pot		AZ3/AZ4, %, Countertorque Meter	
		DSS-27	DSS-28	DSS-27	DSS-28	DSS-27	DSS-28	DSS-27	DSS-28
CW	16–20%	3.07	3.49	15%	17%	3.07	3.49	18–23%	17%
CCW	—	3.07	3.49	15%	16%	3.07	3.49	20%	21%

Table H-5. EL1 and EL2 percent countertorque for DSS-27 and DSS-28, rate 0.5 deg/s, wind speed approximately 20–25 mph, EL approximately 45 deg.

Direction	Recommended Manufacturer Value	EL1/El2, VDC, E20 Pot		EL1/EL2, %, Countertorque Meter	
		DSS-28	DSS-27	DSS-27	DSS-28
Up	16–20%	3.348	3.50	15%–20%	20%–25%
Down	—	3.348	3.50	20%–25%	12%